TECHNISCHE UNIVERSITÄT DRESDEN

**Faculty of Environmental Sciences**

# Assessing climate change impacts on physical structure of lakes and reservoirs using one, two and three-dimensional hydrodynamic models

**DISSERTATION**

**In fulfilment of the requirements for the academic degree**

**Doctor rerum naturalium (Dr.rer.nat.)**


Presented by: Chenxi Mi,

January 9th 1989 in Shenyang, China

Reviewers: Prof. Dr. Dietrich Borchardt

Department of Aquatic Ecosystem Analysis and Management

Helmholtz Centre for Environmental Research, Magdeburg, Germany

Dr. Karsten Rinke

Department of Lake Research

Helmholtz Centre for Environmental Research, Magdeburg, Germany

Prof. Dr. Thomas U. Berendonk

Institute of Hydrobiology

Technische Universität Dresden, Dresden, Germany

# Declaration of Conformity

I, Chenxi Mi, hereby confirm that this copy conforms with the original dissertation on the topic:

“Assessing climate change impacts on physical structure of lakes and reservoirs using one, two and three-dimensional hydrodynamic models”

.....

Ort, Datum

.....

Unterschrift

# Table of Contents

# List of Tables

# List of Figures

# List of Abbreviations

| | |
|---|---|
| 1D | one dimensional |
| GLM | General lake model |
| DWD | Deutscher Wetterdienst |
| RMSE | root-mean-square-error |
| $K_w$ | light attenuation coefficient |
| $C_{HYP}$ | vertical turbulent mixing coefficient in the hypolimnion |
| 2D | two dimensional |
| W2 | CE-QUAL-W2 |
| m a.s.l | meters above sea level |
| WE | withdrawal elevation |
| CTD | conductivity temperature depth |
| DP | dew point temperature |
| WSC | wind sheltering coefficient |
| SHADE | shading coefficient |
| $C_{KH}$ | Kelvin–Helmholtz turbulent billows |
| CBHE | coefficient of bottom heat exchange |
| ALBEDO | Albedo of ice |
| 3D | three dimensional |
| $K_z$ | vertical turbulent diffusion coefficient |
| EFDC | environmental fluid dynamic code |
| $\rho_o$ | reference water density |
| $A_v$ | vertical turbulent viscosity |
| MOM | metalimnetic oxygen minimum |
| GCM | global circulation model |
| RCP | Representative Concentration Pathway |
| ISIMIP | Inter-Sectoral Impact Model Intercomparison Project |
| RH | relative humidity |
| GAM | generalized additive model |
| $A_s$ | surface area of the reservoir |
| PAR | photosynthetically available radiation |

# 1. Introduction

Inland surface waters (i.e. rivers, lakes, and reservoirs), which account for only 0.8% of the earth's area, not only harbor more than 100 000 aquatic species (ca. 6% of the total global diversity, see Malmqvist and Rundle 2002) but also provide several ecosystem services which are very important for human development (Rinke et al. 2019):

1) provisioning services: food, fiber and medicines generated from waters, drinking water supply;

2) regulating services: maintenance of water quality, flood management, climate regulation;

3) cultural services: cultural heritage landscapes, religious cultures, recreation and tourism;

4) supporting services: soil formation, primary production, nutrient cycling.

However, on a global scale, quality of inland waters and their ecosystem services have been increasingly suffered from a plethora of anthropogenic stressors, including widespread pollution, river damming, habitat loss and invasive species introductions, overexploitation and climate change (Cowx and Portocarrero Aya 2011,Tan et al. 2018). Accordingly, model-based predictive tools for inland waters and their application to aid optimization of management strategies, ecosystem restoration and protection or to better understand the driving processes of their dynamics are currently critical concerns in environmental science and related research fields.

Within inland waters, lakes (including reservoirs) occupy around 24% of the total area and the remaining 76% are rivers and wetlands (Rinke et al. 2019). Despite the differences of hydrological properties (e.g. flow velocity, residence time) and shapes, a major difference between lakes and rivers is the occurrence of vertical gradients in lentic ecosystems while lotic ecosystems rather show longitudinal gradients. Rivers are usually shallow and fully mixed for the whole year round, while most lakes show a vertical stratification of their water masses at least for some extended time periods. Any modelling tool for lakes therefore has to take into account the occurrence and dynamics of vertical stratification. In fact, most lake models include a hydrophysical model that simulates stratification and mixing in different dimensionalities (Janssen et al. 2015,Trolle et al. 2012). The focus of this thesis is therefore on modelling the dynamics of stratification and mixing in standing waters.

Previous research has shown that water temperature structure is always changed over time, which is strongly controlled by meteorological drivers (Adrian et al. 2009,Shimoda et al. 2011). This is why stratification patterns are different between climate zones (e.g. amictic in the polar regions, dimictic in temperate regions). Changes in climate conditions, therefore, have a big influence on physical dynamics and thermal structure. This does mostly apply to changes in air temperature and wind speed, from which the effect would be stronger than that from changes in other climate variables (e.g. cloud cover, rain and relative humidity). There are a bunch of previous studies, in this field, analyzing the influence of different climate factors by gradually increasing or decreasing their specific values without altering the other climate variables. This method is quite close to sensitivity analysis in modelling studies, while it fails in predicting

future stratification structure under real climate changes. With the development of climate models (e.g. those used in ISIMIP or CORDEX), it is now possible for the scientists to accurately mimic the future conditions of stratification pattern in standing waters by coupling real climate projections with hydrodynamic simulations. Such issues mentioned above will be discussed in detail in this thesis.

## 1.1. Thermal stratification

Thermal stratification is the phenomenon referring to a variation in water density at different depths in inland waters and usually arises from changes in water temperature in the vertical direction of a water column. In freshwater systems, water density is temperature-dependent and its maximum value, 1g/cm$^3$, appears at 4 °C (Boehrer and Schultze 2009a).

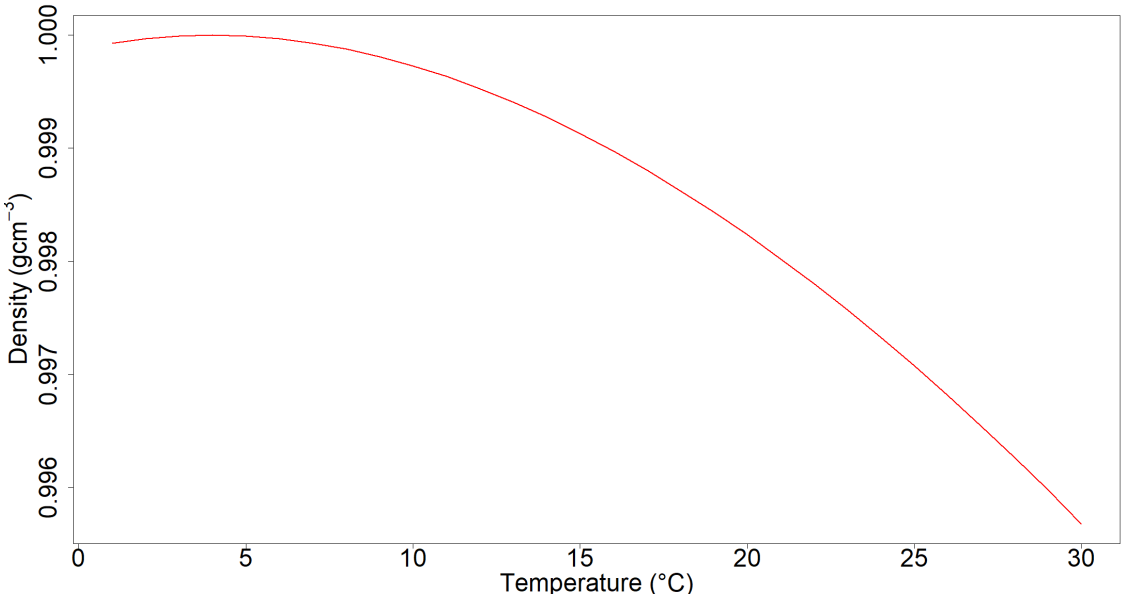


Figure 1.1. Relationship between water density and water temperature (Chen and Millero 1986).

There are two kinds of stratification based on water temperature patterns: (i) summer (direct) stratification occurring when the surface water temperature is higher than the bottom temperature, and (ii) winter (inverse) stratification occurring when surface waters are cooler than bottom waters (Lewis 1983). Based on the stratification and mixing frequency per year, deep waters can be classified into six mixing types (Hutchinson and Loffler 1956):

1) amictic: always ice-covered and inversely stratified throughout the year;
2) cold monomictic: inversely stratified for most of the year and only mixing in the summer;
3) warm monomictic: directly stratified in most of the year and only mixing in winter;
4) dimictic: stratified in summer and winter, mixing in spring and fall;

5) oligomictic: directly stratified for most of the time and mixing at irregular intervals longer than 1 year;

6) polymictic: mixing several times per year.

In temperate regions, most of deep waters can be classified into dimictic or warm monomictic types (Lewis 1983). In such water bodies, stratification in summer includes the occurrence of three layers along depth: the warm surface waters (i.e. epilimnion), the cold bottom waters (i.e. hypolimnion) and the layer in between (i.e. metalimnion) with steep temperature (thermocline) and density gradients. The intensity of vertical mixing, expressed as the vertical turbulent diffusion coefficient $K_z$ , is typically high in the epilimnion due to wind stirring and convection (often larger than $10^{-4}$ $m^2$ $s^{-1}$), and much smaller in the hypolimnion (usually lower than $10^{-5}$ $m^2$ $s^{-1}$), where internal waves (Boehrer 2000), bottom friction and shear stress drive turbulent mixing (Goudsmit et al. 1997,Valerio et al. 2012,Wüest and Lorke 2003). The metalimnion is characterised by extremely low vertical mixing because of its strong temperature gradient.

Stratification is a key factor for water quality and significantly affects biogeochemical cycling in aquatic ecosystems (Boehrer and Schultze 2009b,Kirillin and Shatwell 2016,Winton et al. 2019). Because of the stratification, oxygen from the atmosphere cannot be effectively transported into the hypolimnion which can result in the environmental problem of hypolimnetic anoxia (Snortheim et al. 2017). On the other hand, high mixing in the epilimnion keeps the phytoplankton stay in the layer. Its growth and the following sedimentation lead to the formation of a nutrient-rich bottom water and a nutrient-poor surface water (Read et al. 2011). Additionally, by influencing metabolism and flux of gases between the water surface and atmosphere, stratification can also affect the role of lakes in the global carbon cycle (Bastviken et al. 2011).

## 1.2. Recent studies on stratification and current research gaps

Given the significance of stratification for aquatic ecosystems, numerous investigations have focused on this phenomenon and its influencing factors. Previous studies have proven that climate change strongly affects the temperature stratification of waters worldwide (Fenocchi et al. 2018,Fink et al. 2014a,Piccolroaz et al. 2015), which then influences phytoplankton growth as well as nutrient cycling in aquatic ecosystems (Fenocchi et al. 2019,Sahoo et al. 2013). Wilhelm and Adrian (2008) reported that the strong summer heatwave in 2003 and 2006 significantly increased the stratification duration and intensity of Lake Müggelsee. Schlabing et al. (2014) projected a strong increase in surface water temperature in Lake Constance under future climate conditions, resulting in a more prominent phytoplankton bloom in the spring. Ladwig et al. (2018) found that elevated air temperature will significantly extend the summer stratification period in Lake Tegel at the second half of 21$^{st}$ century, which promotes the growth of harmful cyanobacteria. Most of the related studies paid attention to the response of stratification

phenology to climate changes in natural lakes, whereas very few specifically focused on this response in reservoirs.

A big difference between lakes and reservoirs is that in lakes water always overflows at the surface when its volume is in excess of the maximum storage, but water in reservoirs can be taken out at different withdrawal elevations to meet the requirements of different usages. This selective withdrawal strategy in reservoirs is considered to be an effective way to control their water temperature structures. For example, Ma et al. (2008) simulated the stratification phenology in the Kouris Dam in Cyprus and concluded that the water temperature profiles in the reservoir were noticeably influenced by water withdrawal schemes. In comparison to bottom water withdrawal, surface withdrawal tends to decrease water temperature in the whole column as well as epilimnetic water volume; Carr et al. (2019) used a well-established water quality model to illustrate the response of water temperature and nutrient distribution to changing withdrawal elevations in Lake Diefenbaker reservoir, and found that deep withdrawal would decrease the hypolimnetic volume and draw in more nutrients into the hypolimnion. Weber et al. (2017) employed a one-dimensional model (GLM-AED) to elucidate the decisive impact of withdrawal depth on the thermal structure of Grosse Dhuenn Reservoir. The results showed that selective withdrawal of water from the 14 °C isotherm can significantly shoal thermocline depth and increase the temperature difference between epilimnion and hypolimnion. However, all these studies only tested the influence of the withdrawal strategy on stratification under current climate conditions. Whether the strategy can be adopted to effectively control the thermal structure under future climate change or can even alleviate some effects from a warming climate is far less studied.

Furthermore, when evaluating the response of thermal dynamics to climate change, most research focused on the influence of climate warming. Very few studies, however, considered the effect of other meteorological factors, e.g. changing wind speed. This is astonishing because previous studies have clearly pointed out the significance of wind speed on stratification structure. For example, Woolway et al. (2019) used a well-established hydrodynamic model to simulate the thermal structure of lakes across the Northern Hemisphere and found that lake warming has accelerated due to atmospheric stilling, the reduction in observed wind speed. By evaluating the influence of wind speed on the thermal structure in Lake Biwa, Japan, Koue et al. (2018) illustrated that if the magnitude of wind is strong enough, stratification in the lake will collapse and water can be fully mixed even in the midsummer. Based on the observed data in Lake Annie, Read et al. (2011) demonstrated that its thermocline depth increased by more than 2 m and surface water temperatures decreased by around 3 °C due to a sudden increase in wind speed. However, most of the related studies either simply checked the response of stratification dynamics to global changes of wind speed or just draw conclusions from a single observation. The response of thermal structure to different magnitude and timing of wind events is still not fully understood.

Another stratification aspect which is mostly overlooked in the previous studies is winter inversed stratification. Summer stratification is intensively researched by limnologists but this is not true with respect to the winter stratification. As shown above, the occurrence of winter inversed stratification is an important criterion to distinguish between dimictic and monomictic

waters and it is also a prerequisite for the formation of ice cover, so more attention should be paid to this kind of stratification and its influencing factors. By analyzing long-term water temperature profiles of three deep lakes in Austria, Ficker et al. (2017) found that winter stratification has disappeared in all three lakes due to climate warming, which caused a transition of their mixing regimes from a dimictic to a monomictic type. Similar conclusions were also drawn from the research in Kirillin (2010) and Peeters et al. (2002). Shimoda et al. (2011) even concluded that the disappearance of winter stratification and the following transformation of lake types is not a local phenomenon but will happen in numerous deep lakes around the world, which can strongly affect the hypolimnetic water temperature as well as the sediment-water interactions like internal phosphorus release from the sediment. Even worse, this change in winter conditions will make deep-water mixing much more susceptible to interannual variations in climate conditions and suppress the oxygen recovery in the bottom layer of very deep (i.e. $z > 100$m) lakes (Peeters et al. 2002).

Moreover, when analyzing stratification dynamics, researchers always focused on the dynamics of water temperature (i.e. the state variable), but neglected the dynamics of mixing, e.g. as expressed by vertical diffusivity (i.e. the process). This is due to the fact that the diffusivity is not easy to measure *in situ* and requires measurements at high accuracy with sufficient temporal and spatial resolution, which are not available in most standard lake monitoring programs. It is believed that compared to water temperatures, vertical diffusivity is a variable providing a more direct view on physical transport within the water column (Wahl and Peeters 2014). In particular, the reduced vertical diffusivity within the metalimnion limits the transportation between surface and bottom waters, which strongly influences the nutrient availability (Leach et al. 2018), composition of plankton communities (Karpowicz and Ejsmont-Karabin 2017) and oxygen dynamics (Kreling et al. 2017). Therefore, it is valuable to comprehensively elucidate the dynamics of vertical diffusivity, especially the strong diffusivity gradients around the metalimnion and its influencing factors.

To address the research gaps shown above, several hydrodynamic models were applied in this thesis to simulate stratification in two water bodies (i.e. Lake Arendsee and Rappbode Reservoir) and disentangle its response to climate changes and different withdrawal scenarios (see Table 1.1).

Table 1.1. Influencing factors on stratification checked in each chapter

| Influencing factor | Chapter 2 | Chapter 3 | Chapter 4 | Chapter 5 |
|---|---|---|---|---|
| Wind speed | × | × | | |
| Air temperature | × | | × | |
| Selective withdrawal | | | × | × |
| Future climate projection | | | | × |

Detailed introduction for each chapter is shown below:

- The first analysis (see Chapter 2) describes the application of a 3D hydrodynamic model (EFDC) to study the stratification phenology in Lake Arendsee. Unlike most of previous related research, which only simulated the dynamics of water temperature, this study explicitly evaluated the model performance in reproducing vertical turbulent diffusion, especially the minimum diffusion in the metalimnion of the lake. Additionally, the study demonstrated sensitivity of the metalimnetic diffusion against two climate drivers (i.e. air temperature and wind velocity) and further confirmed importance of wind on the intensity of vertical mixing.
- The second study (see Chapter 3) deals with the impact of wind speed on the thermal structure in Rappbode Reservoir. Simulations were conducted with the 1D hydrodynamic model GLM to assess the response of stratification in the reservoir to changing wind speed, as well as magnitude and timing of short-term strong wind events.
- The third model experiment (see Chapter 4) refers to the application of two hydrodynamic models (i.e. GLM and CE-QUAL-W2) in elucidating the combined effects of potential climate warming and selective water withdrawal strategies on winter stratification in Rappbode Reservoir. Evaluating the scenario results of 1420 simulations by these two widely used models, the study also provides an excellent opportunity to systematically compare the models' performances, which will benefit researchers with respect to model selection and application.
- The fourth study (see Chapter 5) combines future climate projections under different RCP greenhouse gas emissions scenarios (RCP 2.6, RCP 6.0 and RCP 8.5) and the 2D hydrodynamic model CE-QUAL-W2 to elucidate the response of thermal stratification in Rappbode Reservoir to future climate change. The study also illustrated how different withdrawal strategies can be used to alleviate climate warming effects on thermal structure.

Finally, a general discussion critically reflects the methods adopted and results produced in this thesis. Additionally, according to the newly gained knowledge, a comprehensive outlook gives guidance for further research and discusses limitations identified within this thesis.

## 1.3. Main research questions and hypotheses

### 1.3.1. Assessing vertical diffusion in a stratified lake using a 3D hydrodynamic model

This study tightly combined model application and *in situ* measurements related to vertical mixing, so as to evaluate the model results not only by comparing measured and observed states (i.e. water temperature), but also comparing results on the process level (i.e. vertical diffusion coefficients). We were particularly interested in evaluating the model's ability to simulate the highly constrained vertical mixing within the metalimnion as these low mixing intensities play an important role in the formation and persistence of metalimnetic oxygen minima in the studied lake. Moreover, we elaborate to analyse the response of the metalimnetic diffusivity to

meteorological forcing, particularly changing wind speeds and warming.

The main research questions of this study were:

A1: Is the well-established 3D model capable of reproducing the summer stratification and water temperature dynamics in Lake Arendsee?

A2: How does the intensity of vertical turbulent diffusion (as quantified by the turbulent diffusion coefficient $K_z$) is changing over depth and season in Lake Arendsee and can these intensities be modelled properly? Is the metalimnetic minimum of $K_z$ well simulated?

A3: Is changing wind speed is a more influential factor on the metalimnetic diffusion minimum than changing air temperature?

### 1.3.2. Stratification dynamics in Rappbode Reservoir under different wind conditions

The aim of this study was to comprehensively disentangle the response of the stratification dynamics in Rappbode Reservoir to different wind conditions, including overall and episodic changes in wind speed. The study not only confirmed the decisive impact of wind speed on stratification of lakes and reservoirs, but also effectively demonstrated the sensitive time window of thermal dynamics to episodic wind events.

The study was developed based on the following research questions:

B1: Does wind speed have a significant influence on the stratification phenology of the reservoir? It is hypothesized that an increase in wind speed will decrease the stratification stability, shorten the stratification duration and increase the hypolimnetic water temperature.

B2: Does the impact of episodic wind events on the thermal structure of the reservoir is different for different timings over the season? It is hypothesized that the events will be more influential if they took place at the beginning of the stratification period (i.e.in early summer).

B3: What is the impact of the duration of episodic wind events on stratification phenology?

### 1.3.3. Variable withdrawal elevations as a management tool to counter the effects of climate warming in Rappbode Reservoir

The aim of this model experiment was to illustrate the response of winter stratification in Rappbode Reservoir to increasing air temperature, and to analyze the effects of selective withdrawal strategies on controlling winter conditions under climate warming. This study also contained a novel approach by applying two different lake models (i.e. GLM and CE-QUAL-W2) and provided an opportunity to compare and evaluate the performance of these two models. From the comparison of results, the strengths and weaknesses of each model became clearly visible. This helps, on the one hand, developers to improve the models in the future and on the other hand guides practitioners in making a good choice when models have to be selected for a given purpose.

The hypotheses of this study were:

C1: Climate warming tends to shorten and weaken winter stratification in the reservoir and can change the lake type from dimictic to warm monomictic.

C2: Selective withdrawal strategy can control duration of the winter stratification and changing the reservoir management from deep withdrawal to shallow withdrawal elevations can prolong the winter stratification period.

C3: The two hydrodynamic models differ in their quantitative predictions but their qualitative outcomes are comparable.

### 1.3.4. Ensemble warming projections in Rappbode Reservoir and potential adaptation strategies

In this study we aimed at predicting the thermal structure in the Rappbode Reservoir until 2100 under different future IPCC climate projections (RCP 2.6, RCP 6.0 and RCP 8.5). Each climate scenario in this study was driven by an ensemble of four GCMs in order to account for model uncertainties. Additionally, we checked the effect of using adaptive withdrawal strategies for adapting the influences of climate warming on water temperatures and stratification pattern. This study is linked to the ISIMIP2b-project initiative.

The following hypotheses were tested in the modelling study:

D1: Stratification intensity in the reservoir will significantly increase under severe climate warming (i.e. RCP 6.0 and RCP 8.5), but not change so much under low climate warming (RCP 2.6).

D2: Uncertainties of future projections for stratification intensity become larger over time, especially under severe climate warming scenarios.

D3: Under intense warming not only epilimnetic water temperatures will increase, but also hypolimnetic temperatures will display warming.

D4: The surface withdrawal strategy can be used as an effective way to decrease the magnitude of the climate warming effects on the physical structure including potential effects on the hypolimnion.

# 2. Assessing vertical diffusion in a stratified lake using a 3D hydrodynamic model

## 2.1. Abstract

Vertical turbulent diffusivity ($K_z$), which can be estimated from water temperature, is a key factor in the evolution of water quality in lentic waters. In this study, we analysed the capability of a three-dimensional hydrodynamic model (EFDC) to capture water temperature and vertical diffusivity in Lake Arendsee in the Northern German plain. Of particular interest to us is to evaluate the model performance for capturing the diffusion minimum within the metalimnion and analyse the response of the metalimnetic $K_z$ to meteorological forcing, namely changing wind speed and warming. The comparison confirmed that the calibrated model could reproduce both stratification dynamics and vertical diffusion profiles in the lake. The model was also shown to be able to capture the duration and vertical extent of the metalimnetic diffusion minimum. The scenario results illustrate that, compared to air temperature, wind velocity appeared to be the more influential meteorological variable on the vertical exchange within the metalimnion. While increasing wind velocities mostly affected the minimum values of $K_z$ in the metalimnion and thus led to intensified vertical exchange, the reduction of wind velocity mostly affected the depth of minimal $K_z$ , but not its absolute value.

## 2.2. Introduction

Thermal stratification is a key feature in many lentic waters such as lakes and reservoirs (Boehrer and Schultze 2008). During warm seasons, surface waters heat up and have a lower density than the colder deeper waters. The two layers are separated by the metalimnion, a distinct zone with steep temperature (thermocline) and density gradients. Given the fact that lakes are most abundant between subarctic and Mediterranean climates (Lehner and Döll 2004,Pekel et al. 2016), i.e. in a seasonal temperature regime that strongly supports the occurrence of thermal stratification, the vast majority of lakes undergo some degree of thermal stratification. In a stratified lake, the intensity of vertical mixing, expressed as the vertical turbulent diffusion coefficient $K_z$ , is typically high in the epilimnion (often more than $10^{-4}$ $m^2$ $s^{-1}$) because of wind stirring and convection, and much lower in the hypolimnion (usually less than $10^{-5}$ $m^2$ $s^{-1}$) where internal waves (e.g. Boehrer 2000,Boehrer et al. 2000), bottom friction and shear drive turbulent mixing (Goudsmit et al. 1997,Valerio et al. 2012,Wüest and Lorke 2003). The layer in between, i.e. the metalimnion, is characterized by extremely low vertical mixing because of its strong density gradient. This makes the metalimnion a separate layer where local phenomena can persist for a long time before being dispersed by a large mixing event. Examples of such phenomena

within the metalimnion are chlorophyll maxima (Leach et al. 2018), oxygen maxima (Wilkinson et al. 2015), or oxygen minima (Kreling et al. 2017,Wentzky et al. 2019).

The consequences of stratification are multifaceted, affecting physical, chemical and biological processes in several ways (Luo et al. 2018,Yang et al. 2018). Most importantly, the temperature and density gradients along the vertical axis suppress vertical exchange between the epilimnion and hypolimnion and thus give rise to the formation of chemical gradients (e.g. Dietz et al. 2012) or oxyclines (Boehrer and Schultze 2008). Atmospheric oxygen cannot replenish the hypolimnetic oxygen deficit because of the mixing barrier of the metalimnion (Fenocchi et al. 2019). Phytoplankton, on the other hand, often profit from stratification because the reduced vertical mixing protects algal cells from being mixed down into dark layers where low light conditions limit photosynthesis. In many deep lakes, therefore, algal growth can only start once stratification is established and algal cells remain suspended within the epilimnion (Peeters et al. 2007,Sommer et al. 1986).

Stratification models have been developed for more than 30 years (Imberger 1981,Riley and Stefan 1988). Meanwhile, temperature variations, both in depth and time, achieve high coefficients of determination in many cases (often above 95%, see Arhonditsis and Brett 2004,Mi et al. 2018) when simulations are compared with observed data as several model tools and case studies have described (e.g. see Frassl et al. 2018,Mi et al. 2019,Perroud et al. 2009,Wahl and Peeters 2014). Since water temperature variability over a season is very high in the epilimnion and comparatively low in the hypolimnion, the high model performance for temperature dynamics of existing models mostly reflects their excellent ability to simulate temperature dynamics in the surface layers. In that sense, model skill estimates like RMSE or $R^2$ are biased if they incorporate all values aggregated over the whole depth range. These dynamics are strongly controlled by meteorological variables and therefore largely a direct response to the input data (Woolway and Merchant 2017). The direct effect of meteorological drivers, however, diminishes with depth and below the thermocline their contribution to mixing is only indirect.

In fact, many models show small but systematic differences in simulated hypolimnion temperatures (e.g. Perroud et al. 2009). Stepanenko et al (2010) even concluded, in a comparison study of 1D lake models, that temperature dynamics below the thermocline are notoriously difficult to simulate. This limitation is a consequence of the fact that turbulent kinetic energy in the hypolimnion is mostly created by the dissipation of basin scale internal waves, i.e. a three-dimensional process, and therefore cannot be properly mimicked in a 1D approach. Although existing 1D models are undergoing further improvements in order to account for effects from basin scale internal waves (Gaudard et al. 2017,Yeates and Imberger 2003), we usually expect better performance from a 3D model, compared to a 1D model, with respect to hydrodynamics simulation in the hypolimnion. Our study was motivated by the question of how well a 3D hydrodynamic model is able to reproduce vertical transport beneath the surface layer, i.e. within the metalimnion and the hypolimnion of a deep, stratified, temperate lake. For this purpose, we chose a lake with simple basin morphometry and only marginal hydrological forcing, but with pronounced gradients and distinct physicochemical patterns along the vertical axis.

Unlike most other studies using hydrodynamic models, we do not only use the dynamics of water temperature (i.e. a model state variable) for model assessment but also explicitly check its

abilities on the process level by comparing observed and simulated vertical diffusivity (i.e. a process) quantitatively. We believe that this is a more informative approach because any deviation on the level of the model states is not necessarily informative regarding the corresponding deviation of the involved processes due to non-linearities and non-additive interactions with other processes. We therefore followed the concept established in Wahl and Peeters (2014), who also used a 3D model for comparing observed and simulated vertical diffusivity in deep Lake Constance. We extended their study by (i) including a detailed analysis of vertical diffusivity within the metalimnion, (ii) designing a detailed field program using high-resolution monitoring, and (iii) applying a high spatial resolution in the model grid in order to better resolve 3D effects.

The focus of this study is on a tight combination of a 3D hydrodynamic model application and *in situ* measurements related to vertical mixing in a large and stratified lake. The major novelty of our study is the detailed investigation of the diffusion minimum in the metalimnion of a deep lake using a combination of high-frequency *in-situ* measurements and 3D modelling, as well as the sensitivity of this diffusion minimum to external forcing from wind and air temperature. Unlike other modelling studies, we are not focusing our analysis on comparing model states (e.g. water temperature) but on the comparison of key characteristics at the process level (e.g. vertical turbulent diffusion). We pursued the following three research objectives: (i) establish a detailed, high resolution field monitoring program for water temperature in order to calculate turbulent vertical diffusion coefficient $K_z$ with the gradient flux method (Heinz et al. 1990), (ii) perform simulations with a 3D lake model and derive lake-wide estimates of modelled turbulent vertical diffusion, and (iii) analyse the turbulent vertical diffusion within the metalimnion and its sensitivity to the meteorological drivers (i.e. air temperature and wind velocity).

## 2.3. Materials and Methods

### 2.3.1. Study site

Lake Arendsee is a dimictic temperate lake located in the North German Plain (55°53’21’’N, 11°28’27’’E, 23.3 m above sea level). The lake originated from a collapsed salt doline, has an elliptical shape, a surface area of 5.14 $km^2$ and maximum and mean depths of 49.5 m and 29 m, respectively (Figure 2.1). The littoral zone is relatively steep and the cross-sectional area at 30 m depth is 3.07 $km^2$. The hard-water lake is mainly fed by groundwater. Currently, four ditches drain adjacent agricultural fields into the lake and a small artificial runoff channel transports water out of the lake. The theoretical water residence time is between 50 and 60 years (Meinikmann et al. 2015). The above-ground catchment area (29.5 $km^2$) is dominated by agriculture (52.1%) and forestry (30.6%). The town of Arendsee is situated directly on the south-west shore. At least since the middle of the last century, the lake has been strongly eutrophied. High total phosphorus concentrations (2013-2017: 0.19 mg $L^{-1}$ on average) often lead to low transparency depths (ca. 1 m) due to the mass development of phytoplankton during the vegetative period. The phytoplankton is dominated by cyanobacteria such as *Planktothrix*

*rubescens*; or diazotrophic *Anabaena flos-aquae*, and *Aphanizomenon flos-aquae*. Dissolved oxygen ($O_2$) in the hypolimnion at the end of summer stratification has continuously decreased over the last four decades. During summer stratification a distinct metalimnetic oxygen minimum extending several meters is formed every year. More detailed information on the lake origin, morphometry, hydrological regime and physical properties may be found in Findlay et al. (1998), Hupfer et al. (2016), Engelhardt & Kirillin (2014) and Bernhardt & Kirillin (2013).

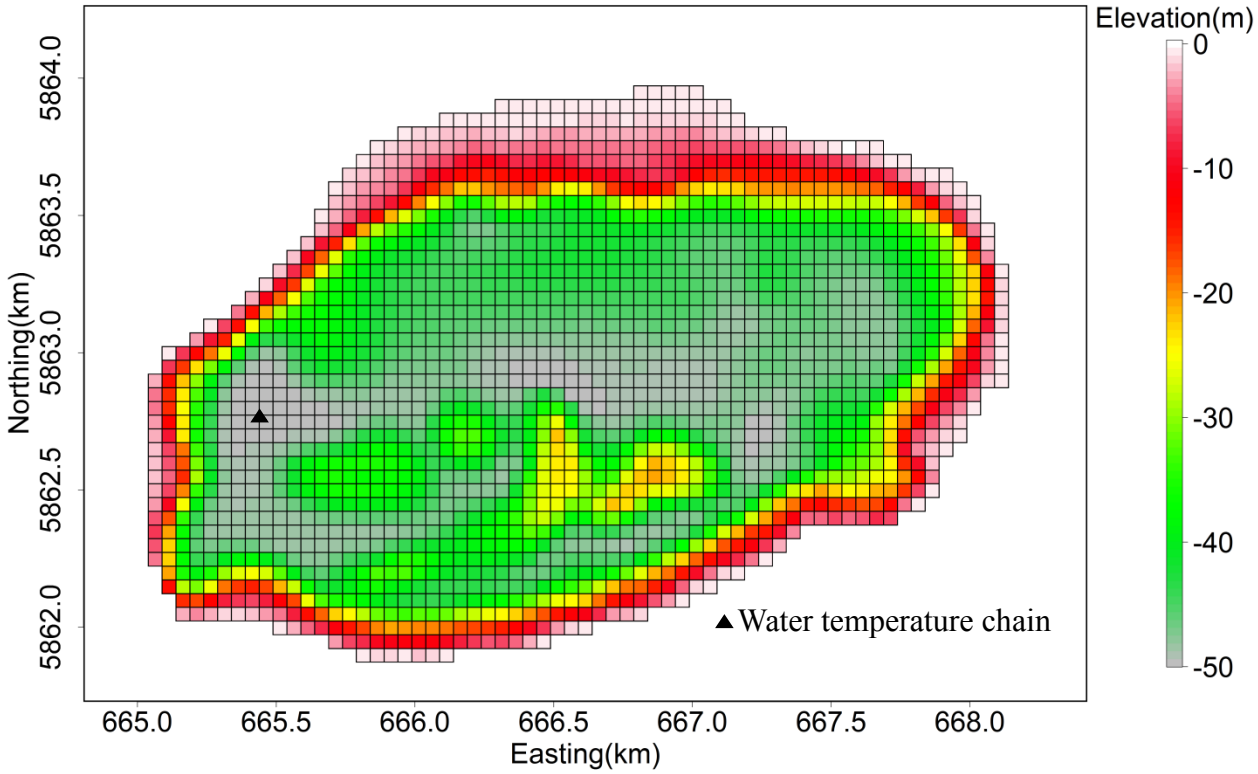


Figure 2.1. Model grid of Lake Arendsee used in the simulations, the horizontal resolution is 50m x 50m. The color scale represents the maximum depth in each grid cell. The black triangle marks the location of sampling point (temperature chain). Coordinates are given in UTM.

### 2.3.2. Numerical model

The three-dimensional model of Lake Arendsee was established using the Environmental Fluid Dynamic Code (EFDC, the utilized distribution is EFDC Explorer Release 8.2.5, DSI LLC), a public domain, open source, surface water modeling system that can be downloaded at https://www.epa.gov/exposure-assessment-models/efdc. EFDC includes routines for one-dimensional, two-dimensional, and three-dimensional hydrodynamics with module extensions for various processes, such as sediment transport, ecosystem dynamics, submerged aquatic vegetation and sediment diagenesis (Hamrick 1992). EFDC was originally developed at the Virginia Institute of Marine Science and the School of Marine Science in the College of William and Mary in Virginia (Tetra 2007). EFDC has been applied to more than 100 water bodies including rivers, lakes, reservoirs, wetlands, estuaries, and coastal ocean regions for

environmental assessment and management. It is recommended by the US EPA as a standard 3D hydro-environmental simulation tool (Wang et al. 2013,Wu and Xu 2011). EFDC uses a three time level, finite difference scheme with an internal-external mode splitting procedure to separate the internal shear or baroclinic mode from the external free surface gravity wave or barotropic mode. The vertical diffusion coefficients for momentum, mass and temperature are determined by the turbulent closure model of Mellor and Yamada (1982), which involves the use of analytically determined stability functions and the solution of transport equations for the turbulence intensity and length scale (Hamrick 1996).

The momentum and continuity equations and the transport equations for salinity and temperature are shown below (Hamrick 1992):

$$\frac{\partial(mHu)}{\partial t}+\frac{\partial\left(m_yHuu\right)}{\partial x}+\frac{\partial\left(m_xHvu\right)}{\partial y}+\frac{\partial(mwu)}{\partial z}-Hv\left(mf+v\frac{\partial m_y}{\partial x}-u\frac{\partial m_x}{\partial y}\right)$$
$$=-m_yH\frac{\partial(g\zeta+p)}{\partial x}-m_y\left(\frac{\partial h}{\partial x}-z\frac{\partial H}{\partial x}\right)\frac{\partial p}{\partial z}+\frac{\partial}{\partial x}\left(\frac{mA_v}{H}\frac{\partial u}{\partial z}\right)+Q_u \tag{2.1}$$

$$\frac{\partial(mHv)}{\partial t}+\frac{\partial\left(m_yHuv\right)}{\partial x}+\frac{\partial\left(m_xHvv\right)}{\partial y}+\frac{\partial(mwv)}{\partial z}+Hu\left(mf+v\frac{\partial m_y}{\partial x}-u\frac{\partial m_x}{\partial y}\right)$$
$$=-m_xH\frac{\partial(g\zeta+p)}{\partial y}-m_x\left(\frac{\partial h}{\partial x}-z\frac{\partial H}{\partial x}\right)\frac{\partial p}{\partial z}+\frac{\partial}{\partial x}\left(\frac{mA_v}{H}\frac{\partial v}{\partial z}\right)+Q_v \tag{2.2}$$

$$\frac{\partial p}{\partial z}=-gH\frac{\rho-\rho_0}{\rho_0}=-gHb \tag{2.3}$$

$$\frac{\partial(m\zeta)}{\partial t}+\frac{\partial\left(m_yHu\right)}{\partial x}+\frac{\partial\left(m_xHv\right)}{\partial y}+\frac{\partial(mw)}{\partial z}=0 \tag{2.4}$$

$$\frac{\partial(m\zeta)}{\partial t}+\frac{\partial\left(m_yH\int_0^1udz\right)}{\partial x}+\frac{\partial\left(m_xH\int_0^1vdz\right)}{\partial y}=0 \tag{2.5}$$

$$\rho=\rho\left(p,S,T\right) \tag{2.6}$$

$$\frac{\partial(mHS)}{\partial t}+\frac{\partial\left(m_yHuS\right)}{\partial x}+\frac{\partial\left(m_xHvS\right)}{\partial y}+\frac{\partial(mwS)}{\partial z}=\frac{\partial}{\partial z}\left(\frac{mA_b}{H}\frac{\partial S}{\partial z}\right)+Q_S \tag{2.7}$$

$$\frac{\partial(mHT)}{\partial t}+\frac{\partial\left(m_yHuT\right)}{\partial x}+\frac{\partial\left(m_xHvT\right)}{\partial y}+\frac{\partial(mwT)}{\partial z}=\frac{\partial}{\partial z}\left(\frac{mA_b}{H}\frac{\partial T}{\partial z}\right)+Q_T \tag{2.8}$$

where, $u$, $v$ are the horizontal velocity components in the curvilinear coordinates (m $s^{-1}$), $x$, $y$

are the orthogonal curvilinear coordinates in the horizontal direction (m), $z$ is the sigma coordinate (dimensionless), $t$ is time (s), $m_x$, $m_y$ are the square roots of the diagonal components of the metric tensor (m), $m$ is the Jacobian with $m = m_x m_y$ (m²), $p$ is the physical pressure in excess of the reference density hydrostatic pressure (m² s$^{-2}$), $\rho_o$ is the reference water density (kg m$^{-3}$), $b$ is the buoyancy, $f$ is the Coriolis parameter (s$^{-1}$), $A_v$ is the vertical turbulent viscosity (m² s$^{-1}$), $Q_u$ and $Q_v$ are the momentum source-sink terms, $Q_S$ and $Q_T$ are the source-sink terms for salinity and temperature respectively, $A_b$ is the vertical turbulent diffusivity (m² s$^{-1}$).

The Mellor-Yamada turbulent closure model connects the vertical turbulent viscosity, diffusivity with the turbulent intensity $q$, turbulent length scale $l$, and Richardson number $R_q$ by equations 2.9-2.11 (Hamrick 1992).

$$A_v = \phi_v q l = 0.4\left(1+36R_q\right)^{-1}\left(1+6R_q\right)\left(1+8R_q\right)ql \tag{2.9}$$

$$A_b = \phi_b q l = 0.5\left(1+36R_q\right)^{-1} ql \tag{2.10}$$

$$R_q = \frac{gH}{q^2}\frac{\partial b}{\partial z}\frac{l^2}{H^2} \tag{2.11}$$

where $\Phi_v$ and $\Phi_b$ are the stability viscosity coefficients, which account for reduced and enhanced vertical mixing or transport in stable and unstable vertically density stratified environments, respectively.

We simulated the oval-shaped Lake Arendsee (Figure 2.1). The computational domain, in the reference simulation, is comprised of a horizontal Cartesian grid of 1,766 cells with a grid size of 50 × 50 m (see Figure 2.1 for model grid and lake bathymetry). The vertical axis was divided into 59 layers at the deepest point using the sigma-z-coordinate grid system. This grid architecture is a new feature in EFDC and computationally more efficient than a similarly configured sigma-coordinate system (Craig et al. 2014). The sigma-z-coordinate system adjusts the number of vertical layers per horizontal grid cell according to the depth below this cell. If depth variations remain relatively small, however, the total number of vertical layers is kept constant and layer thickness is adjusted. In essence, the sigma-z-coordinate system is a combination of features from sigma grids and z-grids and provides an efficient way to balance vertical resolution, allowing the horizontal gradient error in sigma grids to be reduced. We used a relatively small vertical layer thickness of 0.5 m between 5 m and 15 m depth, i.e. at the depth region where the metalimnion can be expected to form during summer, a layer thickness of 2 m for the surface layer (i.e. between 0-2 m depth), and a vertical layer thickness of 1m elsewhere in the water column. The vertical grid was designed in this way to achieve a higher vertical resolution at the metalimnion in order to minimize numerical diffusion. This provides sufficient spatial discretization to investigate the dynamics of vertical density stratification and the corresponding gradients of vertical diffusivity. Total active wet cells amounted to 75021 cells. We further built a model with a grid size of 100 × 100 m to test the influence of the horizontal resolution of the model on the results. All parameters and the vertical configuration, in the new

model, were kept unchanged and this simulation was only used for comparison, not for the climate scenarios in the study.

### 2.3.3. Model setup and parameters

The simulation period covered the stratification period for the year 2013 and was performed from 4th April 2013 to 31st October 2013. The simulation was started on 4th April 2013, when the lake showed a homogeneous vertical temperature. The initial temperature was set to 2.51°C based on the observed value. The time step used for the model simulation was 30 seconds and the frequency of the simulation output was 1h.

Bathymetry data of the lake area with a vertical resolution of 1 m were provided by the State Agency for Flood Protection and Water Management, Saxony-Anhalt. Meteorological input data were obtained from meteorological stations at or close to the lake. Wind velocity and direction were taken from local measurements from a meteorological station located directly on the lake (Ultrasonic anemometer, EcoTech, Germany). The data for air pressure, rain, relative humidity, air temperature, solar radiation and cloud cover were obtained from the Seehausen station of the German Weather Service (DWD), about 15 km east of Lake Arendsee. All meteorological data were provided in hourly resolution.

Since the small annual inflow (water residence time > 50 years) has a negligible effect on the hydrodynamics, we excluded all inflows and outflows from our simulations. Seasonal water level fluctuations in Lake Arendsee remained within the order of a few decimeters. In order to keep the water balance of the lake constant, we excluded precipitation and evaporative loss of water in our model. However, heat loss through evaporation was included in the thermodynamic heat budget and, therefore, temperature effects from evaporation were fully accounted for.

Near the monitoring station at the deepest point of the lake, the seasonal dynamics of water temperature over the entire water body depth were measured using a thermistor logger chain containing 15 optodes (D-Opto Logger, Zebra-Tech, New Zealand). The thermistors were moored at 2.5, 5, 7.5, 10, 12.5, 15, 17.5, 20, 22.5, 25, 30, 35, 40, 45 and 48 m depths. The optodes measured temperature every hour between 28th March and 18th December, 2013. The nominal accuracy of the temperature measurements was ± 0.1K with a resolution of ± 0.01K and these measurements were used for the model calibration. The main hydrodynamic and temperature parameters used in the model are listed in Table 2.1 and were not calibrated but just set to values common in other EFDC applications.

Table 2.1. Summary of the main model parameters used in the simulations.

| Parameter | Values |
|---|---|
| Background horizontal eddy viscosity | $2.5 m^2 s^{-1}$ |
| Dimensionless horizontal momentum diffusivity | 0.1 |
| Background vertical eddy viscosity | $0.00001 m^2 s^{-1}$ |
| Background vertical molecular diffusivity | $0.0000001 m^2 s^{-1}$ |
| Solar radiation minimum fraction absorbed in the top layer | 0.6 |
| Background light extinction coefficient | $2 m^{-1}$ |
| Bed temperature | 4 ℃ |
| Bed thermal thickness | 0.1m |

### 2.3.4. Calculation of vertical turbulent diffusion coefficient $K_z$

To calculate vertical diffusion coefficients, the three-dimensional dynamic description of water temperature in a lake-averaged vertical distribution was achieved by averaging water temperature within each horizontal layer of the grid. The temporal evolution of this lake-wide vertical temperature gradient was the basis for calculating $K_z$ by following the gradient flux method by Heinz et al (1990), who calculated $K_z$ based on the following equation using temperature:

$$K_z(i,t) = \frac{\sum_{k=i}^{m} \frac{\Delta T_i}{\Delta t} * V_i}{\frac{\Delta T_{i-1}}{\Delta z_i} * A_i} \qquad (2.12)$$

where $K_{z,i}$ is the vertical turbulent diffusivity at the upper boundary of layer $i$, m refers to the deepest layer of the lake, $\frac{\Delta T_i}{\Delta t}$ is the temporal change (here: increase) in temperature, $\frac{\Delta T_{i-1}}{\Delta z}$ is the vertical gradient of temperature at the upper boundary of layer i, $\Delta T_{i-1}$ is the temperature difference between layer $i$-1 and $i$, $\Delta z_i$ is the layer thickness, $A_i$ is the area of the upper boundary and $V_i$ is the volume of the layer.

The model-derived $K_z$ was calculated based on equation 2.12 by using the simulated water temperatures. As an alternative way to calculate $K_z$, a conservative (i.e. non-reactive) tracer was included in the simulation, to further test the model capability of reproducing $K_z$ of the lake. The initial condition for the tracer vertical distribution was a linear gradient with 2 mg $l^{-1}$ at the surface and 99 mg $l^{-1}$ at the maximum depth of 49.5m. The formula to calculate $K_z$ by tracer concentrations then became:

$$K_z(i,t) = \frac{\sum_{k=i}^{m} \frac{\Delta C_i}{\Delta t} * V_k}{\frac{\Delta C_{i-1}}{\Delta z} * A_i} \qquad (2.13)$$

where $\frac{\Delta C_i}{\Delta t}$ and $\frac{\Delta C_{i-1}}{\Delta z}$ are the temporal change and vertical gradient of tracer concentration at layer $i$. Whenever vertical mixing conditions were intense, e.g. in early spring, vertical tracer gradients diminished quickly over time, making it impossible to calculate $K_z$. We therefore re-established the vertical tracer concentration every 30 days and the initial tracer distribution was re-established at the start of every calculation period, i.e. on Apr 4th, May 4th, Jun 3rd, Jul 3rd, Aug 2nd, Sep 1st, and Oct 1st. EFDC allows the definition of breakpoints, where all model states are conserved, the model stops and can be reactivated by a warm start. We used this breakpoint feature every 30 days in the simulation to freeze all model states, to re-establish the vertical tracer distribution, and to proceed with the simulation for another 30 days by warm-starting from the last breakpoint. This allowed a continuous simulation of hydro-and thermodynamics while tracer distribution was re-established every month. We calculated $K_z$ on a biweekly basis during the simulation period.

### 2.3.5. Model performance and uncertainty analysis

Simulated and measured water temperatures , for the same time at the same depth, were compared by calculating the root mean squared error (RMSE) according to equation 2.14 to determine model performance.

$$RMSE = \sqrt{\frac{\sum_{i=1}^{n}\left(T_{i,obs} - T_{i,sim}\right)^2}{n}} \qquad (2.14)$$

We then compared our model-based vertical diffusion coefficients $K_z$ in the metalimnion, calculated from simulated water temperatures based on equation 2.12, with corresponding vertical diffusion coefficients computed in an independent study by Kreling et al. (2017), who quantified $K_z$ at the depth of the metalimnion by using the measured water temperature according to the same equation above. Furthemore, we used the in-situ $K_z$ values computed from the thermistor data for a direct comparison with the model-based $K_z$ over the full depth range and stratification period. Notably, in this step the simulated $K_z$ was calculated based on different approaches (i.e. from simulated water temperatures as well as tracer concentration) and horizontal grid resolutions. We used multiple ways to calculcate model-derived vertical diffusivity in order to make our results robust against model specifications and in order to assess the uncertainty in estimated vertical diffusivity that would eventually arise from these specifications. The RMSE and values of $K_z$ were calculated in R Statistical Software (R Core Team 2016a).

### 2.3.6. Scenarios

We defined two scenarios for studying the effect of meteorological drivers on mixing conditions in the metalimnion. The scenarios concentrated on wind velocity and air temperature because both are highly influential for stratification dynamics and are expected to undergo

changes in the future. Note that only water temperature, rather than tracer substance, was included in the scenario simulations with respect to calculating $K_z$:

**Warming scenario:** Due to global warming, we expect average air temperatures to rise in a range between 1K and 4K by the end of the century (IPCC 2014). Although the effect of global warming on lake temperatures (O'Reilly and Sharma 2015a) and stratification (Kraemer et al. 2015) have been thoroughly documented, its effects on the metalimnion have never been analysed in detail. We therefore simulated a simplified warming scenario by increasing air temperatures in our simulation by 2K and analysed the mixing conditions at the thermocline.

**Wind scenario:** Future projections of wind velocity are uncertain. While the phenomenon of global wind stilling has been reported (Vautard et al. 2010), leading to globally declining wind velocities, other authors stress the increasing frequency of storm events (Easterling et al. 2000). Interannual variability in wind velocity is high at Lake Arendsee. For the 42 years from 1976 until 2017, for which continuous data are available from the Seehausen station, yearly averaged wind velocities varied from 2.4 to 4.1 m $s^{-1}$ and showed a coefficient of variation of about 10%. The average wind velocity in the simulated year 2013 was 3.51 m $s^{-1}$, which is relatively close to the overall mean wind velocity over the 42 year period (3.56 m s-$^{1}$). Given the uncertainties in global projections of wind velocities, we defined the wind scenarios based on the historical observations since 1976 and varied wind by +20% and -20% relative to the reference year 2013. This change in wind speed corresponds approximately to the 95% confidence interval of average wind conditions over the past 42 years.

## 2.4. Results

### 2.4.1. Model performance and validity

The temporal and spatial dynamics of water temperatures in Lake Arendsee were well captured by EFDC (Figure 2.2) and the overall RMSE was relatively low (0.78 K). Although absolute differences between simulated and observed temperatures remained low, a systematic difference was recorded in the deep hypolimnion (i.e. at 25m depth and below), where modelled temperatures were always higher than observations from July onwards and the difference reached 0.8 K at the end of October (Figure 2.2 & Figure 2.3). A high RMSE of 1.76 K was observed within the metalimnion, where internal wave activity at high frequencies led to relatively large temperature variations *in situ* at high frequencies (see Figure 2.3 at 7.5m depth). The deviations between observed and simulated water temperatures at this depth reached up to 5 K. However, such large deviations were the exception and the vast majority of simulated temperatures were close to the observations (Figure 2.4 & Figure S1 in Appendix 2): less than 2 ‰ of the simulated temperatures, for example, showed a deviation from observations of 5K or more and less than 5 ‰ showed a deviation of 4 K or rmore. In a plot of simulated versus observed temperatures , most values closely followed the 1:1 line and the overall $R^2$ of the respective linear regression was about 0.98 (Figure 2.4). Finally, important phenomenological aspects, such as the onset of stratification or the depth of the thermocline, were properly reproduced by the model (Figure 2.2).

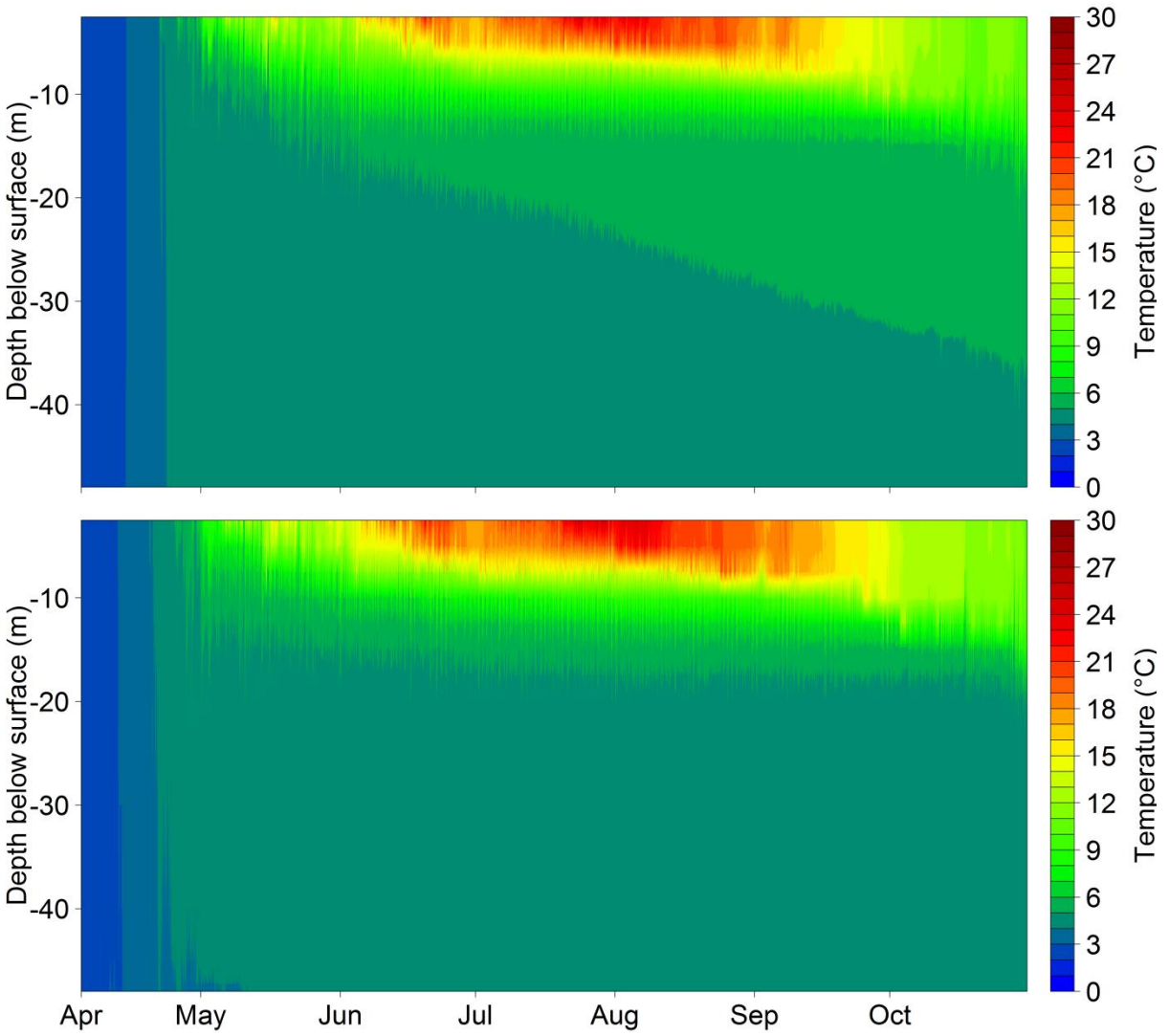


Figure 2.2. Contour plot of the simulated (above) and observed (below) water temperature in Lake Arendsee for the simulation period (04/2013-10/2013).

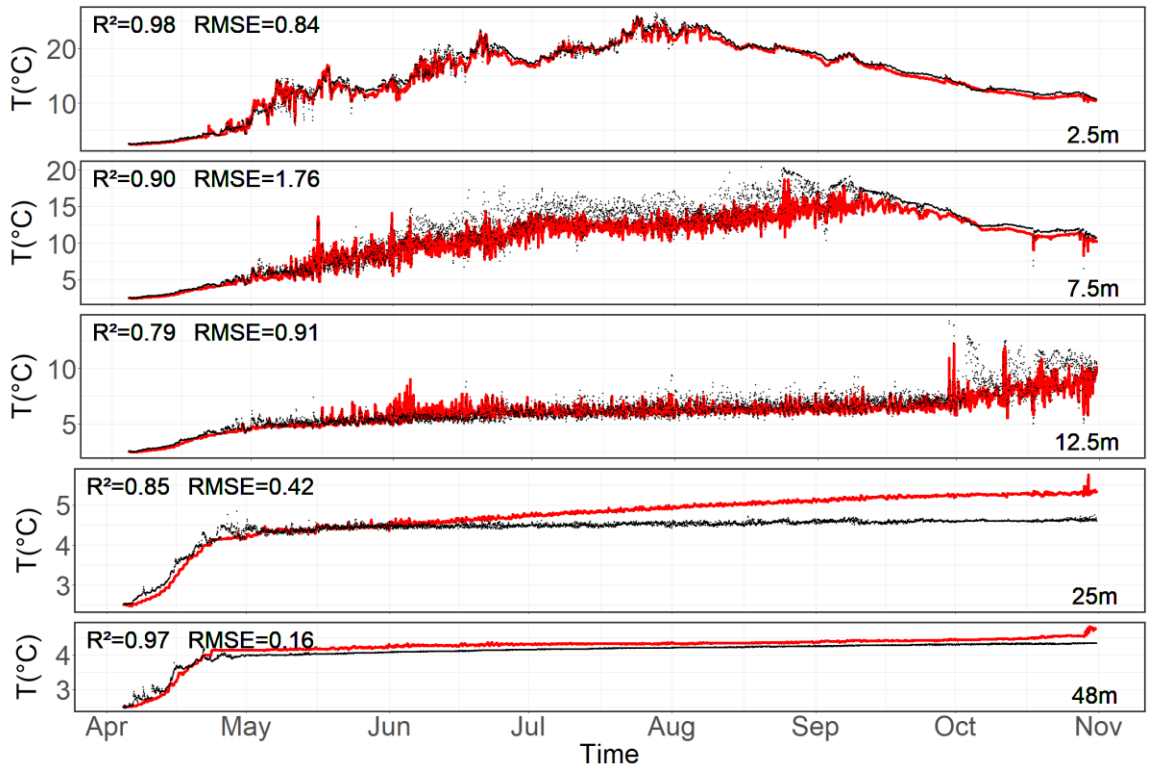


Figure 2.3. Simulated (red) versus observed (black) water temperatures in Lake Arendsee at different water depths (given at the right margin). The coefficient of determination and RMSE are given in the upper left corner for each depth.

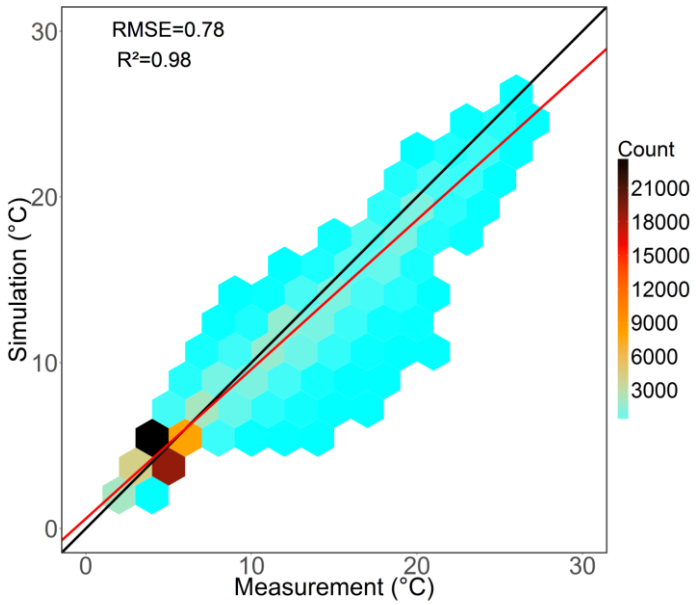


Figure 2.4. Comparison between simulated and measured water temperature for all depths (n=75615). The color bar depicts the amount of samples per hexagon. The black line has a slope of one and an intercept of zero (1:1 line). The red line shows the linear regression between the simulated and measured water temperatures in Lake Arendsee.

Comparing the model-based vertical diffusion coefficients $K_z$ with the values shown in Kreling et al. (2017), it turned out that the model reproduced the magnitude of $K_z$ in the metalimnion as well as the temporal trend of $K_z$ over the season (Figure 2.5). Both model-based and measurement-derived values of $K_z$ yielded minimal values below $1.25\times10^{-6}$ $m^2$ $s^{-1}$ in the middle of July and 5-10 times larger values in early summer. The agreement between the model-based and measurement-based vertical diffusion coefficient was particularly high in the four weeks from mid-June until mid-July, when vertical diffusion reached very low values. Before that period, i.e. before June, the simulation overestimated vertical diffusion coefficients by a factor of two. Moreover, modelled $K_z$ , calculated from water temperature as well as tracer concentration over the full depth range, followed $K_z$ profiles from measurements during midsummer (mid-July – end of August) but showed some overestimation in early summer and early September (Figure 2.6). Although the model predicted a minimum of $K_z$ within the metalimnion and the patterns appeared to be similar to field conditions, the quantitative values were systematically higher in the model during some periods and the depth of minimum $K_z$ was shallower during early autumn. Values of $K_z$ calculated on the basis of tracer and temperature were very close to each other (Figure 2.6), indicating that both methods resulted in similar estimates. Additionally, comparing results of the models with different horizontal resultions showed that grid size only marginally affected the simulated diffusivity and the vertical pattern of $K_z$ was not sensitive to the grid resolution (Figure S2 & S3 in Appendix 2).

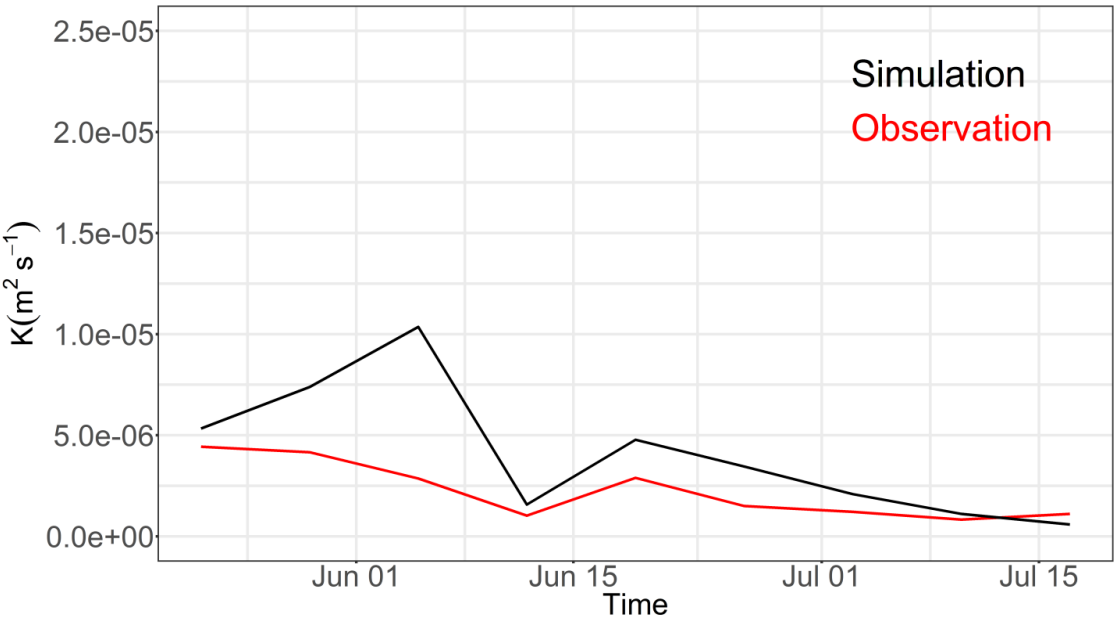


Figure 2.5. Dynamics of simulated (black) and observed (red) vertical diffusion coefficient ($K_z$) during summer 2013 in the metalimnion of Lake Arendsee (i.e. at the depth of the MOM, which is located at a depth of 8.2 m). Observed $K_z$ were taken from Kreling et al. (2017) and based on in situ temperature measurements.

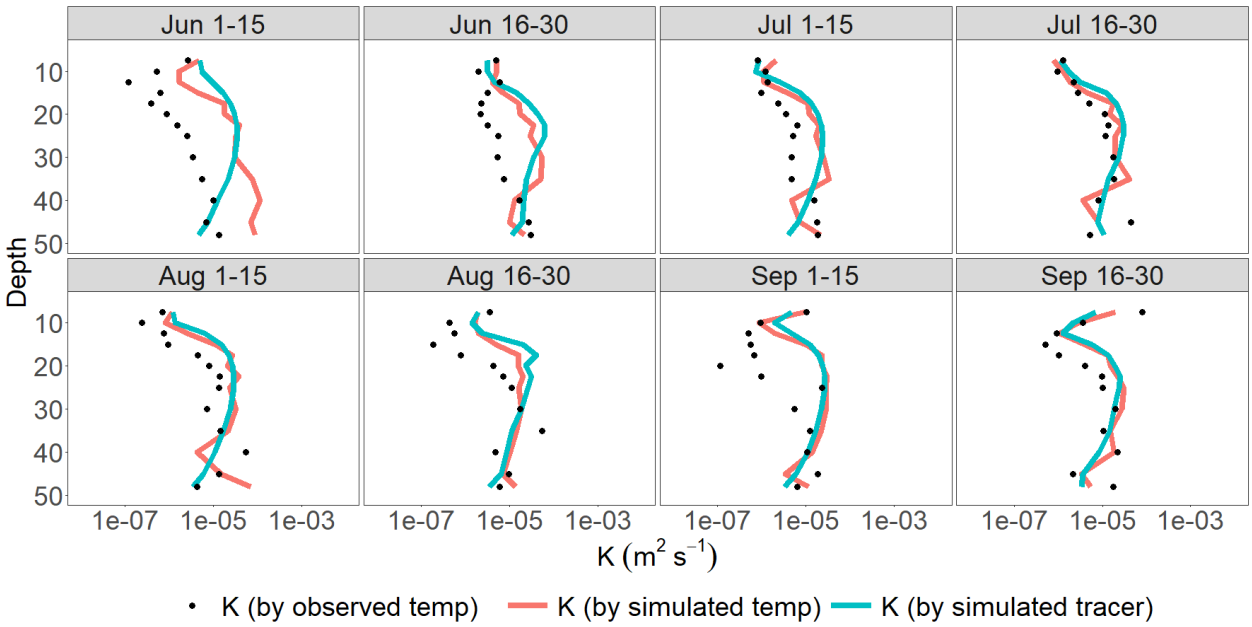


Figure 2.6. Comparison of simulated vertical diffusion coefficient $K_z$ (derived from water temperature and tracer concentration results from the reference simulation) with observed $K_z$ (calculated from observed water temperature dynamics) over biweekly intervals in Lake Arendsee.

### 2.4.2. Mixing conditions in the metalimnion

Observed and simulated vertical diffusion coefficients clearly indicated very low values within the metalimnion (Figure 2.6). The zone of low vertical exchange remained constrained over a narrow depth range that fully corresponded to the region with strong temperature gradients, and had a spatial extent of 2 to 4 meters. The minimum of $K_z$ occurred at depths between 8 and 10 m. In July, when wind velocities remained low and heating was high, the minima in vertical diffusion coefficients was most pronounced and reached values as low as $6\times10^{-7}$ m² $s^{-1}$ in our simulation. At depths 20m and deeper, vertical diffusion coefficients were more than one order of magnitude larger than those in the metalimnion. At most times, the vertical diffusion coefficients slightly decreased towards the lake bottom so that hypolimnetic vertical diffusion showed a slight peak between 20 and 30 m depths, reaching maximum values of up to $5\times10^{-5}$ $m^2$ $s^{-1}$.

Observed and simulated $K_z$ in the metalimnion showed a clear seasonal development with sharply decreasing values in May, when $K_z$ dropped from approximately $10^{-5}$ to $10^{-6}$ $m^2$ $s^{-1}$ (Figure 2.7). The low values of metalimnetic $K_z$ persisted until October (Figure 2.7). The location of the minimum $K_z$ along the vertical axis also remained rather constant during the period from July until September, at depths around 8 m and moving progressively deeper thereafter due to autumnal cooling in October (Figure 2.8).

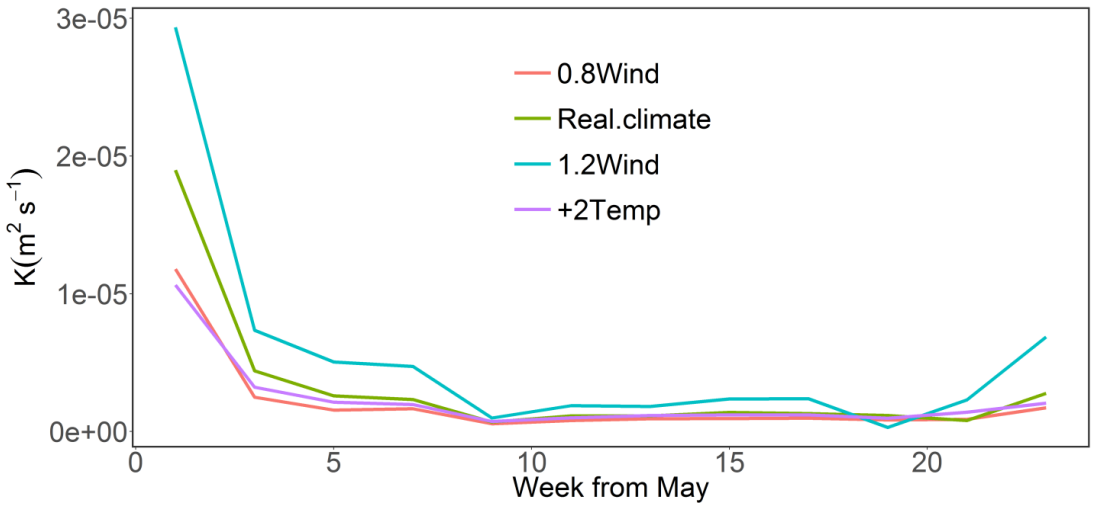


Figure 2.7. Absolute value of the minimum in vertical diffusion coefficient within the metalimnion of Lake Arendsee at different simulation scenarios with respect to wind velocity and air temperature during summer 2013.

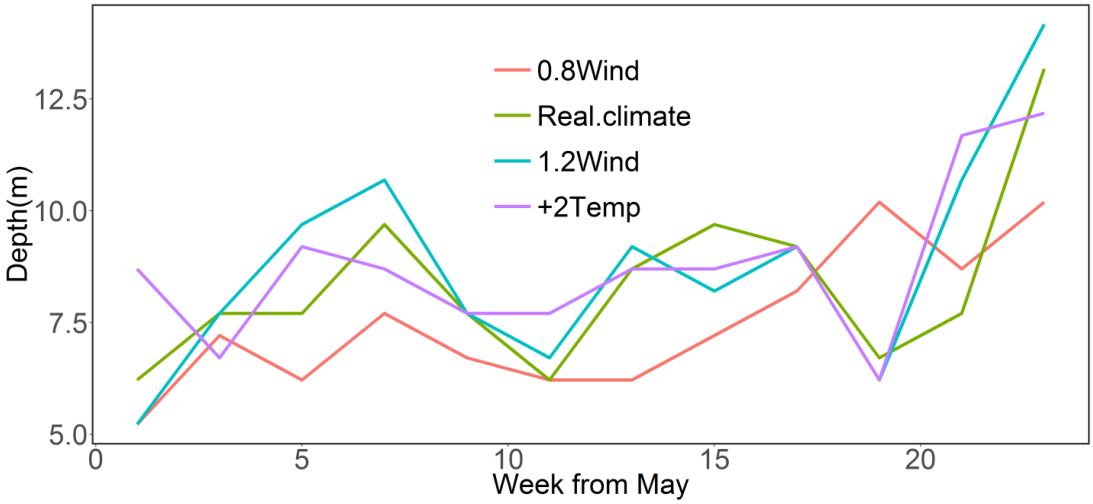


Figure 2.8. Depth of the metalimnetic minimum in vertical diffusion coefficient (as given in Figure 2.7) in Lake Arendsee at different simulation scenarios with respect to wind velocity and air temperature during summer 2013.

### 2.4.3. Effects from changing temperature and wind conditions

The application of changing meteorological conditions with respect to wind velocity (±20%) and air temperature (+2K) showed a high resistance of the metalimnetic zone, with low vertical exchange, against atmospheric forcing (Figure 2.9). This was particularly true for the period from July until September, when the metalimnetic vertical diffusion minimum was most pronounced. With respect to the minimal value of $K_z$ within the metalimnion, warming and wind stilling had only marginal effects but increasing wind velocities markedly increased its value (Figure 2.7). At these elevated wind velocities, the duration of periods with very low vertical diffusion in the metalimnion ($K_z$ below $5\times10^{-6}$ $m^2$ $s^{-1}$) was notably shorter (3 weeks) than in the

other scenarios. The depth of the minimal $K_z$ in the metalimnion, however, was more sensitive to wind stilling, while warming and wind intensification did not show marked effects (Figure 2.8). At reduced wind velocities, the zone of low vertical exchange was about 1 to 2 m shallower than in the other scenarios. In conclusion, wind velocity appeared more influential on metalimnion depth than air temperature. While increasing wind velocities mostly affected the minimum values of $K_z$ in the metalimnion and led to intensified vertical exchange, the reduction of wind velocity mostly affected the depth of minimal $K_z$ t not its absolute value.

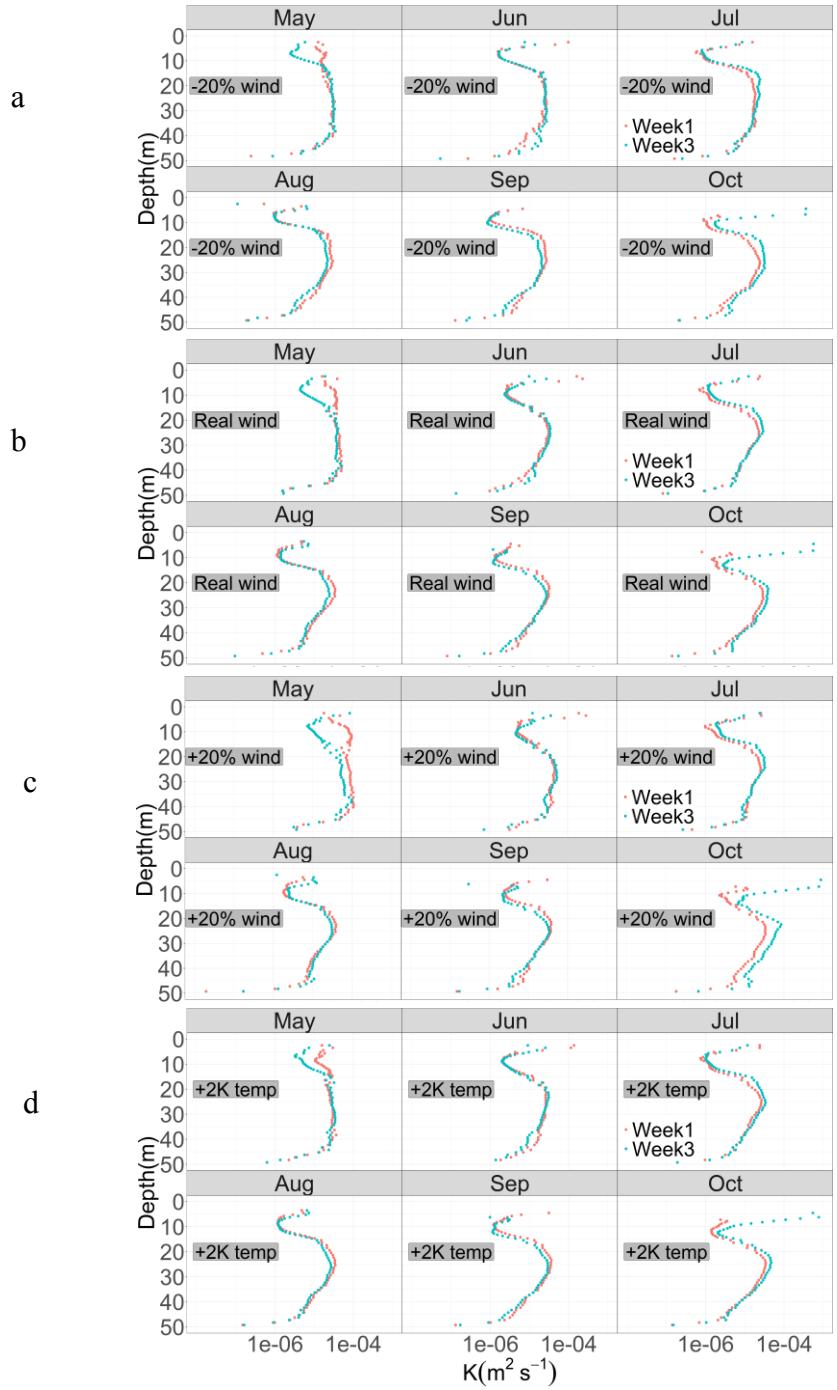


Figure 2.9. Vertical turbulent diffusivity ($K_z$) under different climate scenarios: (a) wind speed reduced by 20% , (b) real climate , (c) wind speed increased by 20% and (d) air temperature increased by 2 K. Values of $K_z$ were calculated on biweekly basis (two weeks per subplot).

## 2.5. Discussion

### 2.5.1. Evaluation of the modelling approach

We showed that the 3D model EFDC was able to simulate stratification dynamics in Lake Arendsee with high precision, resulting in an overall RMSE of only 0.78 K between modelled and observed water temperatures. The errors in our study were much lower than those presented in recent studies in which EFDC was applied (Bai et al. 2018,Zheng et al. 2018). The RMSE was different between layers and generally lower within the hypolimnion towards the lake bottom, which is related to lower temperature variations in this region (Figure 2.3). Increased discrepancies between the simulated and observed temperature profiles were only noticeable in the metaliminion, i.e. at 7.5 m, from June to September (Figure 2.3) when the lake was strongly stratified and high internal wave activity was observed. Usually, 3D models are capable of simulating the spatiotemporal dynamics of internal waves, but this holds mostly true for basin-scale internal waves (Bocaniov et al. 2014). The wave activity in the metalimnion of Lake Arendsee, however, showed higher frequency waves and EFDC is obviously not able to capture these high frequency phenomena. The model slightly overestimated temperatures in the hypoliminion, i.e. at depth 25m and 48m from July to October, indicating that vertical mixing in the model was higher than in reality. This turned out to be exactly the case because modelled vertical diffusion coefficients in the hypolimnion were larger than observed vertical diffusion coefficients (see Figure 2.6). Obviously, the model has difficulty in predicting vertical diffussion properly at the start of the stratification period, when temperature gradients are not as steep as later on. Our efforts to quantify *in situ* $K_z$ values, i.e. the installation and evaluation of high resolution measurements of water temperature dynamics, were beneficial to the modelling process because they allowed us to link emerging deviations between modelled and observed state variables to the underlying processes.

Our study contained three innovative points. Firstly, we evaluated our model results, not only by comparing measured and observed states (i.e. water temperature), but also by comparing results at the process level (i.e. vertical diffusion coefficients). This was a powerful approach in environmental modelling because deviations of the model outputs from observations could be attributed to specific processes. Secondly, we confirmed the ability of a 3D hydrodynamic model to realistically simulate the diffusion minima within the metalimnion, which was an important prerequisite for simulating biogeochemical gradients in the metalimnion (e.g. oxygen minima and nutrient gradients) correctly. Based on different approaches (i.e. from water temperature as well as tracer concentration), the simulated $K_z$ followed the same patterns and the model was able to reproduce the duration and vertical extent of the metalimnetic diffusion minimum in agreement with observations, although the absolute values of $K_z$ were sligthly overestimated in early summer and early autumn. Additionaly, the model showed robust performance in capturing the observed $K_z$ independent of the applied horizontal grid resolution (see Figure S2 & S3 in

Appendix 2). Thirdly, we analysed the sensitivity of the metalimnetic diffusion minimum to changing meteorological conditions. We found that wind speed had noticeable effects on vertical exchange within the metalimnion and formation of the metalimnetic diffusion minimum, while air temperature remained less influential. This is in line with the paper from Magee and Wu (2017), which analyzed the influence of climate changes on thermal dynamics in three lakes and found that, compared to air temperature, wind speed had a more significant effect on the stratification variables.

We used a vertical grid structure in our simulations that contained a higher resolution between 5 and 15 m depths, in order to better reproduce the conditions in the metalimnion. Vertical exchange in hydrodynamic models, i.e. the vertical discretization that is used to solve the underlying partial differential equations, is dependent on this vertical resolution. The larger the vertical layers become, the greater the contribution of numerical diffusion to the overall diffusion. This is a critical issue and one may ask whether the minimum $K_z$ within the thermocline is just a consequence of the finer grid structure at these depths. In order to rule out this concern, we repeated our simulations with a uniform grid where all layers between 2 and 50 meters had a thickness of 1 m (the top layer was kept at 2m thickness as before). It turned out that the uniform grid indeed produced slightly higher $K_z$ values in the metalimnion (see Figure S4 in Appendix 2) but the overall patterns of the vertical profiles of $K_z$ remained similar. Hence, we concluded that the contribution of finer vertical grid structures between 5 and 15m depths only marginally contributed to the low values in the metalimnion. In general, the vertical resolution chosen in hydrodynamic models is always influencing the effective diffusion between layers and modelers have to find a good compromise between model performance and computation time. In our case, the vertical resolution had no major effect on our results. Finally, we noted that the simulated $K_z$-values below the 20 m depth showed only little variation over time and the patterns seen in Figure 2.6 had a high self-similarity between different biweekly periods. This observation deserves further study but probably indicates that simulated $K_z$ in the hypolimnion are slightly but systematically overestimated and the calculation of mixing intensities in the hypolimnion by EFDC requires improvement.

### 2.5.2. Opportunities and limits of the 3D hydrodynamic model

Three-dimensional lake models are powerful tools in hydrodynamical studies because they can account for complex spatial currents and wave patterns such as internal waves, differential cooling and upwelling. It has been shown that 3D models can realistically simulate lake-wide flow dynamics at a high spatial and temporal resolution (e.g. Appt et al. 2004,Hodges et al. 2000b). This has enabled the systematic analyses of hydrodynamical effects from wind forcing (Valerio et al. 2012), the prediction of lake wide transport processes (Hillmer et al. 2008), and management-relevant water-quality dynamics to be addressed (Vilhena et al. 2010). In comparison to classic one-dimensional models, they can more realistically simulate mixing processes that involve three-dimensional dynamics. In a study by Bocaniov et al. (2014), for example, the diapycnical mixing during a large upwelling event in a deep reservoir could be

quantified. Although these features enable 3D models to account for mixing processes in a more mechanistic way, they have also been criticized for systematically overestimating mixing due to numerical diffusion (Hodges et al. 2000a), leading to the development of numerical procedures to minimize numerical diffusion (e.g. Laval et al. 2003). Since numerical diffusion is accumulating over time, 3D models are often assumed to not be applicable when simulation times are long. Our study, however, clearly demonstrates that simulations over several seasons with a 3D model can indeed reproduce temperature dynamics and mixing intensities close to reality. The simulated $K_z$ values in our study are mainly between $1.0\times10^{-6}$ and $1\times10^{-4}$ $m^2$ $s^{-1}$(see Figure 2.6), which is within the range calculated from observed water temperature in previous studies (Imboden et al. 1983,Saber et al. 2018,Wahl and Peeters 2014,Yang et al. 2015). However, a slight, but systematic, overestimation of hypolimnetic $K_z$ was also visible in our study, particularly at the start of the stratified season. Obviously, EFDC could be improved by finding ways to limit numerical diffusion effects in the hypolimnion. We also observed that simulated hypolimnetic $K_z$ peaked at depths between 20 and 30m and slightly decreased towards the lake bottom. Observed hypolimnetic $K_z$, however, showed a uniform depth profile. The dynamics of physical mixing at the sediment-water interface (Wüest and Lorke 2003), therefore, also require a more careful evaluation within EFDC.

The meteorological inputs to nearly all 3D model applications of lakes are very simplified in the sense that uniform fields of meteorological variables are applied. This seems to be a defendable assumption for temperature, radiation and humidity but in many cases not for wind, which can show quite heterogeneous spatial variations. Therefore, using homogenous wind fields to drive lake models will introduce uncertainties in the simulation results. In cases where wind fields are far from being uniform, the application of structured wind fields (Mao et al. 2016) or the simple IBL (Internal Boundary Layer) approach (Fenocchi and Sibilla 2016,Józsa 2014) could be of help. We know little about the wind fields over Lake Arendsee but, given the fact that the sorrounding landscape is flat and relatively unstructured, we believe that the application of uniform wind fields in our study is an acceptable assumption.

### 2.5.3. Limnological processes and lake ecosystem dynamics

The realistic simulation of vertical mixing is an important aspect in lake modelling because the vertical transport of nutrients or other pollutants from the sediment towards the upper water layers is a major component of internal loading. Upward transport of nutrients, for example, can drive eutrophication of lakes and reservoirs (Burger et al. 2008). Similarly, the vertical downward transport of oxygen is relevant for water quality in the hypolimnion, which is of high priority in water bodies used for drinking water supply (Bryant et al. 2011). EFDC appears to be suited for modeling these transport processes and can therefore provide a valuable tool for lake management when appropriate biogeochemical routines are included. Furthermore, since low metalimnetic turbulent diffusivity in Lake Ardensee has been shown to be a prerequisite for forming the metalimnetic oxygen minima (Kreling et al. 2017), further modelling studies should focus on the oxygen dynamics or other limnological features in the metalimnion (e.g. a deep chlorophyll maximum) and pay greater attention to a sound representation of vertical exchange

within the layer. An extension of our model system by including biogeochemical routines would definitely enable us to study these phenomena in a more quantitative way and to provide predictions for lake managers.

From a lake management perspective, simulating the vertical diffusion coefficient may also help in the design of infrastructure for lake water-quality management and restoration efforts. Hypolimnetic aeration by water transfer between epi- and hypolimnion (Tian et al. 2017) or by bubble plume diffusers (Gantzer et al. 2009) requires a quantitative estimate and solid planning for the necessary aeration intensities (Tian et al. 2017). Understanding the dynamics of vertical diffusion can provide guidance regarding the amount of aeration required and the layer of the lake to which the aeration should be applied. The model-based quantification of vertical diffusion could also help in exploring design options for the installation of hypolimnetic bubblers for thermal destratification (Moshfeghi et al. 2005).

From our point of view, the metalimnion is a partly neglected compartment in lake research. In a recent study, Giling et al. (2017b) pointed out that the interplay between physical drivers, chemical conditions and biological activity remained largely unresolved in this layer. The environmental conditions within the metalimnion with respect to light, temperature, or nutrients can vary from lake to lake and even within a given lake these variables change strongly within space and time and, hence, can induce complex local patterns and dynamics such as deep chlorophyll maxima (Leach et al. 2018), oxygen maxima (Wilkinson et al. 2015) or oxygen minima (Kreling et al. 2017). Apart from the case-study level, generalized model-based predictions of biogeochemical activity in the metalimnion are therefore difficult to achieve. However, a special feature of the metalimnion is the very low vertical mixing intensity, making it a highly separated compartment with minimal interactions with the epilimnion above or the hypolimnion below. An important prerequisite for a thorough analysis and reliable prediction of ecological or biogeochemical activity in the metalimnion is, therefore, a sound representation of the physical conditions within this layer. Our study provides evidence that 3D models are able to capture the physical conditions in the metalimnion with reasonable precision and therefore provide a fundament for a more systematic understanding of the ecological dynamics within this fascinating lake compartment.

## 2.6. Conclusion

In this study, we comprehensively evaluated the performance of a well-established 3D hydrodynamic model (EFDC) in capturing the stratification and mixing dynamics of Lake Arendsee. In parallel to the model simulations, we established high frequency monitoring of stratification dynamics that enabled us to compute vertical turbulent diffusion coefficients ($K_z$) from in-situ measurements. The results showed that our model can not only accurately reproduce water temperatures, but can also realistically simulate vertical gradients of $K_z$ within the lake. Moreover, the model predictions regarding the duration and vertical extent of the metalimnetic diffusion minimum were robust with respect to model grid resolution and calculation of $K_z$ (from numerical tracer distribution or from simulated water temperature). Through a scenario analysis

we further illustrated the influence of changing meteorological conditions on the metalimnetic diffusion minimum. Wind speed was shown to be a more influential factor for the spatio-temporal development of the diffusion minimum than air temperature. While increasing wind velocities mostly affected the minimum values of $K_z$ in the metalimnion, wind stilling mostly affected the depth of minimal $K_z$ but not its absolute value. Since low metalimnetic turbulent diffusivity is a prerequisite for the formation of oxygen minima and chlorophyll maxima in the layer, it is recommended that further modelling studies take such biological processes into account in order to obtain a full perspective on the topic.

# 3. Stratification dynamics in a reservoir under different wind conditions

## 3.1. Abstract

Stratification dynamics in reservoirs have a great impact on ecosystem functioning and biogeochemical cycling, and can be strongly influenced by wind events. In this study, a well-established one-dimensional hydrodynamic model (GLM) was used to investigate the response of stratification dynamics in Rappbode Reservoir to different wind conditions, in particular to episodic strong wind events. In years with increased wind speed, stratification duration and intensity were reduced. Episodic wind forcing by strong wind events are important determinants of thermal structure and can induce persisting shifts in the thermal structure that remain over the season until the next overturn. The results showed that reductions in stratification intensity were particularly distinct when the strong wind occurred in early summer. Strong wind events outside of this sensitive time window did not exert an important impact on the thermal dynamics of the reservoir. Our research confirms the decisive impact of wind speed on stratification of lakes and reservoirs. It effectively illustrates the sensitive time window of thermal dynamics to episodic wind events.

## 3.2. Introduction

Stratification is a well-studied key property of standing waters (Boehrer and Schultze 2008). In stratified lakes, the density gradient along the vertical axis gives rise to a series of ecologically relevant biogeochemical gradients like oxygen, nutrients or dissolved metals (Boehrer and Schultze 2008). Therefore, stratification has a great impact on the biogeochemical cycling in lakes and reservoirs (Bueche et al. 2017,Pöschke et al. 2015,Schwefel et al. 2016,Zhang et al. 2015). For example, prolonged stratification will lead to increasing anoxia in lake bottom waters (Foley et al. 2012). Stratification onset is also a key event for planktonic organisms, namely phytoplankton: Stratification limits vertical mixing and the epilimnion offers high average light intensity that alleviates light limitation for algae (Sommer et al. 1986). In deep lakes, the onset of algal spring mass development therefore relies largely on thermal stratification. Additionally, intense vertical stratification, i.e., very steep density gradients that usually emerge when surface temperatures get very hot, can foster the growth and dominance of harmful cyanobacteria (Cao et al. 2016,Paerl and Huisman 2009). Therefore, given the significance of stratification for aquatic ecosystems, it is not surprising that numerous investigations have focused on the dynamics of thermal structure and its influencing factors. One-dimensional hydrodynamic models play an important role in this line of research because they can integrate the different meteorological and hydrological factors and provide quantitative predictions (Fang and Stefan 1999,Frassl et al.

2014,Kerimoglu and Rinke 2013,Snortheim et al. 2017).

Climate change has been shown to exert a strong influence on thermal dynamics of waters worldwide (Fink et al. 2014a,Jansen 2017,O'Reilly and Sharma 2015b,Piccolroaz et al. 2018,Piccolroaz et al. 2015,Wood et al. 2016). Kraemer et al. (2015) used a 1D hydrodynamic model to investigate the impacts of atmospheric warming on the thermal structure of Lake Geneva. The increasing air temperature was found to decrease the duration of complete mixing during winter. Fang and Stefan (1999) reported that an increasing stratification intensity of lakes can be expected under a doubled atmospheric $CO_2$ concentration. Sahoo et al. (2015) predicted an increase in stratification duration of Lake Tahoe as a result of climate warming. However, when evaluating the response of thermal dynamics to climate change, most studies focused on the effect of global warming and little attention has been paid to the influence of other meteorological factors, e.g. changing wind speed. Widespread reductions in wind speed have been observed over the past decades, a trend that is expected to continue in the future (McVicar and Roderick 2010,Read et al. 2011,Roderick et al. 2007). The decrease in wind speed has been associated with changes in surface processes, e.g., an increase in ground roughness and a decrease in sensible heat fluxes (McVicar and Roderick 2010,Roderick et al. 2007,Vautard et al. 2010,You et al. 2010). This phenomenon of reduced wind speeds, known as atmospheric stilling or wind stilling, may play a vital role in stratification dynamics. At the same time, increasing frequencies of storm events are reported (Bromirski et al. 2003,Easterling et al. 2000) that are likely to have profound effects on lakes (Jennings et al. 2012,Rinke et al. 2009). In summary, wind is an important aspect of climatic effects on lakes and appears to be understudied in comparison to the effects from temperature.

Butcher et al. (2015) applied a 1D hydrodynamic model to elucidate the responses of lake stratification structures to climate change and suggested that wind is an important influencing factor for the strength of stratification in deep lakes. Valerio et al. (2015) investigated the response of the thermal dynamics of Lake Iseo to climatic variations and concluded that wind changes will exert strong effects on deep mixing within the hypolimnion. Edlund et al. (2017) reported an increase in thermocline depth due to the stronger wind in eight wilderness lakes in USA. However, the response of stratification to variations in wind speed is still not completely understood and not yet sufficiently quantified. There are basically two different approaches in analysing wind effects: some studies applied global increases or decreases to wind velocity by simple linear factors and others focused more on the importance and scale of single events. A modelling study by Austin et al. (2011) just increased and decreased measured time series of wind velocity by ± 10% or 20% and found systematic effects on stratification phenology and heat fluxes. The study by Churchill and Kerfoot (2007), who made detailed measurements on heat flux and stratification in Portage Lake, pointed to the importance of short storm events. Our study was designed to combine both approaches, we studied the effects of global increases and decreases in wind speed and also specifically analysed the importance of wind events.

In addition, previous studies have shown that sudden changes in wind speed in a specific (i.e., sensitive) period can result in an abrupt variation of thermal structure. Jennings et al. (2012) analysed high-frequency water temperature data from a monitoring station on Lake Leane and

found a sharp increase in thermocline depth following episodic strong wind events during early summer. Read et al. (2011) reported the sudden reduction of water column stability in Lake Annie during a tropical storm in mid-August. We therefore hypothesize that short-term extreme wind events can exert a significant influence on stratification dynamics. Considering the ecological consequences of sudden variations in thermal structure (Jennings et al. 2012), there is a need for a comprehensive understanding of the impact of episodic strong wind events on the physical dynamics within stratified lakes and reservoirs.

In this study, we used the Rappbode Reservoir as a test site to investigate the impact of wind speed on the stratification. The reservoir is the largest drinking water reservoir in Germany, it supplies drinking water for more than 1 million people. Previous studies documented the importance of wind for the hydrodynamics within the reservoir (Bocaniov et al. 2014). The aim of our study is to evaluate the sensitivity of stratification in the reservoir to changing wind speed by using a well-established one-dimensional hydrodynamic model. A particular aspect of our study is to assess the response of thermal dynamics to typical short-term strong wind events in order to identify the most sensitive time windows. Admittedly, 1D models may be insufficient to fully describe the 3D processes like internal waves(Bocaniov et al. 2014). An application of a 3D model would overcome these limitations but would be computationally very demanding without leading to different conclusions in the systematic scenarios we are studying.

## 3.3. Methods

### 3.3.1. Study site

Rappbode Reservoir is located in the eastern Harz Mountains, supplying drinking water to more than 1 million people in central eastern Germany (Figure 3.1, Rinke et al. 2013). It is the largest drinking water reservoir in Germany with a maximum volume of $1.13\times10^8$ $m^3$, a catchment area of 274.0 $km^2$, a mean depth of 28.6 m and a maximum depth of 89.0 m. Rappbode Reservoir is located in a valley and wind sheltering and channeling due to the surrounding hills can be observed. For a more detailed description of the orography refer to Rinke et al. (2013a). The reservoir is the main water body of the Rappbode Reservoir System, a network of 6 water bodies used for flood protection, environmental flows, and drinking water supply (for more details refer to Rinke et al. 2013). It receives water from three smaller upstream reservoirs (Königshütte Reservoir, Hassel and Rappbode Pre-dams) and drains into Wendefurth Reservoir. The Rappbode Reservoir is a typical dimictic water body with mixing in spring and autumn. The reservoir experiences strong stratification in summer and weak stratification in winter with ice cover in some years.

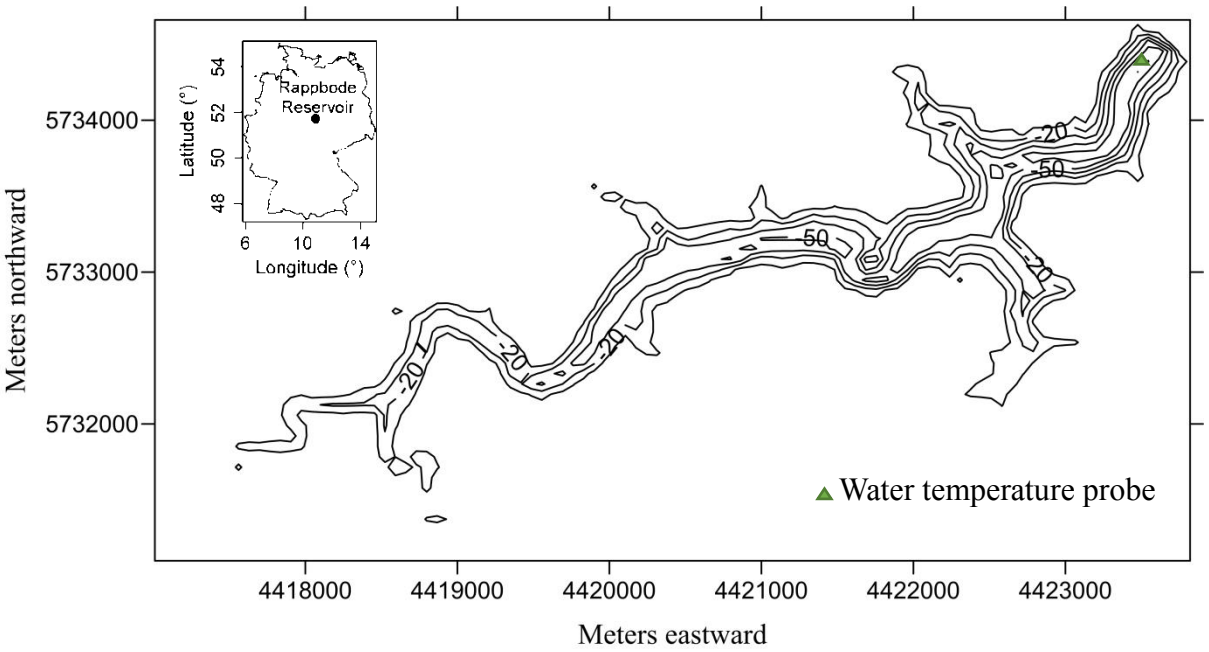

Figure 3.1. The location and contour map of Rappbode Reservoir.

### 3.3.2. Numerical model

The General Lake Model (GLM) version 2.2.0 is a 1D hydrodynamic model developed by the Aquatic EcoDynamics Research group at the University of Western Australia ( Hipsey et al. 2014; Read et al. 2014). It simulates the variations of thermal structures and takes the influence of inflows/outflows, surface energy fluxes and ice cover into account. The code of GLM is open source and freely available.

GLM uses a Lagrangian layer structure, i.e., thickness and volume of each layer change dynamically during the runtime of the model. Minimum and maximum layer thickness can be adjusted by the user. Each layer has homogenous physical properties (Read et al. 2014). The heat budget in GLM consists of shortwave and longwave radiation as well as sensible and evaporative heat fluxes. For more information about the underlying model equations and hydrodynamic closures refer to Hipsey et al. (2014).

### 3.3.3. Model setup and input data

The forcing for running the model includes time-series of meteorological variables, hydrological data on inflows and outflows as well as the morphometric information given as surface area at different water depth (hypsometric curve). The latter was obtained from the reservoir authority (Talsperrenbetrieb Sachsen-Anhalt).

The following meteorological variables were obtained from a water quality monitoring buoy in the central basin of Rappbode Reservoir (see Rinke et al. 2013 and http://www.ufz.de/index.php?de=39919): air temperature, wind speed, shortwave radiation and

relative humidity. Measurements were conducted at high-frequency (every 10 minutes) and subsequently averaged to hourly values. Data gaps were filled with meteorological data either measured at a nearby meteorological station at the Rappbode Pre-dam (see Rinke et al. 2013) or only shortwave radiation from a meteorological station in Harzgerode, which is operated by the German Weather Service, approximately 15 km away from Rappbode Reservoir. Cloud cover data were provided by the Harzgerode station because no cloud cover detection was realized on the buoy. Comparisons of meteorological data between the stations Harzgerode and Rappbode Reservoir showed that values from both stations are highly correlated and there is a relatively low bias between both time series (Table 3.1). Among the different meteorological variables, wind speed showed the largest deviations between the two stations because it is strongly influenced by local orographic features. A graphical comparison of both meteorological stations for the relevant meteorological variables is given in the Supporting Information (see Figure S1 in Appendix 3). Since the replacement of missing values by measurements from Harzgerode was only done for solar radiation and not necessary for the other variables, the consequences from using data from Harzgerode for filling these gaps should be negligible. From these cloud cover data as well as air temperature, incident longwave radiation was computed based on the formula given by Henderson-Sellers (1986).

Table 3.1. Comparison between the measured climate data in 2015 from the weather station at Harzgerode (DWD) and from the buoy on Rappbode Reservoir

| Climate Variables | Mean DWD | Mean Buoy | Bias | r |
|---|---|---|---|---|
| Air Temperature (˚C) | 8.65 | 8.51 | 0.14 | 0.98 |
| Shortwave Radiation (W $m^{-2}$) | 201.85 | 209.98 | -8.13 | 0.80 |
| Wind Speed (m $s^{-1}$) | 3.71 | 3.19 | 0.52 | 0.72 |
| Relative Humidity (%) | 80.44 | 79.02 | 1.42 | 0.86 |

Hydrological data, i.e. daily aggregated inflow and outflow discharges, were provided by the reservoir authority. Inflow salinity and water temperature were available from a YSI-6200 probe (Yellow Springs, USA) deployed in the tributaries of the reservoir. These hydrological data were put into the GLM with a daily resolution.

The model was run and calibrated by using data from Jan 2$^{nd}$ to Dec 30$^{th}$ in the year 2015. The time step for the simulation output was one hour in order to be consistent with the hourly meteorological data. The initial conditions for water temperature and salinity were derived from a vertical profile measured with a Hydrolab DS5 probe (OTT Hydromet, Kempten, Germany) at the start of the year.

### 3.3.4. Model calibration

High-resolution CTD measurements, taken with a Hydrolab DS5 probe, were used to evaluate the performance of the model. The water temperature was observed every week and its measured interval was averaged to 0.3 m from the surface to the bottom of the reservoir. It was our intention to leave the internal mixing parameters of GLM unchanged as they are physically or empirically derived and transferable between different lakes (Bruce et al. 2018,Fenocchi et al. 2017,Read et al. 2014). We therefore restricted the calibration of GLM to the following three lake-specific parameters: wind factor (correcting the wind speed by a constant factor, see study site description above with respect to wind sheltering effects), light attenuation coefficient ($K_w$) and vertical turbulent mixing coefficient in the hypolimnion ($C_{HYP}$). All other parameters are considered to be lake independent as in the study of Weber et al. (2017) and should remain unchanged unless detailed empirical evidence for required parameter changes is available. The root-mean-square-error (RMSE) of water temperature was applied to assess the model performance:

$$\mathrm{RMSE}=\sqrt{\frac{1}{n}\sum_{i=1}^{n}e_i^2} \qquad (3.1)$$

where $e_i$ is the difference between observed and simulated water temperature and $n$ is the number of observations. We chose the RMSE as the model fit criteria because it is a standard indicator for model errors, used in many lake modeling studies (Schwefel et al. 2016,Weber et al. 2017).

### 3.3.5. Wind scenarios

*Scenario S1: Stratification phenology in 2015 at different wind conditions*

In order to show the effect of a different wind speed on the stratification in Rappbode Reservoir, we used the reference simulation of 2015 and compared the stratification phenology with simulations having wind speed increased by 10% and 20%.

*Scenario S2: Sensitivity to wind speed under averaged meteorological conditions*

In the local climate of Rappbode Reservoir, all meteorological variables except the cloud cover follow a specific seasonal pattern (see Figure S2 in Appendix 3). Each individual year, however, has characteristic periods of cold/warm, windy/calm, wet/dry, etc. weather conditions making each year different from the others. These characteristic stochastic fluctuations of meteorological variables (i.e. weather) around the average seasonal pattern (i.e. climate) in a given year complicate the interpretation of model outcomes derived from a single year. In order to make the model outcome independent from a specific year, we calculated hourly averaged climatological conditions for all required meteorological variables based on long-term data of meteorological observations as outlined in Table 3.2 (see Figure S2 in Appendix 3). Note that for the calculation of average climatological conditions no measurements from the reservoir could be used because these time-series were too short. We therefore applied long-term meteorological conditions at nearby stations for the scenario simulations. This may include some minor differences in local meteorological conditions (compare Table 3.1) but such differences are unproblematic in a scenario-based approach where only relative differences between different scenarios are interpreted. These averaged climatological conditions, defined as the 50% quantile,

represents the present, average climatic conditions in the region of Rappbode Reservoir. As inspired by a study by Persson and Jones (2008), we used the averaged meteorology as a reference scenario and compared model results with simulations using the 20%, 40%, 60%, 80%, and 100% quantile of wind speed. Note that all other meteorological variables were left unchanged at the 50% quantile, i.e., at the median values. Additionally, input data for inflow and outflows were kept the same as those in 2015. These quantile-based wind scenarios have a very artificial character in the sense that they have a strongly dampened annual cycle without any disturbing wind events. This artificial setting is helpful, however, to systematically analyse the effect of wind speed on stratification independent of short-term events.

Table 3.2. Summary of data for meteorological drivers

| Meteorological Drivers | Time Range | Data Source(Name of the Weather Station) | Location |
|---|---|---|---|
| Wind Speed | 1981-2015 | Harzgerode | 51.65° N, 11.14° E |
| Air Temperature | 1981-2015 | Harzgerode | 51.65° N, 11.14° E |
| Relative Humidity | 1991-2015 | Harzgerode | 51.65° N, 11.14° E |
| Cloud | 2008-2015 | Harzgerode | 51.65° N, 11.14° E |
| Precipitation | 1995-2015 | Harzgerode | 51.65° N, 11.14° E |
| Shortwave Radiation | 1981-2015 | Halle | 51.51° N, 11.95° E |

*Scenario S3: Effects of short-term wind events on stratification*

This scenario focuses on the effects of short-lasting strong wind events on stratification. A typical strong wind event in Rappbode Reservoir has a duration of 1-2 days and reaches daily averaged values up to 10 m $s^{-1}$ representing the 95% quantile of all wind speed recordings at Harzgerode station (see Table 3.2).

As a starting point we used the averaged meteorological conditions (see scenario S2) over the course of one year. We then created a series of simulations having a strong wind event (10 m $s^{-1}$ for 2 days, see above) progressing over the whole year, i.e., the first simulation has the strong wind event on day 1-2, the second simulation from day 3-4, the third simulation from day 5-6, and so on. We completed this simulation series from the beginning to the end of one year.

*Scenario S4: Effects of short-term wind events on stratification (seasonally varying)*

The scenario S4 is basically the same as S3 but the wind speed applied in the wind event was not set to 10 m $s^{-1}$ but to the maximum observed wind velocity at the respective day of the year (100% quantile in Figure 3.2). In this way, the wind velocity of the wind event becomes seasonally varying with approximately 25% lower wind speeds in summer compared to winter. The motivation to create the scenario S4 came from the fact that a 2-day lasting wind with 10 m $s^{-1}$, as applied in S3, is an extremely powerful event. The additional scenario S4 is therefore

closer to the real local conditions at Rappbode Reservoir, while the scenario S3 may represents a strong wind event as it can be observed at other places in central Europe. We ran this scenario two times, in a first run we applied a wind event lasting over two days and in a second run we let the wind event to last only over 1 day.

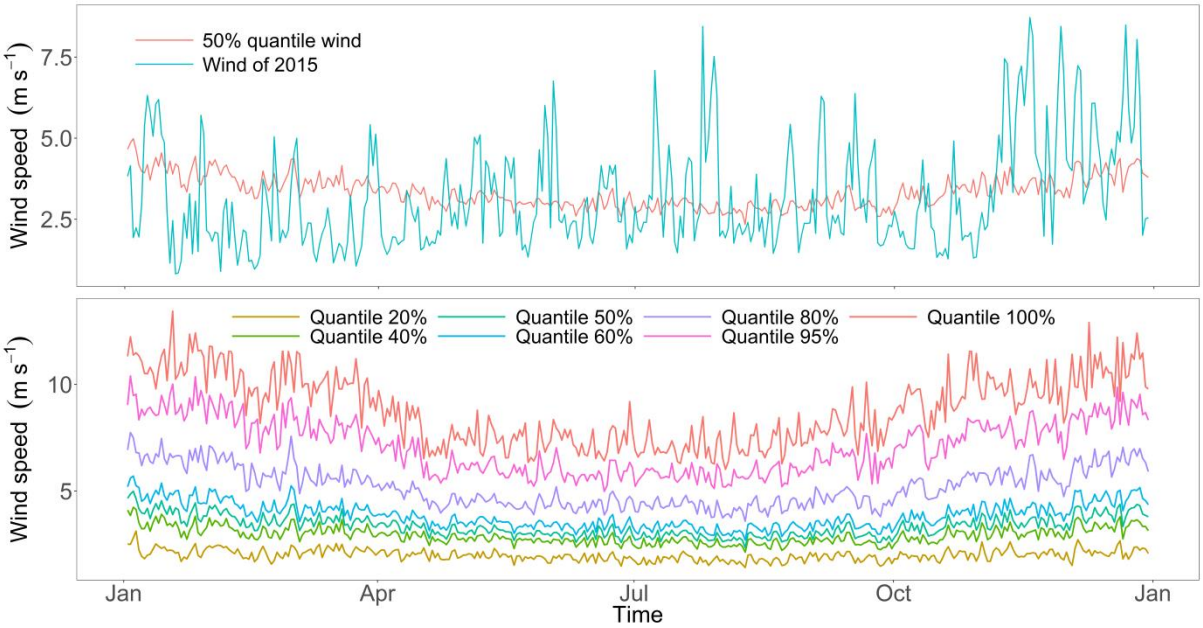


Figure 3.2. Comparison between daily median wind speed (calculated from 35 years of measurements) and daily averaged wind speed of 2015 (upper panel); long-term annual pattern of wind speed at Harzgerode station (lower panel).

### 3.3.6. Evaluation of simulations

We calculated five indices to evaluate the strength and duration of stratification in the different scenarios: Schmidt stability, open water stratification ratio, onset of stratification, 10 °C isotherm depth and hypolimnion temperature. These five indices were frequently used in related research (Butcher et al. 2015,Fang and Stefan 2009,Kraemer et al. 2015,Schwefel et al. 2016,Valerio et al. 2015). The Schmidt stability, reflecting the difference in potential energy between a stratified lake and the same lake at hypothetically mixed conditions (Boehrer et al. 2014,Boehrer and Schultze 2009b,Idso 1973,Schmidt 1928), was defined as:

$$S = \frac{g}{A_0} \int_0^{z_{max}} (z - z_*)(\rho_z - \rho_*) A_z dz \qquad (3.2)$$

where $g$ is the gravitational acceleration, $A_0$ the surface area, $\rho_z$ and $A_z$ are the water density and area at depth $z$, $z_*$ and $\rho_*$ are the center depth of the volume and its corresponding density.

The open water stratification ratio is defined as the fraction of simulation time in which the temperature difference between the top and bottom layer of the water is greater than 1 K (Fang

and Stefan 2009). We used this ratio to evaluate the duration of stratification. The first time when the temperature difference between surface and bottom is larger than 1 K was defined as stratification onset. The hypolimnion temperature was calculated as the volume-weighted average water temperature in the hypolimnion. To define the hypolimnetic water body, we used the function "meta.depth()" from the R package "rLakeAnalyzer" ( R Development Core Team 2016; Winslow et al. 2017). This function first defines the thermocline as the depth of the maximum density gradient found in the profile. An upper and lower end of the metalimnion was then derived by assuming a critical threshold in the density gradient of 0.1 kg $m^{-4}$, i.e., the value of the metalimnion depth is defined as the range around the thermocline where the density gradient is steeper than this threshold. Accordingly, the hypolimnion is then defined as the water masses between the lower end of the metalimnion and the lake bottom.

The R packages "glmtools" and "rLakeAnalyzer" were used for calculating the stratification indices mentioned above. Furthermore, these two packages were also applied for pre- and post-processing of the model simulations.

## 3.4. Results

### 3.4.1. Calibration results

After the calibration of water temperature for the year 2015, the parameter values for wind factor, light attenuation coefficient ($K_w$) and vertical turbulent mixing coefficient in the hypolimnion ($C_{HYP}$), respectively, were identified as 0.92, 0.87 $m^{-1}$ and $5\times10^{-6}$ $m^2$ $s^{-1}$. The values of these calibrated parameters are in a reasonable range for the local conditions in Rappbode Reservoir. Modelled water temperatures were in good agreement with measurements. The simulated mean water temperature was 6.33 °C for all measured depths, which is close to the observed temperature of 6.62 °C. The RMSE of vertical temperature profiles was 0.89 and the $R^2$ was 0.97 (n = 19081, see Figure 3.3). The RMSE in our study was in the range of that in other recent studies using GLM (Bueche et al. 2017,Fenocchi et al. 2017,Weber et al. 2017). The simulated hypolimnetic temperature at 50 m depth was slightly lower than the measured value. The modeled surface and metalimnion water temperature showed an excellent agreement with the observed data (Figure 3.4). In general, the calibrated model successfully reproduced the stratification phenology of the reservoir.

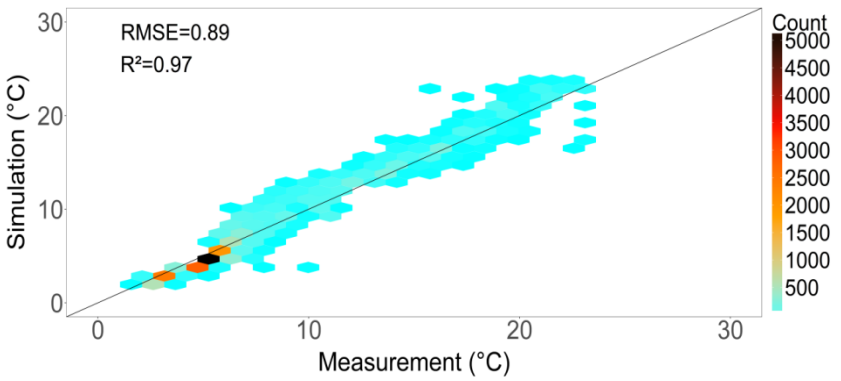


Figure 3.3. Comparison between simulated and measured water temperature for all depths (n = 19081). The color bar depicts the amount of samples per hexagon. The 1:1 line has a slope of one and an intercept of zero, indicating a perfect fit.

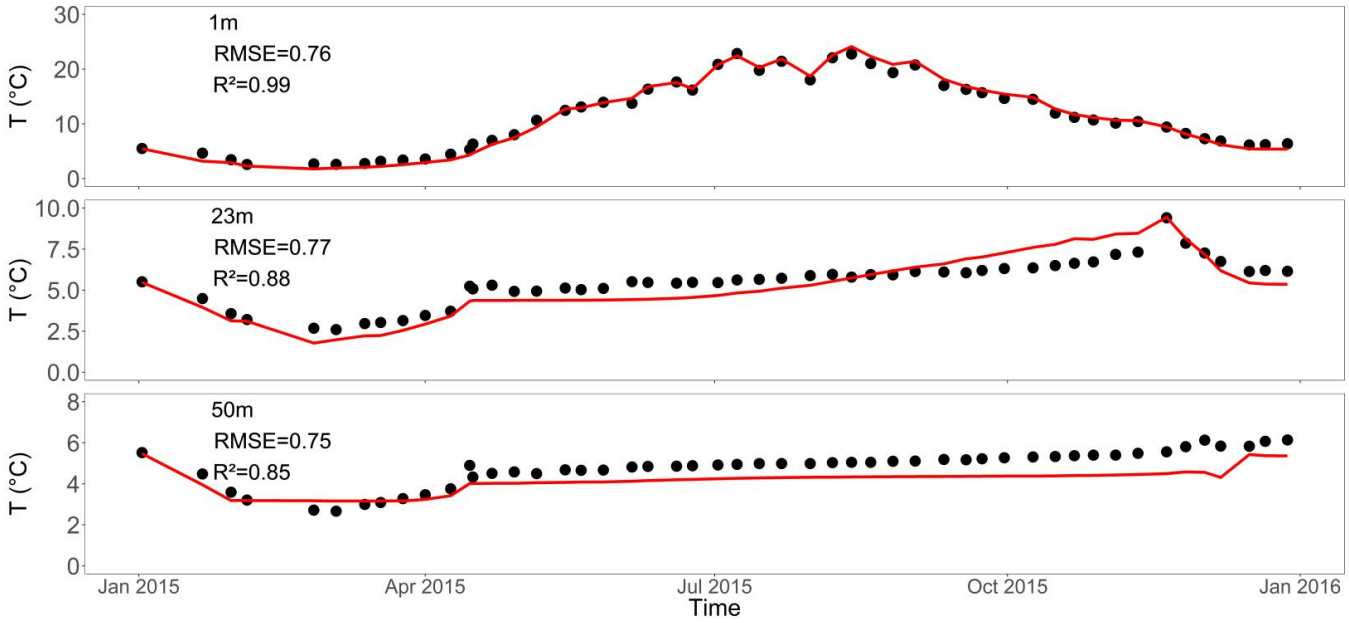


Figure 3.4. Simulated (red line) versus measured (black dot) water temperature at 1 m, 23 m and 50 m depths.

### 3.4.2. Statistical properties of wind velocity at Rappbode Reservoir

The analysis of 35 years of wind speed measurements at station Harzgerode revealed a clear seasonality with high wind speeds in winter and low wind speeds in summer (Figure 3.2). Absolute differences in seasonal wind speed remained low between the 20% and 60% quantile, but they became larger and more variable over the year for the 80%, 95% and 100% quantile. At the 20% quantile, wind speed was always lower than 4 m $s^{-1}$ and calm conditions (wind speed < 2 m $s^{-1}$) prevailed over 54% of the year.

### 3.4.3. Scenario S1: Stratification phenology in 2015 at different wind conditions

Comparing the standard simulation of 2015 with simulations using 10% and 20% higher wind speed revealed that wind plays a significant role in stratification phenology, which could even result in variations of the hypolimnion temperature (Figure 3.5). Its mean increased from 4.9 °C in the 2015 reference simulation to 6.9 °C at 10% increased wind and further to 7.2 °C at 20% increased wind (Figure 3.5). Additionally, wind speed directly affected the isotherm depths of different temperatures. For example, the average depth of the 10 °C isotherm increased from 15.7 m in the 2015 reference simulation to 30.8 m at 10% increased wind and further to 33.0 m at 20% increased wind (Figure 3.5).

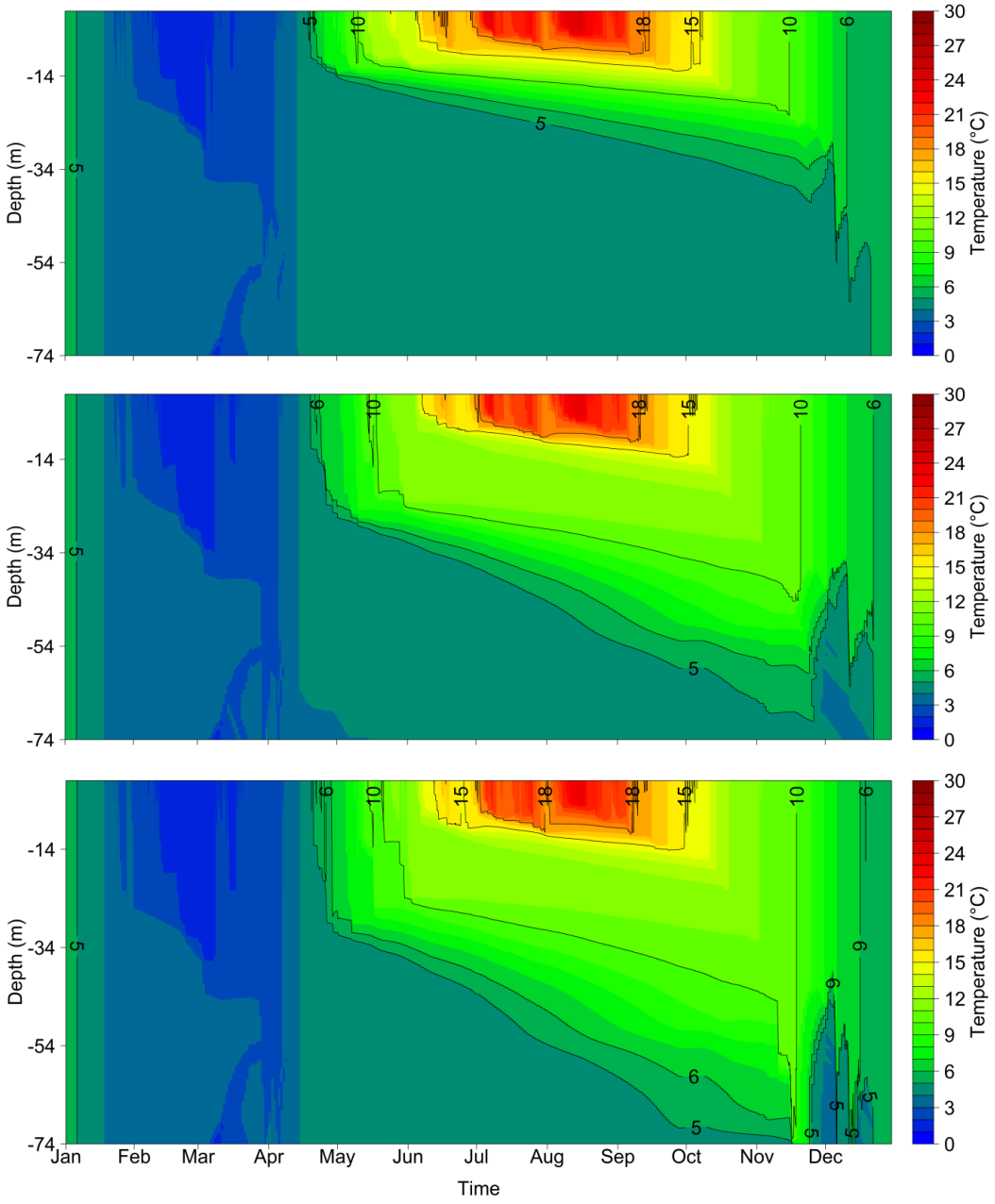


Figure 3.5. Water temperature under different wind scenarios. Temperature with wind speed measured in 2015 (top), wind speed from 2015 increased by 10% (middle) and 20% (bottom).

### 3.4.4. Scenario S2: Sensitivity to wind speed under averaged meteorological conditions

As can be seen in Figure 3.6 and Figure 3.7, it is evident that wind speed had a significant influence on the stratification duration: the higher the wind speed the later the stratification started and the shorter the stratification lasted. When comparing the 20% with the 100% quantile scenario, the start date of stratification was delayed by one month (from April 14$^{th}$ to May 15$^{th}$) and the stratification ratio was reduced by 17% (from 67% to 50%, see Figure 3.6). Also, Schmidt stability decreased markedly under increasing wind speed (Figure 3.7). For example, from the 20% to the 100% quantile of wind speed, the maximum Schmidt stability was reduced from 2803 to 1943 J m$^{-2}$, which corresponded to a reduction of 31% in stability. Finally, wind was an important factor on the variability of the 10 °C isotherm depth. At wind speed below the 80% percentile, the maximum 10 °C isotherm got shallower than 30 m. At 100% percentile, however, the maximum isotherm was deeper than 40 m (Figure 3.7).

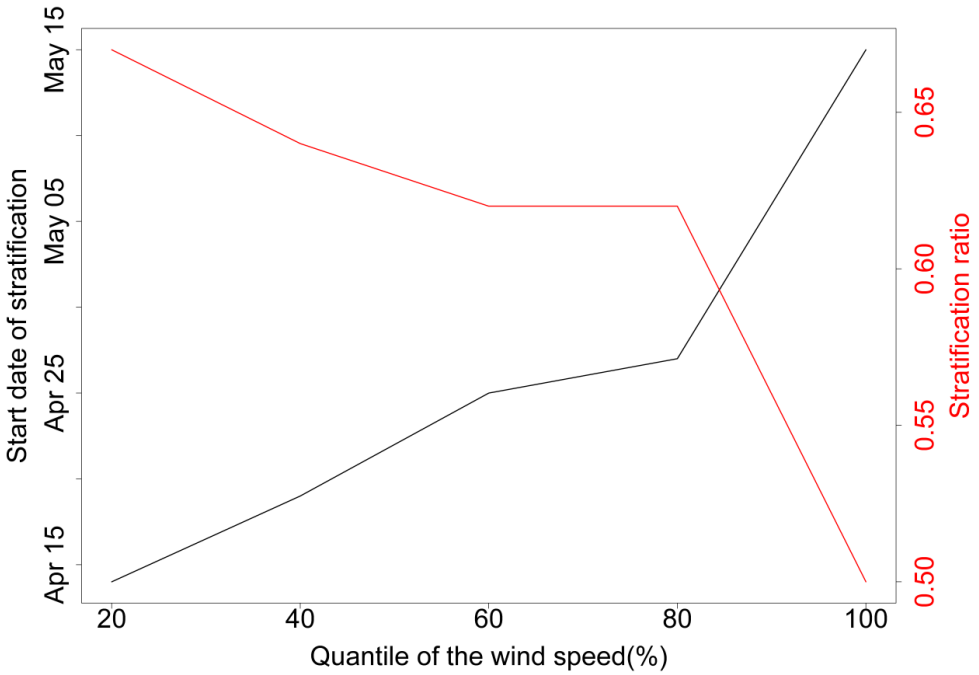


Figure 3.6. Comparison of stratification onset and open water stratification ratio under different wind forcing, given as quantiles of long-term wind speed observations.

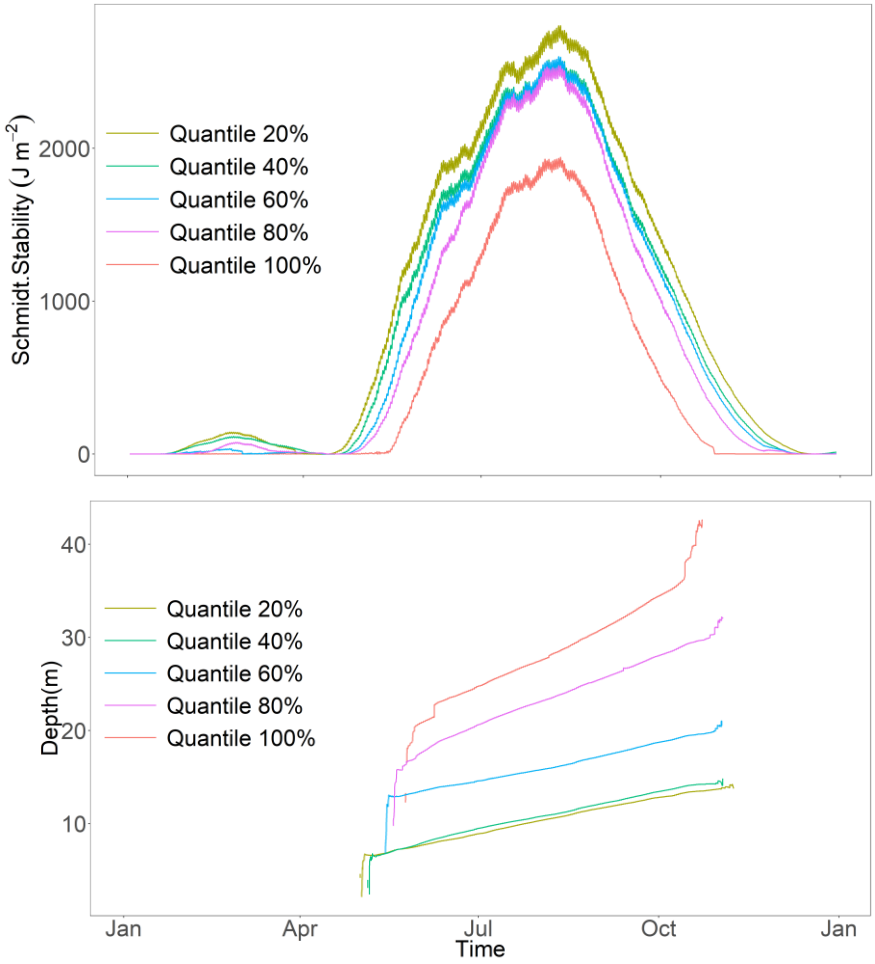


Figure 3.7. Comparison of Schmidt stabilities (top) and 10 °C isotherm depths (bottom) under different quantile wind scenarios.

### 3.4.5. Scenario S3: Effects of short-term wind events on stratification

Simulating a strong wind event (10 m $s^{-1}$ over 48 h), progressing over the whole year, illustrated the sensitive time window of lake stratification against such winds. We used three indices to evaluate the sensitivity of the thermal dynamics against strong wind events: hypolimnetic water temperature, 10°C isotherm depth, and Schmidt stability.

Stratification strength decreased when a strong wind occurred between end of April and beginning of July, i.e. in early summer (Figure 3.8c). As a matter of fact, strong wind events had negligible effect during overturn, i.e. before mid-April. A strong wind event after the beginning of July did not exert a significant impact on the evolution of thermal structure because the stability of the existing stratification was high enough to withstand the mixing forces from the

wind event. Under a strong wind event between end of April and early July, the hypolimnetic temperature and the 10 °C isotherm depth in summer were increased by up to 10 °C and 45 m respectively. The Schmidt stability during this period was decreased to around 2500 J $m^{-2}$. Although a strong wind event after July did neither affect hypolimnion temperature nor the 10 °C isotherm, small reductions of Schmidt stability can be recorded due to intensified cooling by evaporation, which scales with wind velocity.

The later the strong wind event occurred in early summer, the warmer got the hypolimnion since the down-mixed surface waters had a higher temperature and more heat was transported downward. Given this higher hypolimnion temperature, convective mixing during the autumnal cooling was also earlier reaching the hypolimnion (see Figure 3.8a). In case of a strong wind in early July, for example, the hypolimnion temperature reached more than 10 °C and convective cooling reached the hypolimnion already in early October. In contrast to this, a strong wind in early May increased the hypolimnion temperature to around 6 °C but convective cooling affected the hypolimnion only in late November (Figure 3.8a).

In conclusion, it turned out that the sensitive time window of thermal dynamics to episodic wind events was from the end of April to the beginning of July. This was also verified by an apparent reduction of surface water temperature (> 4 ˚C) if the strong wind occurs on June 30$^{th}$ (Figure S3 in Appendix 3). A short-term strong wind on April 9$^{th}$ (i.e. before the sensitive time window) and July 14$^{th}$ (i.e. after the sensitive time window), however, did not exert an important impact on the temperature in the top layer.

,

(a)

(b)

(c)

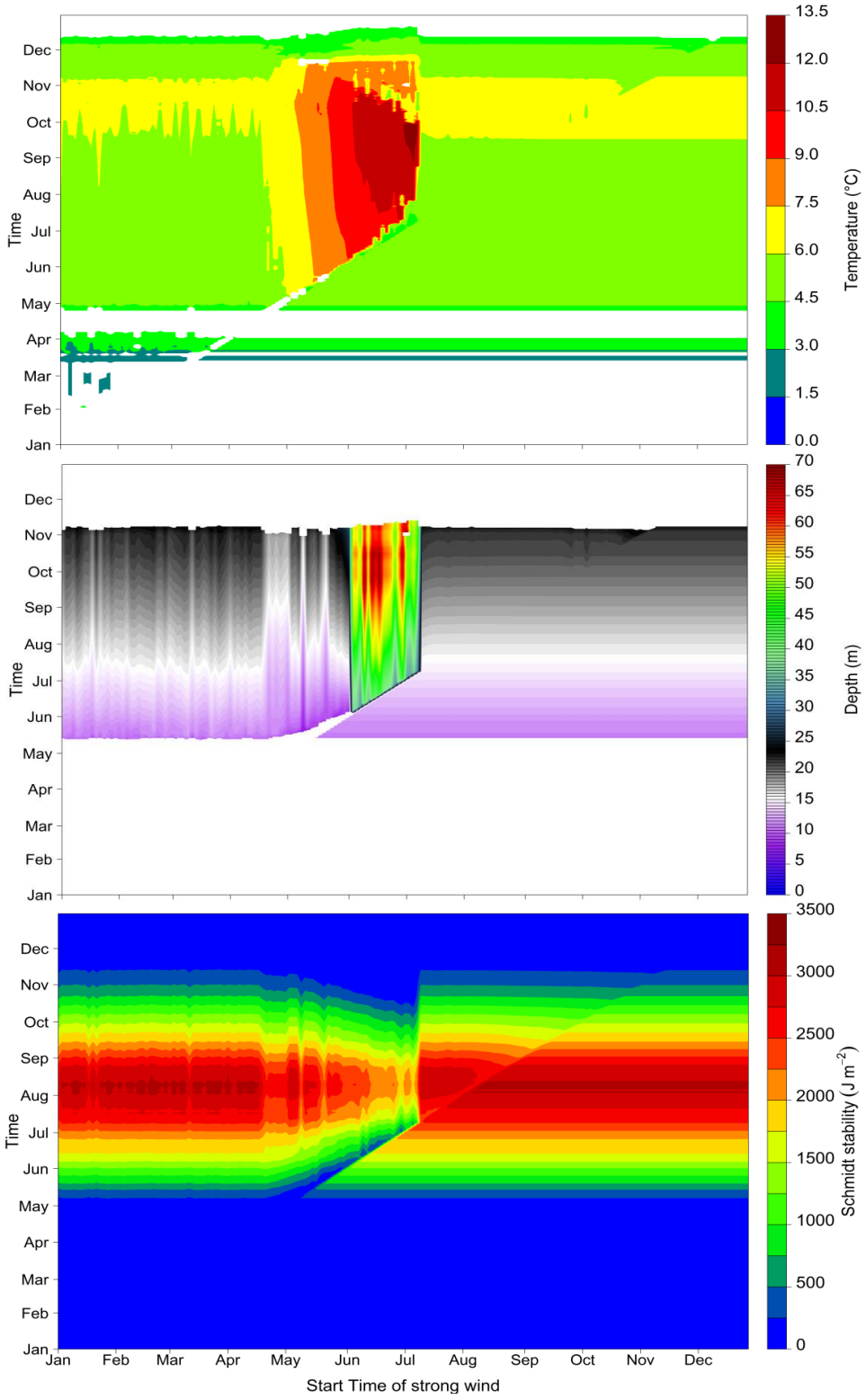


Figure 3.8. Hypolimnetic temperature (a), 10 °C isotherm depth (b) and Schmidt stability (c) modeled over the entire year (vertical axis) for different timing of the strong wind event (horizontal axis).

### 3.4.6. Scenario S4: Effects of short-term wind events on stratification (seasonally varying)

When applying less intense, seasonally varying wind speeds in the wind event, the resulting perturbations in stratification showed similar patterns like observed in scenario S3. The downward shift of the 10 °C isotherm (Figure 3.9) was, however, less strong than in S3 because the applied wind velocities were approximately 25% lower during summer. Nevertheless, in this scenario the duration of the sensitive time window for wind events was almost the same as in S3. We also applied two different durations of the wind event, lasting either over one or two days and clearly identified that the duration is an important factor for the impact of the wind event. The longer the wind is blowing, the stronger the effect on the stratification as indicated by the deepening of the 10 °C isotherm. Similar results can also be found for the hypolimnetic temperature and the Schmidt stability (Figure S4 and S5 in Appendix 3). This wind induced disturbance, however, remains only effective when the wind event occurs within a certain time window. Interestingly, the beginning and end of this sensitive time window is almost independent of the duration and strength of the wind event.

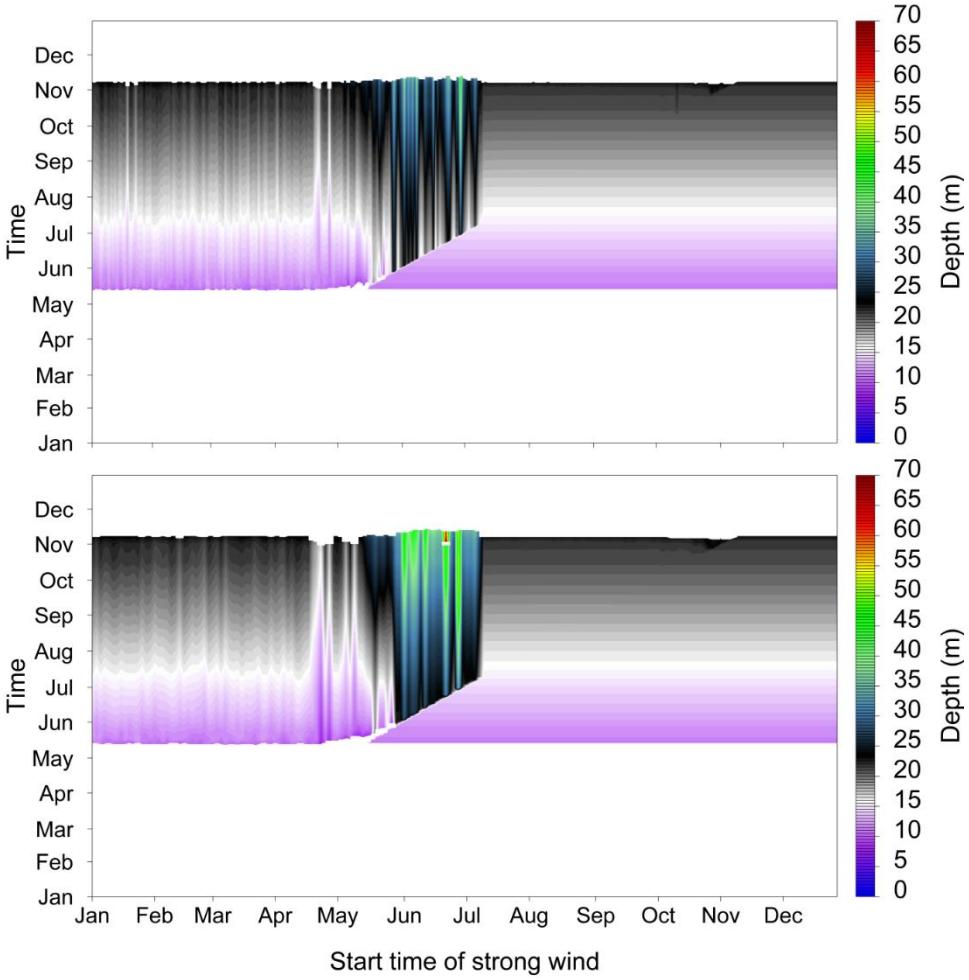


Figure 3.9. Depth of the 10 °C isotherm depth in the scenario S4 for a strong wind event lasting over either one (top) or two days (bottom) modeled over the entire year (vertical axis) for different timing of the strong wind event (horizontal axis).

## 3.5. Discussion

In the paper, the one-dimensional hydrodynamic model GLM was used to investigate the evolution of thermal structure in the Rappbode Reservoir. First, the parameters wind factor, light attenuation coefficient and vertical turbulent mixing coefficient in the hypolimnion were calibrated. Although the hypolimnetic temperature was slightly underestimated, the calibrated model reproduced the stratification pattern well and captured the variation of the thermal structure over the whole year (Figure 3.4). The discrepancies between measured and simulated temperature may be associated with the insufficient modeling of three-dimensional processes (e.g., internal waves, upwelling, etc.), which can be important processes for vertical transport of heat below the epilimnion (Hodges et al. 2000b). Previous research has confirmed the significant influence of internal wave activity on the stratification dynamics in Rappbode Reservoir (Bocaniov et al. 2014). Since a 1D model is not capable to fully account for these processes, a 3D simulation model may be used to evaluate the influence of three-dimensional processes on the thermal structure and its sensitivity to wind. Additionally, GLM uses a constant light attenuation coefficient ($K_w$) which cannot be changed during the simulation period. As indicated by Bueche et al. (2017), a lack of seasonal variation of $K_w$ may also exert a negative influence on the simulation accuracy.

The calibrated model was then used to investigate the effect of wind variations on stratification. It should be noted that since the wind direction is neglected by the model, only the influence of changing wind speed was taken into account. Averaged seasonal conditions were used for the other meteorological variables to run the model. In this way, effects from variations in other meteorological variables on simulation results were excluded. By simulating seasonal wind forcings of different intensities (quantile scenarios, S2), the decisive influence of wind speed on the thermal structure was substantiated. It is apparent that a decrease in wind speed moved the 10 °C isotherm depth upwards, extended the duration of the stratification season, increased the Schmidt stability, and therefore reduced the vertical mixing (Figure 3.6 and Figure 3.7). These findings extend those of previous research (Desai et al. 2009,Magee and Wu 2016) stating that decreasing wind speed reduces heat flux from the surface into deep layers due to lower mixing intensities. Under these conditions, the hypolimnion is more sheltered from the top layer and stratification can persist longer.

To our knowledge, this is the first study investigating the response of thermal stratification to seasonally changing wind, i.e. to episodic strong wind events, in detail. From Figure 3.8c, it can be seen that the maximum Schmidt stability decreased gradually when the strong wind took place from the end of April to the start of July (i.e., late spring and early summer). The strong wind event in the other periods, however, did not exert an important impact on the thermal dynamics of the reservoir. Before late April, stratification had not yet developed (Schmidt stability < 1000 J $m^{-2}$) and wind-induced mixing accordingly was not relevant. During May till June, stratification became stronger with Schmidt stability approaching 2000 J $m^{-2}$. In this period, however, the thermal structure of the reservoir is not stable enough to resist the influence of strong wind events. After this period, i.e. from mid July onwards, stratification is so intense and

stable (stability > 2000 J $m^{-2}$) that the wind-induced mixing cannot penetrate into the deep hypolimnion. Our simulations show a marked warming of the hypolimnion in Rappbode Reservoir when a strong wind occurs at the right time of the year. Following such an event, hypolimnion temperature can be far higher than the usual 4 to 6 °C and reach values up to 10°C. Long term-temperature records from Rappbode Reservoir indeed showed warmer hypolimnion temperatures in some years and reached values up to 9 °C (Wentzky et al. 2018a). This temperature is a little lower than in scenario S3 but given the high wind velocities and long durations in this scenario, a less intense hypolimnion warming *in situ* appears reasonable.

A difference should be noted when comparing our results with the studies of Lake Annie in the USA (Jennings et al. 2012,Read et al. 2011). In the latter, a strong mixing event in mid-August was observed as a result of high wind speed at that time (up to 8 m $s^{-1}$). In our study, however, the strong wind at that time did not show a strong influence on the thermal structures of the Rappbode Reservoir. The discrepancy could be attributed to the different morphometry of two lakes. As shown by the previous studies (Butcher et al. 2015,Magee and Wu 2016), lake morphometry exerts an important impact on stratification phenology. The deep basin of the Rappbode Reservoir (89m maximum depth) allows a very cold hypolimnion of 4-5 °C and this induces strong density gradients towards the surface. It indicates that the episodic strong wind in the hot summer cannot provide enough energy to alter its stratification structure. The maximum depth of Lake Annie, in contrast, is only 19 m. Under the strong wind event during midsummer, energy can be easily transferred into the deep hypolimnion to fully mix the water column.

Our scenarios S3 and S4 documented the importance of wind events for stratification phenology. It appears that not the average wind conditions predetermine the stratification phenology but rather the occurrence of strong wind events within a sensitive time window. Although wind strength and duration hardly affected the timing of this sensitive time window，the wind-induced perturbations on stratification phenology are, of course, affected by wind strength and duration. We did not evaluate how perturbations at shorter time-scales, e.g., sub-daily events, may influence the stratification dynamics in Rappbode Reservoir. Diurnal asymmetry in meteorological drivers can exert a strong impact on the thermal structure of different water systems (Ishikawa and Tanaka 2010,Snortheim et al. 2017) suggesting that more knowledge is required about the duration of a wind event necessary to be effective for changing stratification phenology. Consequently, future work should focus on the combined effect of diurnal and seasonally changing wind so that we can get a better understanding about the mechanisms of stratification variability.

We also noted that emerging patterns in the simulation results in Figure 3.8 showed distinct fluctuations in their numerical values. The 10°C isotherm in scenarios with strong wind events within the sensitive time window, for example, varied between 40 m and 55 m over the summer (shown as yellow and red vertical bands in the contour). Also the Schmidt stability showed some of these fluctuations, partly even for strong wind events before April. We assume that sometimes small changes in the model input can show discontinuously strong effects in GLM due to its Lagrangian layer structure. Since GLM is self-optimizing the layer structure and dynamically adapts layer thicknesses, small changes can sometimes induce a distinctly different vertical

structure in the model. These changing vertical discretizations are hardly visible in the contour plots for simulated temperature but affect derived variables like Schmidt stability or isotherm depth. These consequences from the dynamic Lagrangian model structure can induce slight discontinuities, but, of course, do not destroy the prominent patterns in simulation studies like ours. Moreover, the Langrangian model structure has many advantages in water bodies with subsurface inflows and outflows (e.g. in reservoirs) because of low numerical mixing and is therefore an important feature of GLM for its high transferability between different water bodies.

Finally, changes in thermal structure have a great impact on oxygen dynamics. An increase in stratification, e.g., as a consequence of wind stilling, will result in increased extent of anoxia, which will exert a negative influence on aquatic ecosystems. Based on this, to extend the present research, it is worthwhile to elucidate the quantitative relationship among dissolved oxygen concentration, stratification dynamics and wind changes in further studies. Strong wind events are, however, destabilising the stratification and lead to earlier overturn and shorter stratification period. In conclusion, the effects of wind are not easy to quantify, because they strongly depend on the timing and strength of key events and therefore have a highly stochastic component. Our study was able to characterize the sensitive time window when wind is highly effective and underpins the importance of short-term events. More systematic research is required to study the consequences of wind events in situ and how these events affect ecosystem features (e.g., Giling et al. (2017a)) like nutrient cycling or plankton dynamics.

# 4. Variable withdrawal elevations as a management tool to counter the effects of climate warming in Germany's largest drinking water reservoir

## 4.1. Abstract

Thermal stratification in reservoirs is a significant factor affecting water quality, and can be strongly influenced by climate change and operational strategies. Reservoirs in the temperate zone react most sensitively to climate warming during winter as ice cover and inversed stratification are about to disappear in a warmer world. In this study, two well-established hydrodynamic models, the one-dimensional General Lake Model (GLM) and the two-dimensional CE-QUAL-W2 (W2), were used to investigate the response of winter inversed stratification in the Rappbode Reservoir to future climate warming, combined with different water withdrawal elevations. Results showed that under increased air temperature, the duration of inversed stratification is reduced and the inversion phenomenon will entirely disappear under current management if the air temperature is increased high enough (more than 4.5 K) in the future. Under strong climate warming, the Rappbode Reservoir will therefore change from a dimictic to a monomictic mixing type. Changing the reservoir management from deep withdrawal (e.g. below 350 m a.s.l.) to shallow withdrawal elevations (e.g. above 390 m a.s.l.) reduces internal heat energy stored in the reservoir in summer and prolongs the inversed stratification period in winter. This strategy can retain the dimictic behavior even under strong warming. Our study indicates that adjusting the withdrawal elevation is an effective management instrument in order to control the winter conditions and can, in fact, mitigate climate warming effects on winter hydrodynamics by stabilizing the dimictic mixing type.

## 4.2. Introduction

Thermal stratification is the phenomenon referring to a variation in the water temperature at different depths in a water body, and is the result of changes in water density with temperature (Boehrer and Schultze 2008). The stratification is a significant factor for the evolution of water quality in lentic waters (Boehrer and Schultze 2009a). For example, because of the stratification, connectivity between the bottom and surface layers is suppressed giving rise to a nutrient rich but colder hypolimnion and a nutrient poor but warmer epilimnion (Read et al. 2011). Due to the weakened connectivity, it is difficult to supplement the hypolimnion with oxygen from the atmosphere, which can lead to a serious environmental problem of anoxia in the bottom layer (Snortheim et al. 2017). Additionally, the enhanced stratification throughout summer can lead to an increased occurrence of toxin producing cyanobacteria in the epilimnion, posing a significant threat to water quality (Paerl and Huisman 2009). Furthermore, by influencing the greenhouse gas exchange between the water and atmosphere, stratification can affect the role of aquatic

systems in the global carbon cycle (Coloso et al. 2011,Woolway et al. 2014). Therefore, concerning the importance of stratification for aquatic ecosystems, a large amount of investigations have focused on this phenomenon and its influencing factors. Reservoirs offer opportunities to affect stratification by operational strategies, which are not available for natural lakes, and models can be used to explore the available options.

Based on the stratification patterns (Boehrer and Schultze 2009a), most of the freshwater systems in temperate regions are either dimictic or warm monomictic: a dimictic water body can be ice-covered in winter and is generally stratified both in summer (direct) and winter (inverse) with turnover mixing in spring and autumn; a warm monomictic water is never ice-covered and undergoes only one mixing period in winter in addition to being stratified during the rest of the year. Currently, when evaluating the stratification dynamics in this area, most studies focus on the summer stratification with three identifiable layers, epilimnion, metalimnion and hypolimnion, and distinct water temperature differences along the vertical direction during this period (Foley et al. 2012,Hu et al. 2016,Kerimoglu and Rinke 2013,Mi et al. 2018,Rosner et al. 2012). However, little attention has been specifically given to the winter inversed stratification in dimictic waters and its influencing factors.

For dimictic water bodies, the surface water temperature in winter is lower than the bottom layer which causes the winter inversed stratification (Laybourn-Parry and Wadham 2014). This inversed stratification is a prerequisite for the formation of an ice cover (Boehrer and Schultze 2009a,Marmorino 1978). The winter inversed stratification (and prolonged ice cover) can cause low oxygen and fish kills during long winters, which then can lead to increased grazing of zooplankton on phytoplankton in the following period (and thus increased water quality). Moreover, the existence of the inversion is important evidence in distinguishing between dimictic and monomictic waters. Due to global warming trends over the last decades, the winter inversed stratification and ice cover are shown to have been reduced and even disappeared in numerous lakes around the world, which leads to potential changes of mixing patterns from dimictic to monomictic types (Adrian et al. 2009,Ficker et al. 2017,Shimoda et al. 2011). By employing a 1D hydrodynamic model, Peeters et al. (2002) simulated the thermal structure of Lake Zurich over half a century and predicted that under substantially increasing air temperatures in the future, the winter inversion will disappear resulting in the lake shifting from being generally dimictic to generally monomictic. The disappearance of the winter inversion and the subsequent changes in thermal patterns due to the climate warming have a negative influence on the hypolimnetic oxygen concentration and can even change the available habitat for aquatic organisms (Ficker et al. 2017,Peeters et al. 2002). Under high greenhouse gas emissions in the absence of climate mitigation polices, the global average air temperature may increase by 5° C by the end of the 21$^{st}$ century (England et al. 2015). Concerning the importance of the winter inversed stratification for aquatic systems, there is a need to comprehensively illustrate how the inversion responds to such a noticeable warming trend and whether anthropogenic management practices can influence the inversion so as to mitigate the negative effect caused by global warming.

Among various management strategies for waters, selective water withdrawal is considered

to be an effective method to control the thermal stratification for meeting the requirements of different usages. For example, Casamitjana et al. (2003) applied a one-dimensional model (DLM) to elucidate the response of the thermal structure of Boadella Reservoir to different withdrawal scenarios. The results show that the withdrawal location determines the thermocline depth and the hypolimnion volume; Çalıskan and Elçi (2009) investigated the influence of selective withdrawal on the hydrodynamics of Tahtali Reservoir and concluded that hypolimnetic withdrawal is the most effective choice to encourage water mixing and reduce anoxia; Weber et al. (2017) developed an optimization withdrawal strategy which can automatically determine the withdrawal elevation to modify the thermal structures for different water usages. However, all such previous studies focus on the effect of selective withdrawal on summer stratification, they did not take the winter inversed stratification into account.

In this study, two well-established hydrodynamic models (i.e. General Lake Model and CE-QUAL-W2) were selected to elucidate the response of winter inversed stratification in the Rappbode Reservoir to future climate warming combined with different water withdrawal elevations. Considering the importance of ice phenology for the temperature inversion, the ice cover (duration and thickness) is also included in the scenarios. Rappbode Reservoir is the largest drinking water reservoir in Germany and supplies drinking water to more than 1 million people. A previous study predicted that by the end of this century, the winter stratification will completely disappear in most of deep waters in this region as a result of global warming, which will severely threaten their aquatic ecosystems (Kirillin 2010). It is expected that our study will help reservoir operators effectively control the winter inversed stratification so as to mitigate the negative influence caused by the increase in air temperature. Additionally, the two models (General Lake Model and CE-QUAL-W2) are widely used in research to analyze the vertical stratification and thermal dynamics and they both are distributed as open-source software. This study provides an excellent opportunity to compare and evaluate the models' performances in detail, which will benefit researchers for model selection and application. Furthermore, simulation results are more reliable if they are supported by several models so that the outcome becomes independent of one specific model. Additionally, from the comparison of results, the strengths and weaknesses of each model can be clearly seen and it will help developers improve and enhance the models in the future.

## 4.3. Methods

### 4.3.1. Study site

The Rappbode Reservoir is located in the eastern Harz Mountains and has a maximum volume of $1.13\times10^8$ $m^3$. The crest elevation of the reservoir is 423.6 m a.s.l. and its maximum depth is 89 m. It is the largest drinking water reservoir in Germany, supplying drinking water to more than 1 million people in central eastern Germany (Fig 4.1, Rinke et al. 2013b). The reservoir is the core of the Rappbode system, a network of 6 water bodies used for flood protection, environmental flows, hydropower, recreation and drinking water supply. It receives water from three smaller upstream reservoirs (Königshütte Reservoir, and the Hassel and

Rappbode auxiliary reservoirs). The reservoir has five outlets at different elevations (360 m a.s.l-400 m a.s.l in 10 m intervals) for raw water discharge. The outlets with the elevation of 360, 370 and 380 m a.s.l are used for most of the time. The top 2 outlets (390 and 400 m a.s.l) are only open at late December and early January in each year. There is also an additional outlet into the downstream Wendefurth Reservoir from the elevation of 345 m a.s.l. which is active all the time. The Rappbode Reservoir is a typical dimictic water body with mixing in spring and autumn. It experiences strong stratification in summer and weaker stratification in winter with an ice cover in some years. The mean water residence time of the reservoir is a little more than one year (380 days).

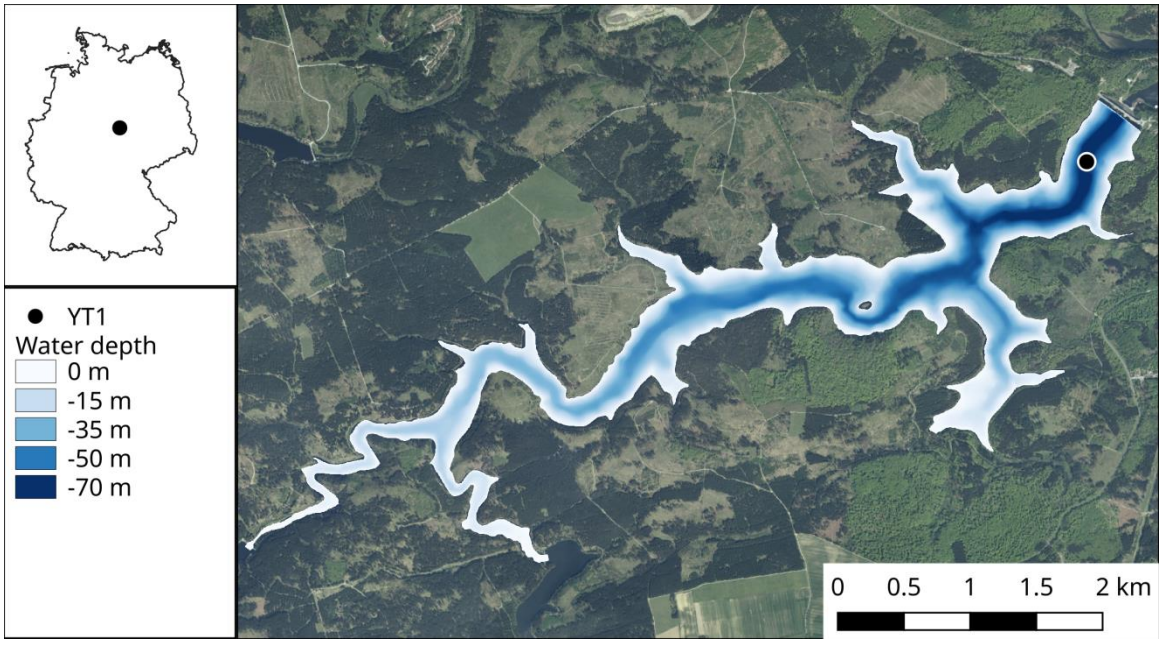


Figure 4.1. Map of Germany (top left). The black point indicates the location of the Rappbode Reservoir within Germany. In the bathymetric map of the Rappbode Reservoir (right), the black point shows the monitoring location for water temperature.

### 4.3.2. Numerical models

We intentionally used two lake models in our study in order to quantify the variability of their outcomes due to different model structures. We selected two established, open source, and broadly accepted models for our study, the General Lake Model (hereafter GLM) and CE-QUAL-W2 (hereafter W2). The main difference between the two models can be seen in Table 4.1.

Table 4.1. Comparison of main features of the used models GLM and W2

| Feature | GLM | W2 |
|---|---|---|
| Dimensionality | 1D | 2D |
| Layer grid | Lagrangian | Eulerian |
| Respository | http://aed.see.uwa.edu.au/research/models/GLM/ | http://www.cee.pdx.edu/w2/ |
| Geometric input | hypsographic curve | topographic map and/or sediment range surveys |
| Meteorological input | Shortwave radiation, cloud cover, air temperature, relative humidity, wind speed, precipitation | Shortwave radiation, cloud cover, air temperature, dew point temperature, wind speed, wind direction, precipitation |
| Reference | Read et al. 2014; Mi et al. 2018 | Sadeghian et al. 2015; Brito et al. 2018 |

(1) GLM is a one-dimensional (1D) hydrodynamic model developed by the Aquatic EcoDynamics Research group at the University of Western Australia (http://aed.see.uwa.edu.au/research/models/GLM/; Hipsey et al. 2014). It simulates the vertical stratification and mixing of lakes taking the influence of inflows/outflows, surface heating and cooling and ice cover fraction into account. The code of GLM is open source which can be freely downloaded from GitHub (https://github.com/AquaticEcoDynamics/GLM).

GLM uses a flexible Lagrangian layer structure, i.e. thickness and volume of each layer can be contracted and expanded dynamically during the runtime of the model. Minimum and maximum layer thickness can be adjusted by the user. Each layer has homogenous physical properties (Read et al. 2014).

GLM has been widely used to compute the vertical profiles of water temperature and stratification phenology in different water bodies (Read et al. 2011,Snortheim et al. 2017,Weber et al. 2017). In a large multiple lake intercomparison study GLM was shown to reproduce stratification dynamics in various lakes without local calibration (Bruce et al. 2018). The model is also successfully applied to simulate ice dynamics (Bueche et al. 2017,Yao et al. 2014). Three components of ice are included in GLM: black ice (formed at the ice-water interface), white ice (generated because of snowfall) and snow cover. Further details on the ice dynamics and modelling of the hydrodyanmics can be found in the GLM manual (Hipsey et al. 2014) and in Hipsey et al. (2017).

(2) W2 is a two-dimensional, laterally-averaged, hydrodynamic and water quality model. The hydrodynamics component of the model can predict surface water level elevations, flow velocities and water temperatures varying in the longitudinal and vertical directions. The model conceptualises water bodies as a grid discretised as vertical columns and horizontal rows. The cell widths can vary spatially to match the cross-sectional width of the water body at the cell location.

W2 is a wide-spread model and has been successfully applied to various lakes, reservoirs and river systems (Brito et al. 2018,Chang et al. 2015,Sadeghian et al. 2018). Through several decades of model development, W2 has an up-to-date user manual (Cole and Wells 2006) and an active user forum. The source code is freely available with clear comments allowing the extension and application of new formulations and algorithms.

### 4.3.3. Model setup and input data

The input files for running the two models include time-series of meteorological data, hydrological data for inflows and outflows as well as the reservoir bathymetry describing the elevation-area-volume relationship. An overview of such files can be seen in Table 4.2. The hydrological and bathymetry data were provided by the reservoir authority of the state of Saxony-Anhalt (Talsperrenbetrieb Sachsen-Anhalt). The water temperature of inflows were obtained from a YSI-6200 probe deployed in the tributaries of the reservoir (see Rinke et al. 2013b).

Table 4.2. Summary of the model boundary conditions

| Boundary condition | Frequency | Data Source |
|---|---|---|
| Wind speed | Hourly | Station 1,Station 2, Station 3 |
| Wind direction | Hourly | Station 1,Station 2, Station 3 |
| Air temperature | Hourly | Station 1,Station 2, Station 3 |
| Relative humidity | Hourly | Station 1,Station 2, Station 3 |
| Shortwave radiation | Hourly | Station 1,Station 2, Station 3 |
| Precipitation | Hourly | Station 2, Station 3 |
| Cloud | Hourly | Station 3 |
| Inflow discharge | Daily | Reservoir authority (Talsperrenbetrieb Sachsen-Anhalt ) |
| Inflow temperature | Daily | Station 2 |
| Outflow discharge | Daily | Reservoir authority (Talsperrenbetrieb Sachsen-Anhalt ) |

*Station 1: Monitoring station in the central basin of the Rappbode Reservoir; Station 2: Monitoring station at the Rappbode auxiliary reservoir; Station 3: German Weather Service station at Harzgerode

As a 1D model, the model structure of GLM is based on the hypsographic information, and user defined layer properties in terms of maximum number of layers as well as maximum and minimum layer thicknesses. Based on experience and initial testing, the three layer parameters shown above were set to 500, 0.5 m and 0.1 m, respectively.

The Rappbode Reservoir was discretized in W2 using 34 segments along the longitudinal directions of the main stem and side branches (see Figure 4.2). Some of the segments, segments 1, 24, 25, 29, 30 and 34, serve as boundary condition segments, at the model edges and between branches, hence they do not appear in the plan view of the segment discretization. For the discretization in the vertical dissection, the thickness of the top 8 rows is 0.25 m, 0.5 m for the next 6 rows and 1m thick for the remaining rows down to the reservoir bottom.

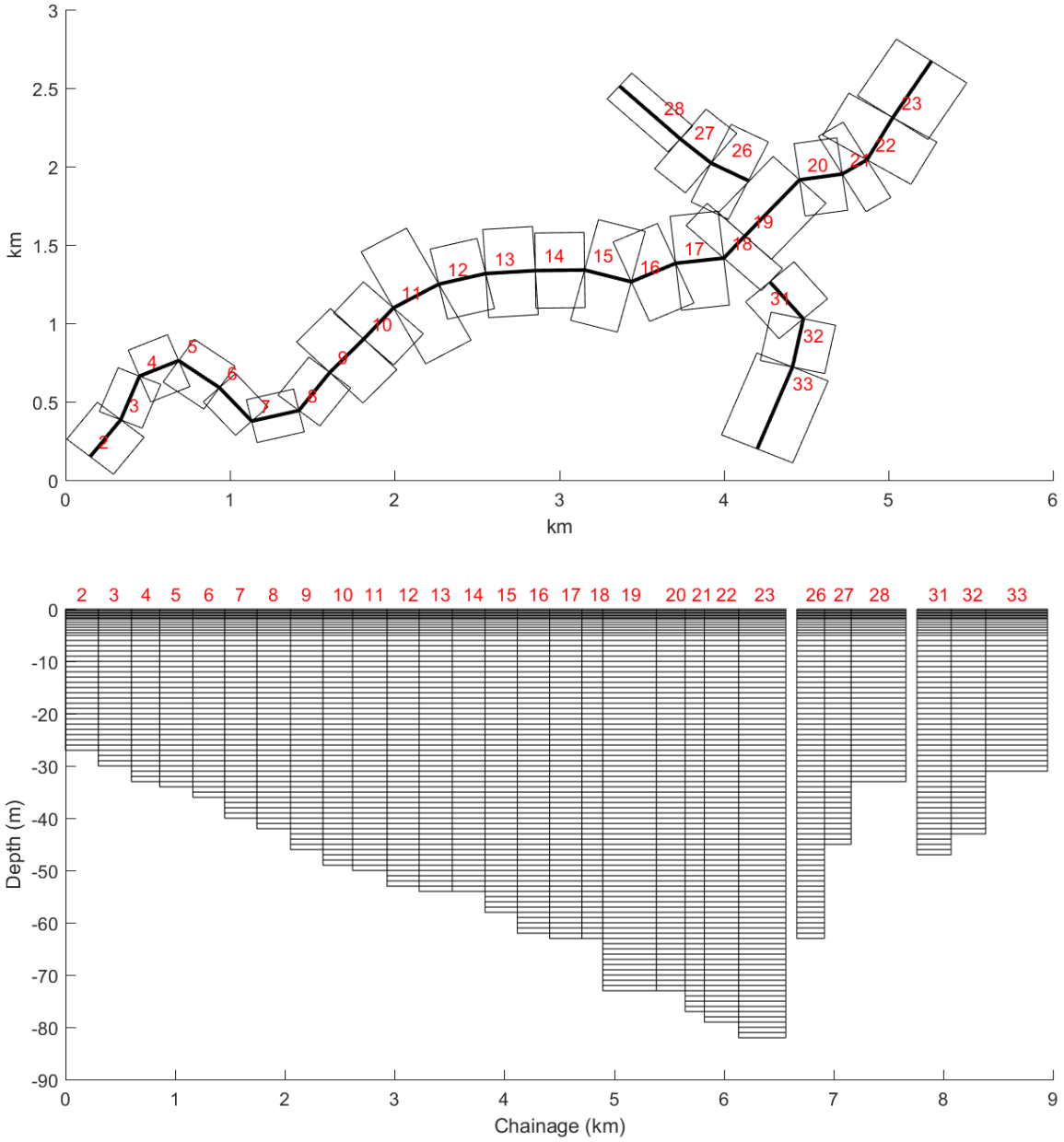


Figure 4.2. CE-QUAL-W2 grid definition for Rappbode Reservoir in profile view (bottom) and plan view (top) along the axis.

The meteorological input data, air temperature, wind speed, wind direction, shortwave radiation and relative humidity, were obtained from a monitoring buoy deployed in the central basin of the Rappbode Reservoir (see Rinke et al. 2013b). High-frequency observed data (every 10 minutes) were averaged to hourly values for the simulations. A small amount of missing values were filled with measurements from a nearby observatory at the Rappbode auxiliary reservoir (Friese et al. 2014,Rinke et al. 2013b) or from the German Weather Service station at Harzgerode ( 15 km away from the research area). The precipitation values were primarily drawn from the Harzgerode station because of sensor failures at the measurement buoy and the gaps

were filled from data recorded at the Rappbode auxiliary reservoir. The cloud cover fraction data were obtained from the Harzgerode station. All meteorological stations delivered air humidity as relative humidity but W2 requires dew point temperature as input. We calculated dew point temperature from relative humidity based on the formula from Lawrence (2005):

$$Dp\ (T,\ RH)=\frac{\lambda\left(ln\left(\frac{RH}{100}\right)+\frac{\beta T}{\lambda+T}\right)}{\beta-\left(ln\left(\frac{RH}{100}\right)+\frac{\beta T}{\lambda+T}\right)} \qquad (4.1)$$

where *Dp (T, RH)* is the dew point temperature (in °C), RH is the relative humidity (in %), T is the air temperature (in °C), the values for the coefficients $\lambda$ and $\beta$ are $243.04$°C and $17.625$, respectively.

The time step of the simulation output was one hour which allows us to capture the sub-daily changes of water temperature and ice-cover. Water temperature profiles extending from the water surface to the bottom layer were available for Rappbode Reservoir. The profiles were recorded using high-resolution CTD measurements with a Hydrolab DS5 probe and used for model calibration. Such data were also used for the model initializations, i.e. the vertical profile of water temperature at the beginning of the simulation. Because the Rappbode Reservoir is a typical freshwater system with low conductivity, the salinity in the models was set to 0.

### 4.3.4. Model calibration

The models were run from January 2nd, 2015 until April 30th, 2017. This period was selected because it included a rather mild winter (2015/2016) and a cold winter (2016/2017) and because high quality observation data were available from this time. For GLM, aside from a few site-specific settings, calibration of physical parameters is usually not required as the process parameters have a solid empirical or physical basis and are independent of local characteristics of the lake and its climate (Bruce et al. 2018,Read et al. 2014). In accordance with the study of Weber et al. (2017), we therefore kept the parameter values the same, as recommended in the scientific manual (see Hipsey et al. 2014) except for the wind factor (correcting for wind speed) and the averaged background light attenuation which are considered to be site-specific.

For the W2 model calibration, the effects of wind and solar radiation are the most important factors influencing the mixing and heat budget of Rappbode Reservoir. The influence of these two factors are adjusted using the parameters WSC (wind sheltering coefficient) and SHADE (shading coefficient). The light extinction coefficient EXT is also an important parameter since it controls the amount of solar radiation penetrating the water column from the water surface. Given the minimal calibration of a few site-specific parameters in each model and the fact that both models were shown to have a transferable (i.e. site-independent) parameterization, we did not perform a separate model validation on further observational data.

The root-mean-square-error (RMSE) of water temperature was used for model calibration. It has been widely accepted as a good indicator for assessing the geoscientific modeling performance (Chai and Draxler 2014).

### 4.3.5. Scenarios

In order to systematically analyse the effects of withdrawal elevation on stratification and mixing regime and to elucidate the management options to influence the winter conditions in the reservoir, we defined two scenarios:

**S1:** Influencing ice dynamics by withdrawal regime. The established model was run with withdrawal elevation varying from the bottom (339 m a.s.l) to the surface (409 m a.s.l) in intervals of 1m, i.e. in total 71 simulations. In this scenario, time-dependent withdrawal discharge was kept the same as in the reference simulation, but all withdrawn water is taken from one single depth as specified in the respective scenario case. Note that in the scenario, all water is withdrawn from one outlet depth and never two separate outtake flows, e.g. one for drinking water and another one for downstream discharge. Since ice formation was only observed in winter 2016/2017, the first scenario was analysed by exclusively evaluating conditions in this winter by calculating the number of days with ice cover, dates of ice-on and ice-off, as well as mean and maximum ice thicknesses.

**S2:** Mixing regimes under different withdrawal and warming regimes. In the second scenario, we focused on the combined influence of air temperature increase and withdrawal elevation on the duration of inversed stratification. We identified the mixing regime of the reservoir by the occurrence of inversed stratification, i.e. if the inversed stratification occurred in winter, the reservoir was regarded as a dimictic water; if not, it was regarded as a monomictic water body. In this scenario, we created a series of simulations for the whole study period (Jan 2015-April 2017) and increased air temperature from +0.25 (K) to +5 (K) in intervals of +0.25 (K) and withdrawal elevation from 339 m to 409 m in intervals of 1 m. In the climate scenarios, we kept the relative humidity in GLM the same as in the original measurements and adjusted dew point temperature in W2 based on Equation (1) so that relative humidity was the same in both model runs. Just like in the first scenario, all withdrawn water is taken from one elevation at one site. All combinations resulted in a series of 1420 simulations, which were evaluated by both models. We then calculated the number of days with inversed stratification (i.e. the duration of inversed stratification) for each simulation.

Note, that temperature differences are given in Kelvin while simulated temperatures are given in degrees Celsius. The R package “glmtools”, combined with other customized R code, was applied for executing GLM and analyzing the simulations (Read et al. 2014,Winslow et al. 2017a). More details about the package can be found at GitHub (https://github.com/USGS-R/glmtools). MATLAB was used to analyze the W2 output.

## 4.4. Results

### 4.4.1. Model calibration

The parameters used in the two models are shown in Table 4.3. Both models were able to accurately reproduce the water temperature and stratification phenology of the Rappbode

Reservoir, with good agreement between simulated and observed water temperature profiles. For the whole time series, the mean water temperature simulated by GLM and W2 were 6.18 °C and 5.82°C, respectively, which are very close to the observed value of 6.17°C. The overall RMSE for both models is less than 1K, which indicates a high accuracy of the simulations (Figure 4.3). Both models successfully reproduced seasonal variations of water temperature for the top layer (at depth 1 m, see Figure 4.4). The models slightly overestimated the metalimnetic water temperature in the summer and early autumn (depth of 23 m, Figure 4.4) whereby GLM showed a more pronounced overestimation in 2015. Both of them performed well in calculating the hypolimnetic temperature (depth of 50 m, Figure 4.4). At the depth of 1 m, the maximum observed water temperature was reached between July and August. For the depth of 23 m, it was delayed towards November. This lag of the maximum temperature was also accurately captured by the two models.

Table 4.3. List of parameters used in the two models. W2 was applied with standard settings for freshwater systems. Note that because of the characteristics of both lake models, settings for specific parameters can have slightly different values due to differences in the underlying model equations.

| Model | Parameter | Description | Value |
|---|---|---|---|
| GLM | $C_K$ | Convective overturn coefficient (-) | 0.2 |
| GLM | $C_{KH}$ | Kelvin-Helmholtz turbulent billows (-) | 0.3 |
| GLM | $C_W$ | Wind stirring coefficient (-) | 0.23 |
| GLM | $K_w$ | Averaged background light attenuation ($m^{-1}$) | 0.83 |
| GLM | $C_E$ | Latent heat transfer coefficient (-) | 0.0013 |
| GLM | $C_H$ | Sensible heat transfer coefficient (-) | 0.0013 |
| GLM | $C_D$ | Coefficient for transfer of momentum (-) | 0.0013 |
| GLM | $F_{wind}$ | Wind factor (-) | 0.89 |
| GLM | $F_{sw}$ | Shortwave radiation factor (-) | 1 |
| W2 | WSC | Wind sheltering coefficient (-) | 1 |
| W2 | SHADE | Shade fraction coefficient (-) | 1 |
| W2 | CBHE | Coefficient of bottom heat exchange (W $m^{-2}$ $^oC^{-1}$ ) | 0.3 |
| W2 | TSED | Sediment temperature ($^oC$) | 8 |
| W2 | TSEDF | Heat lost to sediments that is added back to water column | 1 |
| W2 | EXH2O | Light extinction for pure water ($m^{-1}$) | 0.4 |
| W2 | BETA | Fraction of incident solar radiation absorbed at the water surface | 0.45 |
| W2 | BETAI | Fraction of solar radiation absorbed in the ice surface | 0.6 |
| W2 | ALBEDO | Albedo of ice | 0.25 |

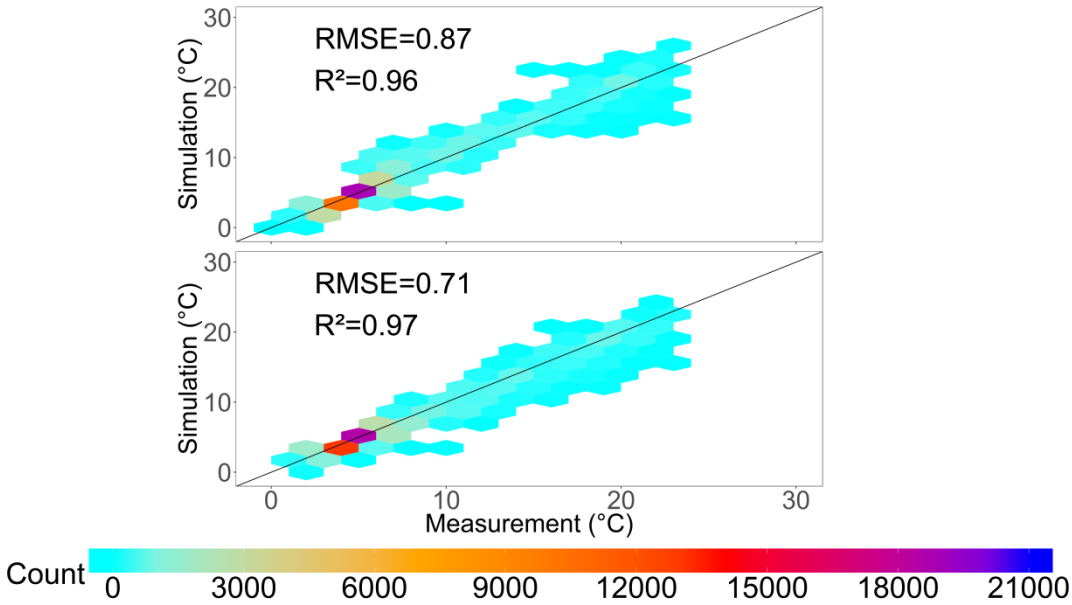


Figure 4.3. Comparison between simulated and measured water temperature during the simulated period (n=47613, from 01/2015 to 03/2017) for GLM (top) and W2 (bottom). The color scale denotes the amount of samples per hexagon. The straight line has a slope of one and an intercept of zero.

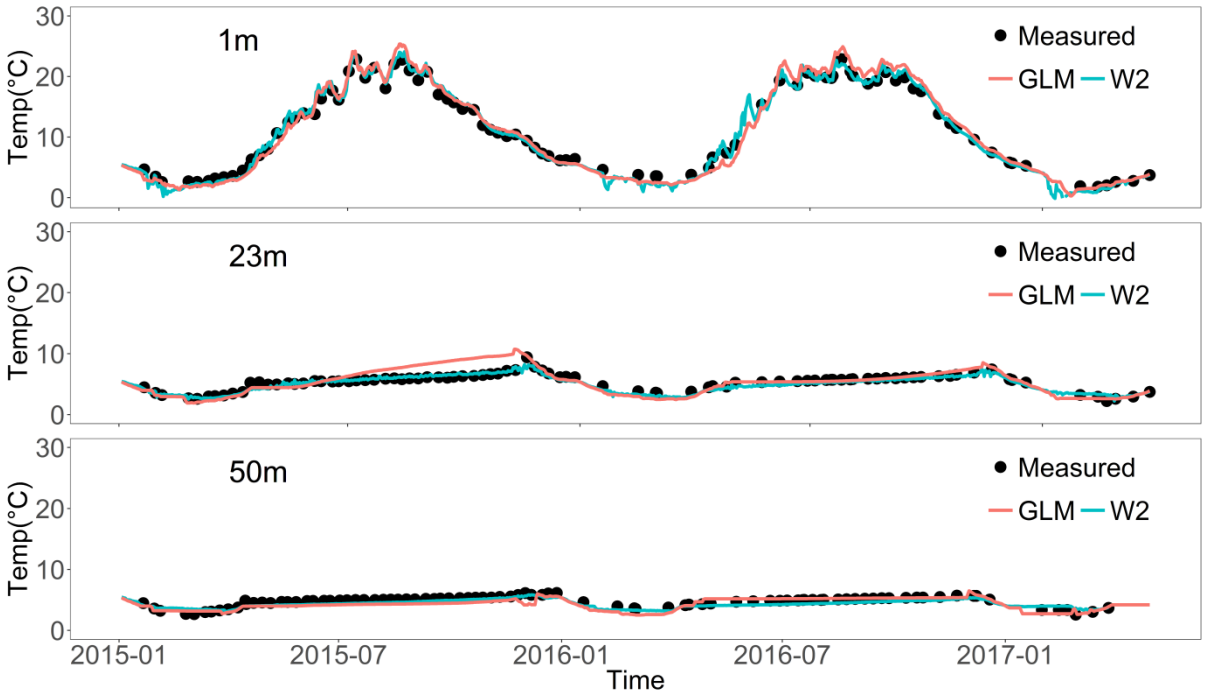


Figure 4.4. Simulated and measured water temperatures at 1 m, 23 m, 50 m depth.

The comparison of simulated and observed ice cover for both models is shown in Figure 4.5. For W2, there were 52 days of ice duration in the 2015/2016 winter, although no ice formation was observed in this winter. But both models successfully captured the observed ice cover for the 2016/2017 winter (Figure 4.5). For GLM, the ice-on date was well reproduced on 23$^{th}$ January but the ice-off was simulated 5 days later than the observation. By contrast, W2

exactly captured the observed ice-off date but simulated 5 days earlier for the ice-on date. Ice thickness was observed two times on January 31st and February 14th, 2017 and was measured to be 5.0 cm and 10.0 cm, respectively (Figure 4.5). GLM simulated ice thickness on these dates as 8.7 cm and 11.5 cm while W2 thicknesses of 7.5 cm and 8 cm, respectively. The results in Figure 4.5 also show that the simulated maximum ice thickness at 2017 appeared roughly at the same time by the two models (February 15th for GLM and February 12nd for W2). However, the maximum thickness by W2 was significantly larger than that by GLM (18.5 cm for the former and 11.7 cm for the latter).

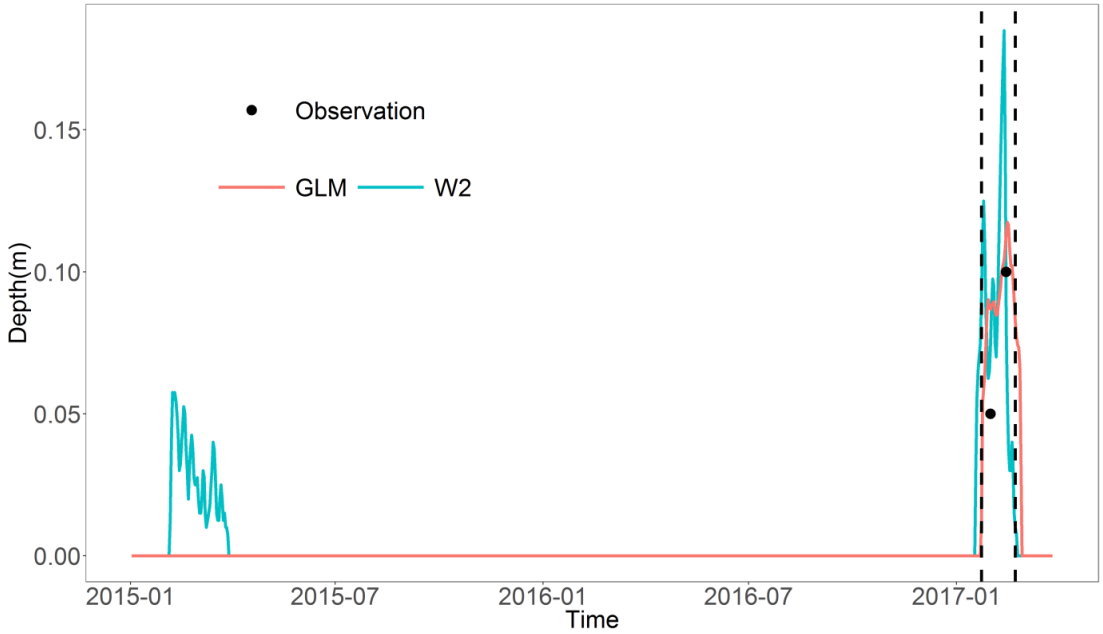


Figure 4.5. Simulated ice cover from W2 and GLM during the winters 2015/2016 and 2016/2017. The observed ice-on and ice-off dates are indicated by the vertical dashed lines. The two black dots indicate the measured ice depth at 2017-01-31 (5 cm) and 2017-02-14 (10 cm).

### 4.4.2. Scenario S1: Influencing ice dynamics by withdrawal regime

GLM and W2 performed differently when simulating ice cover under changing withdrawal elevations. From GLM, a tendency of earlier ice-on, delayed ice-off, and consequently longer ice duration was predicted with a higher withdrawal elevation (Figure 4.6). The duration of ice cover increased from less than 37 days (withdrawal elevation below 380 m a.s.l.) to 39 days (withdrawal elevation at 401 m a.s.l) and further to 41 days (withdrawal elevation 408 m a.s.l). It is reasonable to expect that a longer ice season is linked to larger ice thicknesses and vice versa. This is verified by our results showing that the mean and maximum ice thicknesses are consistent with ice duration: the Pearson correlation coefficient between mean ice thickness and ice duration was 0.91 (p-value $< 0.05$); the coefficient between the maximum thickness and the duration is 0.96 (p-value $<0.05$). By contrast, W2 was less sensitive to different withdrawal elevations. The ice duration was 33.5 days under bottom withdrawal (339 m a.s.l.) and increased very slightly to 34.25 days under top withdrawal (409 m a.s.l.). Similarly, the mean and maximum ice thicknesses calculated by W2 also remained rather stable under different

withdrawal elevations. In line with the calibration results, the maximum thickness predicted by W2 was noticeably higher than that from GLM over the range of withdrawal elevations applied (Figure 4.6).

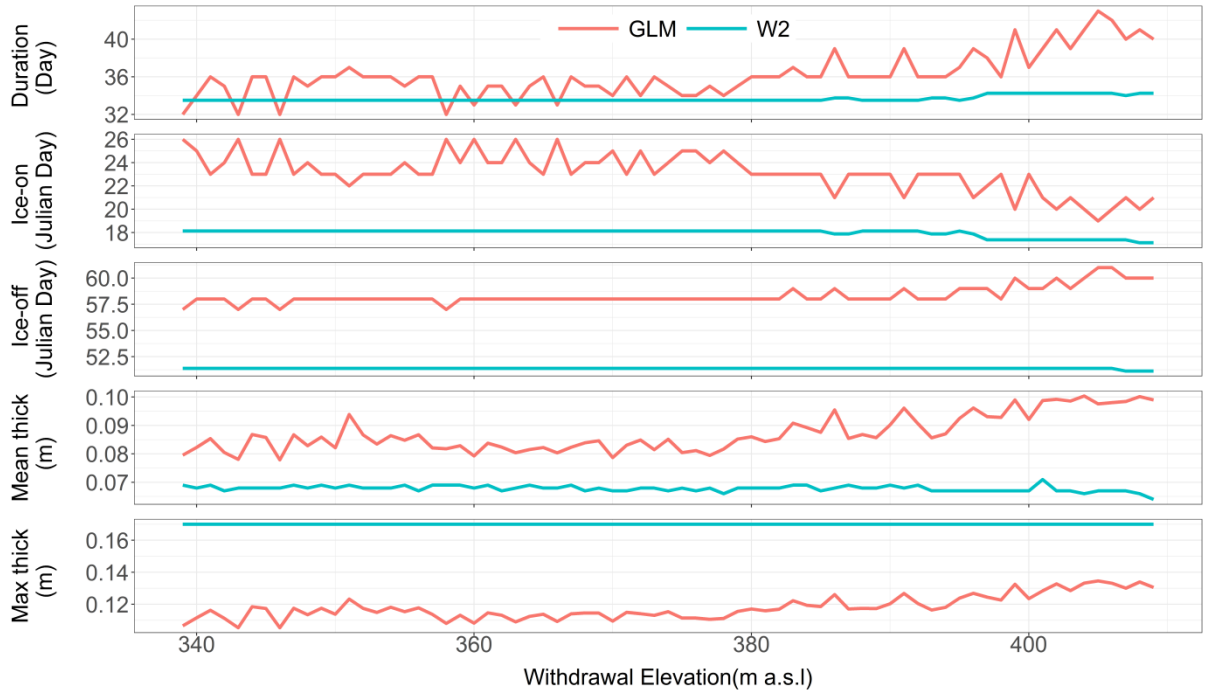


Figure 4.6. Simulation results for ice cover duration, dates of ice-on and ice-off as well as mean and maximum ice thickness for W2 and GLM at different withdrawal elevations during winter 2016/2017.

### 4.4.3. Scenario S2: Mixing regimes under different withdrawal and warming regimes

The duration of the inversed winter stratification in both years decreased with deeper withdrawal elevation and increasing air temperatures (Figure 4.7 and Figure 4.8). As a matter of course, the inversion phenomenon can entirely disappear if the air temperature is increased high enough. At a warming by 3.5 K, for example, results from both the two models showed that the winter inversion disappeared completely for the mild winter of 2015/2016 and the reservoir resorts to a monomictic mixing type (Figure 4.7). In the comparatively cold winter of 2016/2017, however, inverse stratification still persisted at this warming rate under all the withdrawal scenarios. Furthermore, it is possible to obtain the same inversion duration under different air temperature increases by adapting the withdrawal elevation accordingly (see Figure 4.9). According to the results from W2, for example, the inversion duration in the winter of 2016/2017 at 1 K warming increased gradually from 70 days (withdrawal elevation below 380 m a.s.l.) to 88 days (withdrawal elevation at 409 m a.s.l.); under 1.75 K warming the inverse duration can occur for 54 days (bottom withdrawal) or up to 75 days (surface withdrawal). When adjusting the withdrawal elevation to either bottom withdrawal (at 1 K warming) or around 403 m a.s.l (at 1.75 K warming), in consequence, the duration of winter inverse stratification is about the same. The effects from warming in winter conditions can thus be compensated by adjusting the withdrawal elevation to a specifically shallower depth.

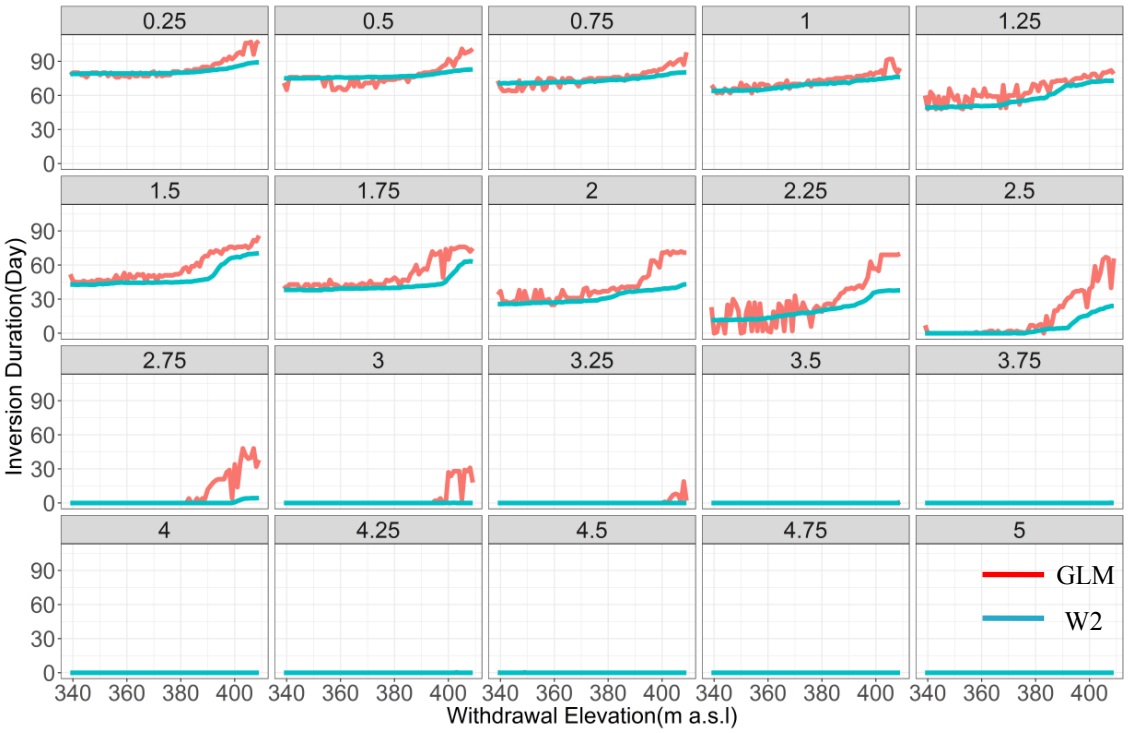


Figure 4.7. Response of the duration of inversed stratification in winter 2015/2016 to changes in air temperature (y-axis) and withdrawal elevation (x-axis).

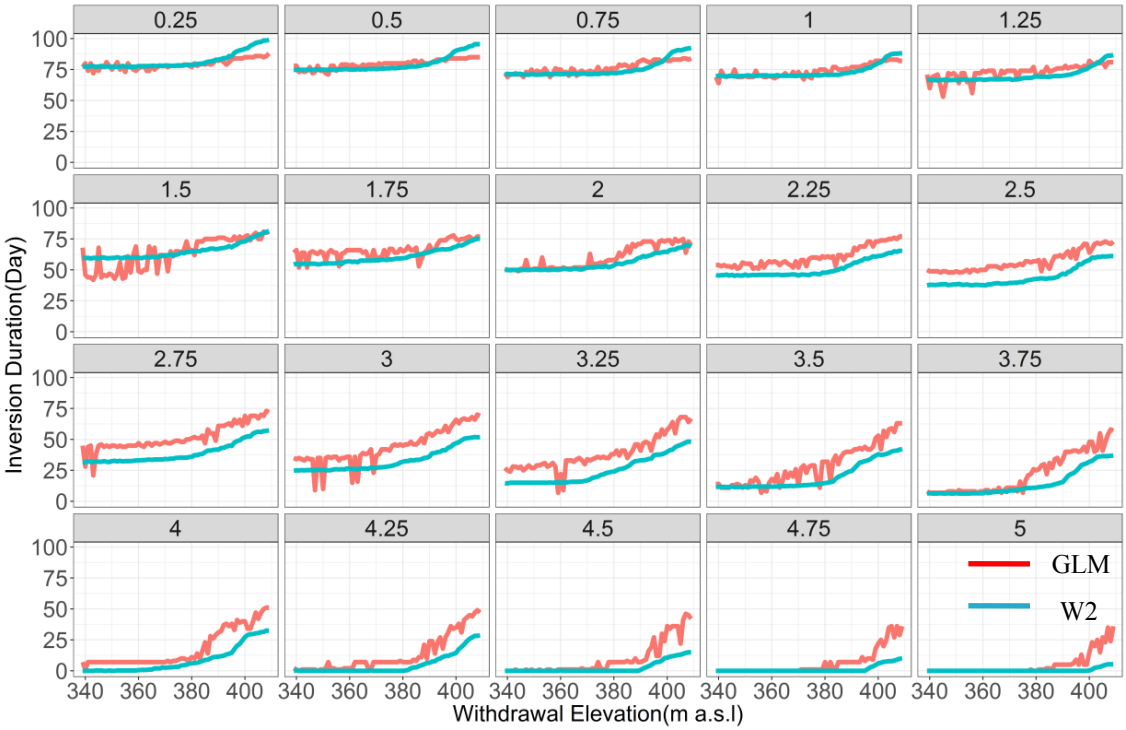


Figure 4.8. Response of the duration of inversed stratification in winter 2016/2017 to changes in air temperature (y-axis) and withdrawal elevation (x-axis).

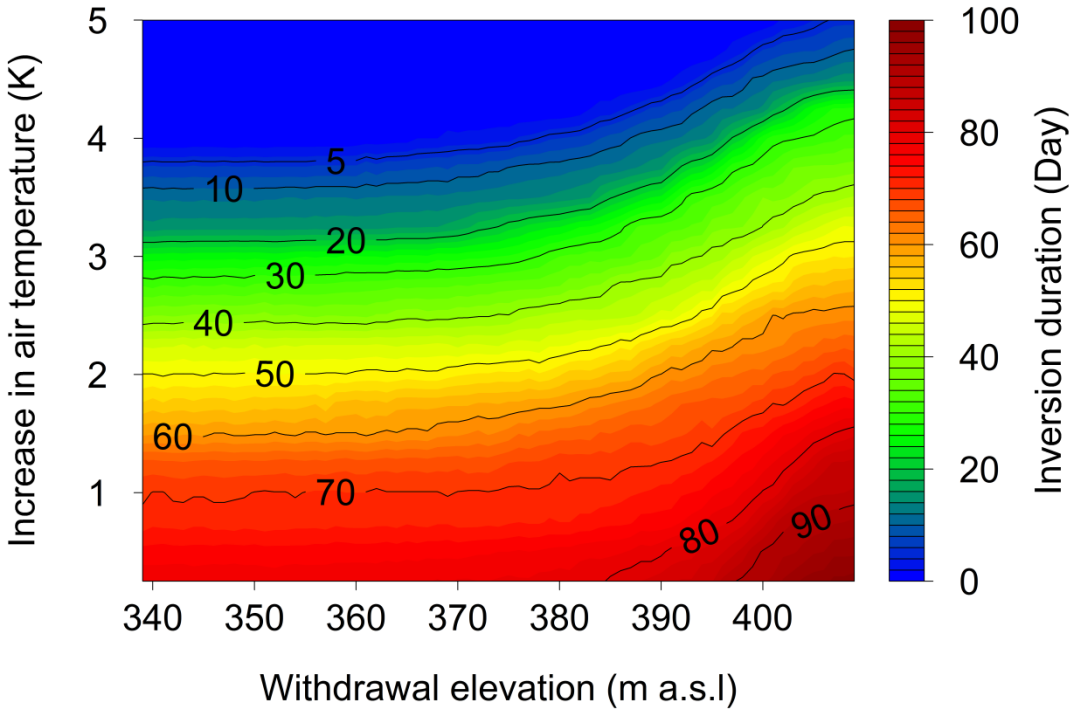


Figure 4.9. Combined effects of changes in withdrawal elevation and air temperature on the duration of winter inversed stratification (for winter 2016/2017, from W2).

However, Figure 4.7 and Figure 4.8 also indicate that the performance of inversion stratification differ between the two models. In each subplot, the inversion duration calculated from W2 shows much smoother changes than that from GLM, which showed discontinuous shifts in the predicted inversion duration making the exact quantitative outcome highly dependent on small scale variations in the simulation settings (e.g. in our case exemplified by the withdrawal elevation). It also appears that, compared to W2, the reaction of GLM to the variation in air temperature and withdrawal elevation was far more sensitive. The qualitative response patterns to warming and withdrawal elevation, however, remained independent of the model as GLM and W2 showed similar response shapes. Noteworthy, in all the climate scenarios, the stratification durations obtained from both models are close to each other. It should also be noted that, for the winter of 2015/2016, the inversion event began to disappear when air temperature increases beyond 2.25 K and 2.5 K, for GLM and W2, respectively. In the winter of 2016/2017, the current air temperature should be increased by 4.5 K and 4K for the two models so as to get the same effect.

## 4.5. Discussion

In this study, we used two hydrodynamic models, GLM and W2, to investigate the dynamics of the thermal structure and ice cover in the Rappbode Reservoir. The simulations of both models performed well in reproducing the water temperatures during the calibrated period

(01/2015 to 04/2017, see Figure 4.3). For the model calibration, the overall RMSE are 0.87 K (GLM) and 0.71 K (W2) both of which are lower than the errors presented in recent studies in which the two models were applied (Brito et al. 2018,Fenocchi et al. 2017,Ladwig et al. 2018,Lee et al. 2018,Park et al. 2018b,Read et al. 2014). Although the models slightly overestimated the metalimnetic temperature in the summer and early autumn (in particular GLM, see Figure 4.4), they performed well in reproducing the variation of surface temperature and stable temperature in the hypolimnion. The discrepancies between observed and simulated water temperatures may be linked to the insufficient modeling of internal waves which has been shown to have a significant influence on the thermal dynamics in the Rappbode Reservoir (Bocaniov et al. 2014). This process is fundamentally three dimensional so that it cannot be fully captured by 1D or 2D models. Moreover, both the two models use a constant light attenuation coefficient ($K_w$) which in reality is dynamic due to varying concentrations of algae and turbidity. As indicated by Bueche et al (2017), no provision of the seasonal variation of $K_w$ in the input file may also exert a negative influence on the simulation accuracy.

An ice cover was not present in the Rappbode Reservoir every winter hence capturing the occurrence of ice in different years can be an important criterion to compare model capability when simulating ice dynamics. For the ice component, GLM performed better than W2 because the former simulated the ice occurrence only for the winter of 2016/2017 which is consistent with the observations. For W2, there were 52 days of thin ice cover (< 5 cm) during the winter of 2015/2016 (Figure 4.5), although no ice was observed in that period. The appearance of additional ice in W2 can be linked to the fact that the model underestimates the surface temperature of that winter (see Figure 4.4). GLM accurately reproduced the ice-on date for the 2016/2017 winter but the simulated ice-off date was delayed by 5 days compared to the observation. These results are in accordance with the previous finding by Yao et al (2014). In their study, GLM was used to predict the ice cover of Harp Lake (Canada) under a future warming climate and the simulated ice-off dates were always later than expected. The delay of ice-off in both results shows that it is necessary to further improve the ice decay process in the model. We noted a few cases with negative surface water temperatures in W2, a phenomenon that is explained by the model specifications on ice dynamics. W2 applies a minimal ice thickness and during cooling episodes, negative water temperatures are accumulated before ice cover is formed in the simulation.

The different performance of inversion stratification between the two models can be clearly seen in Figure 4.7 and Figure 4.8. Compared to W2, the response of GLM seems overly sensitive to small changes in input (e.g. withdrawal elevation and air temperature). It seems that GLM reacts in a discontinuous way to changes in model parameters or model input data, which was already observed in previous research by Bueche et al (2017). It goes beyond the scope of this study to identify the reasons for this problematic behavior in GLM. We also do not exactly know why both models perform differently in our scenarios although it is obvious that both models have clear differences, e.g. in grid architecture (lagrangian vs. eulerian), heat budget calculations, or mixing algorithms. The fact that different models react differently in simulations with the same external drivers is due to structural differences between models (structured uncertainty). The application of model ensembles is the common strategy to account for structural uncertainty,

e.g. in hydrology (Ajami et al. 2007) or atmospheric sciences (Tebaldi and Knutti 2007). In lake modelling, however, the application of model ensembles is still rare although they were proven useful (Trolle et al. 2014). In conclusion, we believe that the application of two models is a major strength of our approach because we can show that quantitative results vary between models but the basic outcome is independent of the used model. We encourage future lake model studies to exploit multi-model ensembles wherever possible in order to provide information on structural model uncertainties and to improve reliability of outcomes. Comparative model applications will furthermore help to identify the strengths and weaknesses of existing models.

Our study clearly elucidates the response of winter inversed stratification to climate change, combined with water management options. It is reasonable that climate warming leads to a shortening of the period of inversed stratification (see Figure 4.7 and Figure 4.8) and the inversion phenomenon can entirely disappear if the air temperature is increased high enough. It implies that, under strong warming in the future, the Rappbode Reservoir may change into a monomictic mixing type. Our findings are confirmed by those of Kirillin (2010) who predicts that by the end of the 21$^{st}$ century, most deep lakes in northeastern Germany will change their mixing type to warm monomictic (Kirillin 2010). In addition to this, our results indicate that under a small increase of air temperature (less than 3 K), adjusting the withdrawal elevation can be used to manage the inversed stratification so as to mitigate the influence caused by climate warming. Under the same weather conditions, a shallower withdrawal elevation will result in longer inversed stratification and, in turn, can offset the effects of further warming. If the air temperature is increased too much (higher than 4 K), however, the potential of withdrawal strategy to stabilize inversed stratification is gradually diminishing. These findings complements the study of Kerimoglu and Rinke (2013), which focused on the response of summer stratification to the changing withdrawal regime (Kerimoglu and Rinke 2013). The latter study confirms that the surface withdrawal reduces the mixing events in summer. Our study emphasizes such effects on the thermal structure in winter, which were not addressed by Kerimoglu and Rinke (2013). A changing wind condition in a warmer climate may be able to modify stratification further (compare Mi et al. 2018) but only very high winter storms could prevent the occurrence of inversed stratification due to high mixing intensities.

The effect of the withdrawal strategies on the duration of winter inversed stratification can be explained by the difference in internal heat energy stored in the reservoir under different withdrawal elevations. The deeper water withdrawals will store more heat energy in the reservoir. For example, we compared the internal heat energy under the real climatological conditions based on the surface (409 m a.s.l) and bottom (340 m a.s.l) withdrawal elevations (see Figure 4.10). The heat energy per surface area can be defined as:

$$E=\frac{\int_0^{z_{max}} CT\rho_z A_z dz}{A_0} \tag{4.2}$$

where C is the specific heat capacity of water (4186 J/kg/K), T is the water temperature (in °C), $\rho_z$ is the water density, $A_z$ is the area at depth z, $A_0$ is the surface area and $Z_{max}$ is the maximum water depth. It can be seen that the internal heat energy of the water column using bottom

withdrawal is far higher than that using surface withdrawal. Therefore, bottom withdrawal will enlarge the heat storage and by that delay the occurrence of inversed stratification because longer periods of cold weather are required to release the stored heat out of the water body.

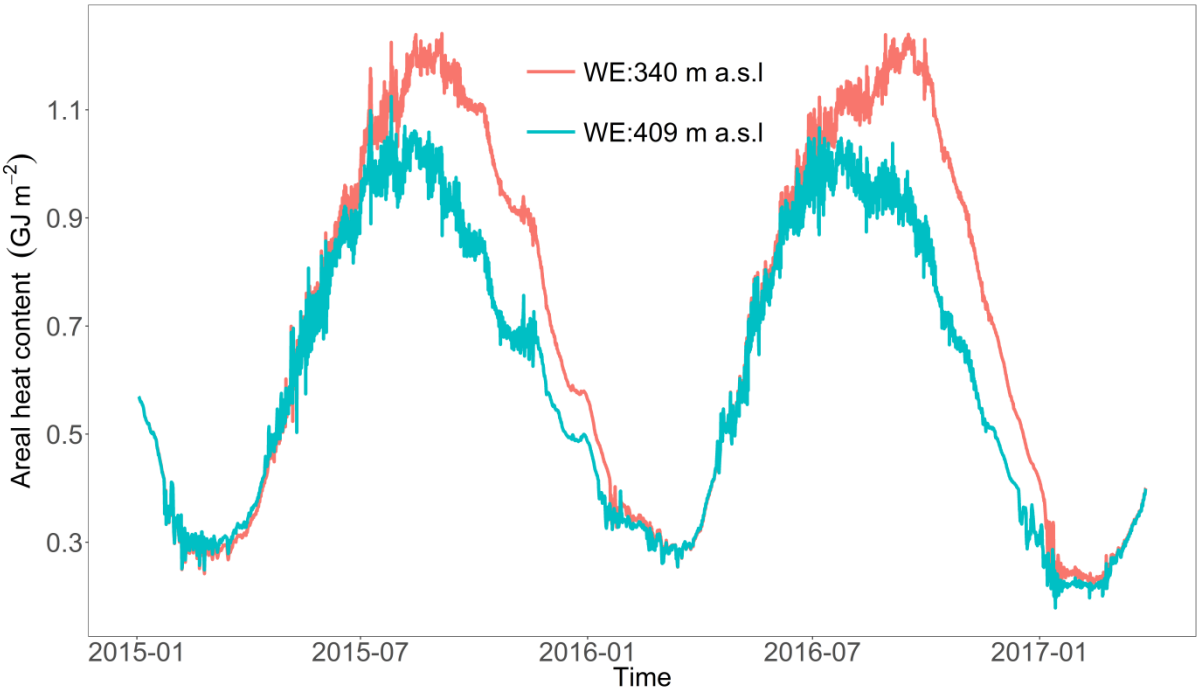


Figure 4.10. Internal heat content per surface under surface (green line) and bottom (red line) withdrawal strategy (from W2).

Previous studies have shown that, under climate warming, numerous dimictic water bodies have the potential to change to a monomictic mixing type which may result in a negative influence on lentic aquatic ecosystems (Ficker et al. 2017,Peeters et al. 2002). Our results indicate that the withdrawal elevation can be used as a management method to mitigate the negative influence caused by warming on the mixing regime. This option is only available in reservoirs with flexible outtake structures while it is unavailable in natural lakes that always withdraw from the surface. Nevertheless, a change from dimictic to warm monomictic in a warmer world can in fact be avoided in many temperate reservoirs by adjusting the withdrawal elevation. This is a new management option in reservoir management that can be relevant for many reservoirs and overlooked in reservoir operation, which typically do not make much use of withdrawal elevation as a management instrument. Before implementation of a changing withdrawal management, however, potential side effects on water quality need to be evaluated, e.g. on deep water oxygen content, internal loading, and nutrient export. Therefore, it is worthwhile for future work to elucidate the response of other water quality variables (i.e. oxygen, nutrients, toxins) to these withdrawal strategies and to integrate such strategies into the multi-objective view required in sustainable reservoir management (Schwefel et al. 2016,Weber et al. 2017).

## 4.6. Conclusions

- Two well-established hydrodynamic models (GLM and W2) showed good performance in reproducing the water temperature and ice cover in the Rappbode Reservoir, the largest drinking water reservoir in central Germany.
- Winter inversed stratification of the reservoir can entirely disappear under the current management regime if climate warming is getting strong (>4 K warming). In other words, the Rappbode Reservoir may change from a dimictic to a monomictic mixing type under strong climate warming.
- Adjusting the withdrawal strategies can strongly influence the winter conditions and can mitigate the effect of climate warming on mixing type. Shallow withdrawal elevations will reduce internal heat energy stored in the reservoir over the summer and thus enable to conserve the dimictic state even in a much warmer climate (>4 K).
- Withdrawal management is a so-far largely unexploited operational tool in climate change mitigation in reservoirs of the temperate zone.

# 5. Ensemble warming projections in Germany's largest drinking water reservoir and potential adaptation strategies

## 5.1. Abstract

Thermal structure in reservoirs affects the development of aquatic ecosystems, and can be substantially influenced by climate change and management strategies. We applied a two-dimensional hydrodynamic model to explore the response of the thermal structure in Germany's largest drinking water reservoir, Rappbode Reservoir, to future climate projections and different water withdrawal strategies. We used projections for representative concentration pathways (RCP) 2.6, 6.0 and 8.5 from an ensemble of 4 different global climate models. Simulation results showed that epilimnetic water temperatures in the reservoir strongly increased under all three climate projections while hypolimnetic temperatures remained rather constant under RCP 2.6 and RCP 6.0 but increased markedly under RCP 8.5. Under the intense warming in RCP 8.5, hypolimnion temperatures were projected to rise from 5 °C up to 8 °C by the end of the century. Stratification in the reservoir was projected to be more stable under RCP 6.0 and RCP 8.5, but did not show significant changes under RCP 2.6. Similar results were found with respect to the light intensity within the mixed-layer. Moreover, the results suggested that surface withdrawal can be an effective adaptation strategy under strong climate warming (RCP 8.5) to reduce surface warming and avoid hypolimnetic warming. This study documents how global scale climate projections can be translated into site-specific climate impacts to derive adaptation strategies for reservoir operation. Moreover, our results illustrate that the most intense warming scenario, i.e. RCP 8.5, demands far-reaching climate adaptation while the mitigation scenario (RCP 2.6) does not require adaptation of reservoir management before 2100.

## 5.2. Introduction

The thermal structure of standing waters, which is the vertical distribution of water temperature, is a key factor for lentic ecosystems and their water quality. The emerging vertical gradients in the water column and their dynamics are strongly affected by meteorological drivers (Read et al. 2014,Trolle et al. 2019) making the thermal structure of lakes highly sensitive to climatic changes (Valerio et al. 2015,Woolway and Merchant 2019). Stratification affects nutrient cycling, algal and cyanobacterial dynamics, and the trophic status of water bodies (Posch et al. 2012,Read et al. 2011,Yang et al. 2018). Vertical gradients of temperature cause density stratification, which limits vertical transport in stratified lakes and leads to hypolimnetic oxygen depletion and subsurface oxygen minima (Kreling et al. 2017,Müller et al. 2012). By analyzing the metabolic rates of lakes, Coloso et al. (2011) even pointed out that primary production and

ecosystem respiration processes were sensitive to short-term dynamics of thermal stratification. Therefore, a sound understanding of thermal stratification and its dynamics is the key for a thorough analysis and prognosis of lentic ecosystems.

Climate change was shown to significantly affect the thermal structure of freshwater systems (Fang and Stefan 2009,Fenocchi et al. 2018,Sahoo et al. 2015,Yang et al. 2019). A long-term analysis of water temperature suggested that lake stratification, at the global scale, is mainly controlled by the climate conditions (Kraemer et al. 2015). Changes of different climate factors (i.e. increase in solar radiation and air temperature, decrease in cloud cover) together explain the high warming rates observed in ice-covered lakes (O'Reilly et al. 2015). Mixing regimes, a key feature of lakes, are particularly sensitive to climatic drivers (Shatwell et al. 2019,Woolway and Merchant 2019). By using a 1 dimensional hydrodynamic model, Sahoo et al. (2013) predicted, for example, that Lake Tahoe will stop mixing to the bottom after 2060 because of climate warming, which will lead to a severe depletion of dissolved oxygen in the hypolimnion. While many studies have focused on the relationship between thermal structure and climate change in lakes, very few studies specifically considered this relationship in reservoirs (Lewis Jr et al. 2019).

Compared to lakes, reservoirs respond differently to climate change because they have a different outlet location: in lakes, water is almost always released from the surface layer, whereas in reservoirs, water is often withdrawn selectively from deeper layers. This can strongly affect the thermal structure (Bonnet et al. 2000,Ma et al. 2008). The deep water withdrawal strategy, which is used in most reservoirs located in Europe and North America, releases the coldest water, weakens stratification and results in hypolimnetic warming (Weber et al. 2017). In contrast, surface withdrawal releases the warmest water and preserves the cold hypolimnetic waters (Ma et al. 2008). Kerimoglu and Rinke (2013) concluded that exporting water from the surface will stabilize summer stratification in Bautzen reservoir by preserving the cold hypolimnetic water. Mi et al. (2019) also showed carry-over effects into winter arising from surface withdrawal in a deep reservoir. These findings gave rise to the idea that selective water withdrawal can be used as a management strategy to dampen the effect of future climate change on mixing regime, which is at the center of this study.

Climate change predictions, however, are associated with uncertainties arising from emission pathways (Lopez et al. 2015) and technical features of the global circulation models (GCM). For example, future climate conditions under RCP 8.5 (representative concentration pathway), which corresponds to the highest greenhouse gas concentration trajectory without adaptation strategies, will be dramatically warmer than under RCP 2.6, representing the lowest concentration trajectory due to a major turnaround in climate policies in the near future (IPCC 2014). On the other hand, even within the same climate trajectory, the future projections of different climate models can vary widely since every model relies on its specific parameters and assumptions to depict the relationship between atmosphere circulations, underlying surfaces and ocean effects (Smith 2002). Drawing conclusions from an ensemble of climate models to portray the future climate conditions is more robust because the model-borne uncertainties in climate projections can be effectively included in this approach (Wiens et al. 2009). It was therefore our intention to explicitly account for uncertainties in climate models by applying outputs from

different GCMs and for different emission pathways as provided by the Inter-Sectoral Impact Model Intercomparison Project (ISIMIP) initiative (Warszawski et al. 2014).

In this study, a well-established hydrodynamic model CE-QUAL-W2 (hereafter W2) was used to analyze the response of thermal structure in the Rappbode Reservoir to future climate change. The innovative points in our study include: (i) a detailed investigation of the stratification dynamics in Germany's largest drinking water reservoir to warming scenarios under different RCP greenhouse gas emissions (RCP 2.6, RCP 6.0 and RCP 8.5) driven by an ensemble of global climate models; (ii) an assessment of whether alternative management scenarios with different water withdrawal depths can be used to mitigate climate warming effects on thermal structure and mixing regimes. The aim of our research is to clarify the response of thermal stratification and physical gradients within the water column in reservoirs to climate change and to guide reservoir operators to optimize their management strategies under the expected global warming trend.

## 5.3. Methods

### 5.3.1. Study site

Rappbode Reservoir, which is located in the eastern Harz Mountains, is the largest drinking water reservoir in Germany with a mean depth of 28.6 m (Figure 5.1). It is the core of the Rappbode system, a network of 6 reservoirs with multiple functions such as providing environmental flows, flood protection, recreation, hydropower, and drinking water supply (Mi et al. 2018). The reservoir receives water from two inflows (Hassel and Rappbode pre-reservoirs) and a transfer gallery from Königshütte Reservoir. It has five outlets from the bottom to the surface (at elevations from 360-400 m a.s.l at 10 m intervals) to discharge raw water towards the drinking water plant. The two hypolimnetic outlets (i.e. 360 and 370 m a.s.l) are used most of the time and the other three are rarely open. There is an additional outlet at an elevation of 345 m a.s.l, which discharges water into the downstream Wendefurth Reservoir (Mi et al. 2019,Rinke et al. 2013b). The reservoir is a typical dimictic water body which is stratified in summer and winter and fully mixed in autumn and spring. Its residence time is a little more than a year (380 days). Based on long-term measurements, the phosphorus concentration in the reservoir decreased strongly after 1991 due to the reduced use of detergents with phosphates so that the reservoir changed from a eutrophic to an oligotrophic state (Wentzky et al. 2018b).

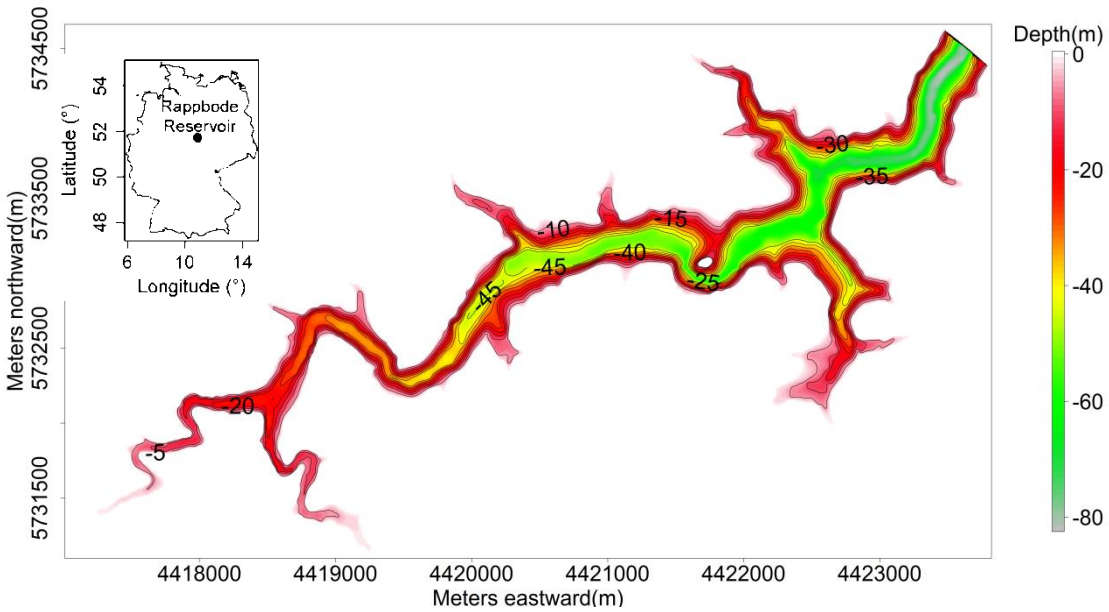


Figure 5.1. The location and contour map of Rappbode Reservoir.

### 5.3.2. Hydrodynamic model

The latest version of W2 (V 4.1) was employed in this study. The source code of the model was written in Fortran and its first version was launched in 1975 by the US Army Corps of Engineers, while the model was further developed and maintained by researchers at Portland State University (Cole and Wells 2006,Sadeghian et al. 2018). The model has been successfully used in simulating hydrodynamics (e.g. stratification, internal waves) and ecological processes (e.g. oxygen dynamics, phytoplankton bloom) in different lakes and reservoirs worldwide (Chuo et al. 2019,Kobler et al. 2018,Terry et al. 2017,Uhlmann 2017). Its source code can be freely downloaded from the official website (http://www.ce.pdx.edu/w2/) so users can modify the model based on their own demands. More information about the algorithms used in the model and its application history can be found in the user manual (http://reviewboard.ca/upload/project_document/EA1314-01_CE-QUAL-W2_2D_Laterally_Averaged_Hydrodynamic__and_WQ_Model_-_User_Manual.PDF).

In this study, we built the computational grid for Rappbode Reservoir according to the geometric data measured by the reservoir authority (Talsperrenbetrieb Sachsen-Anhalt). The input geometry of the model includes four branches, with two branches for side arms, which enables an accurate representation of the reservoir shape (see Figure S1 in Appendix 4). The entire reservoir was split into 106 longitudinal segments with lengths ranging from 100 m to 400 m and widths ranging from 5 m to 700 m, the vertical thickness of all grid cells was 1m resulting overall in 3976 model cells. The elevation-volume relationship generated by the model corresponded well with the original relationship derived from a digital elevation model, which proves the accuracy of the input bathymetry.

### 5.3.3. Model setup and calibration

Boundary conditions for driving the model include time series of meteorological variables (i.e. air temperature, wind speed and direction, shortwave radiation, dew point temperature, cloud cover), inflow data (i.e. discharge and temperature) and outflow discharge. For model calibration, we used meteorological reanalysis data from the EWEMBI dataset after bias correction, based on the ISIMIP dataset (Frieler et al. 2017). The reanalyzed climate data were provided with daily resolution. This database was employed for the calibration because future climate projections in this study were also driven by similar gridded climate products at daily resolution.

The model was calibrated from January 2nd 2015 to December 31st 2016. This two-year period was selected because high-quality water temperature measurements were available in this time. During this period, the bias-corrected reanalysis from the EWEMBI dataset agreed well with climate observations at Rappbode Reservoir (Figure 5.2). The air temperature, wind speed and shortwave radiation were directly taken from EWEMBI. Wind direction was calculated based on the eastward and northward wind speed components from the reanalysis data. We calculated dew point temperatures based on reanalyzed relative humidity and air temperature according to the following equation (Bolton 1980):

$$T_{dp} = \frac{\lambda\left(ln\left(\frac{RH}{100}\right)+\frac{\beta T}{\lambda+T}\right)}{\beta-\left(ln\left(\frac{RH}{100}\right)+\frac{\beta T}{\lambda+T}\right)} \qquad (5.1)$$

where $T_{dp}$ is the dew point temperature (in °C), $T$ is the air temperature (in °C), $RH$ is the relative humidity (in %), and $\lambda = 237.7°C$ and $\beta = 17.27$ are constants. Cloud cover was calculated from the reanalyzed longwave radiation and air temperature based on the formula in the source code of W2 and Swinbank (1963):

$$C = \sqrt{\frac{\frac{R}{0.97\times5.31\times10^{-13}\times(273.15+T)^6}-1}{0.0017}} \qquad (5.2)$$

where R is the incoming longwave radiation (in W $m^{-2}$), and C is the cloud cover (0-10).

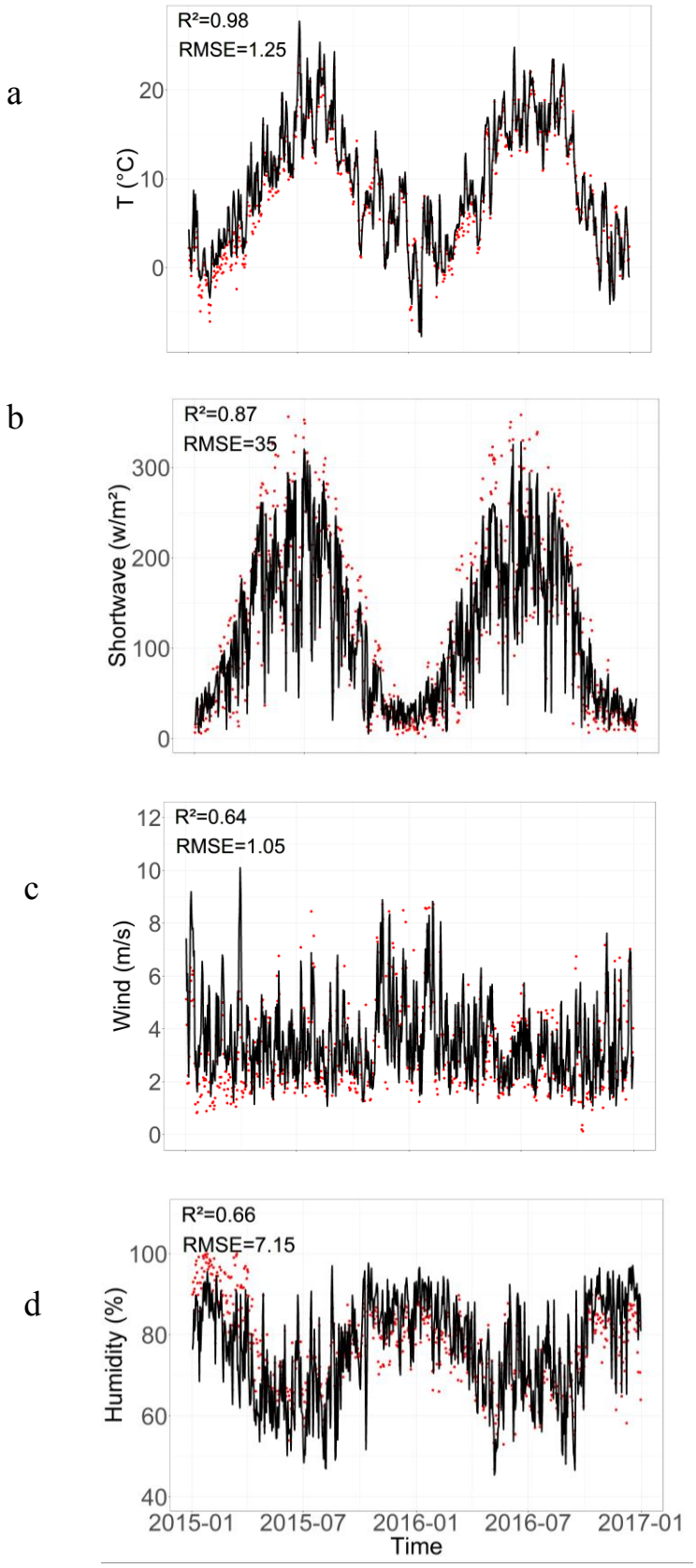


Figure 5.2. Comparison between reanalysis data from EWEMBI (lines) and observed (points) climate data for (a) air temperature, (b) shortwave radiation (c) wind speed (d) relative humidity.

The inflow and outflow rates were provided by the reservoir authority. Inflow water temperatures were drawn from a YSI-6200 probe at the pre-reservoirs and Königshütte Reservoir (see Mi et al. 2018). All hydrological boundary conditions were put into W2 at a daily resolution.

Initial water temperatures for initialising the model were measured by a Hydrolab DS5 probe at the deepest point of the reservoir. Biweekly temperature measurements were used for model calibration (see Mi et al. 2018). Based on the user manual of W2 (Cole and Wells 2006) and our previous study (Mi et al. 2019), WSC (wind sheltering coefficient), SHADE (shade reduction factor) and EXH2O (light extinction coefficient) are the most important parameters for water temperature predictions and were used for calibration. All the other parameters were kept at default values. The coefficient of determination ($R^2$) and root-mean-square-error (RMSE) were used to evaluate the model performance since these two indicators have been widely used in related studies for model calibration (Chuo et al. 2019,Thiery et al. 2014). After a manual "trial and error" procedure, WSC and EXH2O were set to 0.9 and 0.55 $m^{-1}$, while SHADE was kept as its default value (i.e. 1). All the three values were in the appropriate range for the Rappbode Reservoir.

### 5.3.4. Response of thermal structure to climate change

The calibrated model was forced with three climate projections (RCP 2.6, RCP 6.0 and RCP 8.5) to analyze the response of the thermal structure in Rappbode Reservoir to future climate. RCP stands for "Representative Concentration Pathway", which was put forward in the IPCC Fifth Assessment Report in 2014 (IPCC 2014) and the following number represents the assumed increase of radiative forcing values in 2100 (i.e. 2.6, 6.0, 8.5 W $m^{-2}$, respectively , see Moss et al. 2008). In the three projections, RCP 2.6 predicts the lowest global warming trend in which the annual mean air temperature in the period 2081-2100 is expected to increase by 0.26-0.55 °C compared to the period 1986-2005. RCP 8.5 on the other hand predicts the highest trend with a temperature increase of 2.6-4.8 °C. The trend of RCP 6.0 is intermediate with a warming of 1.4-3.1 °C (Meinshausen et al. 2011). The projections were downloaded from the freely accessible ISIMIP database for the years 2006-2099 and each RCP scenario was separately calculated by four climate models, i.e. HadGEM2-ES, MIROC5 GCM, IPSL-CM5A-LR, and GFDL-ESM2M (hereafter HadGEM2, MIROC5, IPSL and GFDL, respectively). The ISIMIP climate data, with daily resolution, have been bias corrected for the required meteorological variables.

Daily averaged inflow and outflow rates were used to derive a long-term average seasonal cycle using a circular generalized additive model (GAM). The GAM was fitted to long-term measurements from 1996-2015 with the day of the year as explanatory variable. These GAM-based long-term averages were used as hydrological boundary conditions in all simulations and repeated for each year in the period (2006-2099). Water withdrawal in the simulations was based on the current management strategy (shown in part 5.3.1), where the two hypolimnetic outlets at 360 and 370 m a.s.l were used for the raw water supply, and the other outlet at 345 m a.s.l was

used for the downstream discharge into Wendefurth Reservoir.

Since no inflow water temperatures were provided from the ISIMIP database, we built a piecewise linear regression between observed water temperature ($T_W$) and air temperature ($T_A$) based on measurements for 2014-2019 ($R^2 = 0.88$):

$$\text{For } T_A \leq 2.275\ °C, T_w = 0.206T_A + 2.49 \qquad (5.3)$$

$$\text{For } T_A > 2.275\ °C, T_w = 0.964T_A + 0.76 \qquad (5.4)$$

This function was used to calculate inflow temperature based on the projected air temperature within each climate scenario. A similar approach can be found in Bueche and Vetter (2015).

### 5.3.5. Alternative management scenarios using different withdrawal strategies

To elucidate how different withdrawal strategies can modify climate warming effects on the future water temperatures, we firstly simulated a scenario in which all the water was discharged from the top outlet (i.e. 400 m a.s.l, the complete surface withdrawal), instead of from several hypolimnetic outlets as described in part 5.3.1. Note that this scenario corresponds to the situation in a natural lake where all water leaves the water body from the surface layer. Secondly we simulated a scenario in which the drinking water was still taken from the hypolimnion (i.e. 360 and 370 m a.s.l), but the downstream withdrawal to Wendefurth was taken from the epilimnion at 400 m a.s.l (i.e. the partial surface withdrawal). This second scenario was implemented because hypolimnetic water is preferred for drinking water due to its low temperature and turbidity throughout the year. Since we were interested in the interactions between withdrawal management and climate change, all management scenarios were based on the most extreme climate scenario (RCP 8.5).

### 5.3.6. Thermal indices and statistics

Thermal indices used in this study include water temperatures at 1 m, 10 m and 50 m depth, Schmidt stability, mixed-layer thickness, and averaged light intensity within the mixed-layer. The mixed-layer was considered as the water stratum between the surface and the layer with minimum second order difference in temperature ($T$) with respect to depth ($z$), i.e. $min\left(\frac{\partial^2 T}{\partial z^2}\right)$ (Kirillin et al. 2013). Schmidt stability, indicating the total energy required to mix the water column, was calculated according to the equation from Schmidt (1928):

$$S = \frac{g}{A_s} \int_0^{z_{max}} (z - z_*)(\rho_z - \rho_*) A_z dz \qquad (5.5)$$

where $S$ is the Schmidt stability (in J $m^{-2}$), $g$ is the gravitational acceleration, $A_s$ is the surface area of the reservoir, $z_{max}$ is the maximum depth of the reservoir, $\rho_z$ and $A_z$ are the water density and area at depth $z$, respectively. The value of $z_*$ denotes the depth at the center of volume calculated as:

$$z_* = \frac{\int_0^{z_{max}} z A_z dz}{\int_0^{z_{max}} A_z dz} \qquad (5.6)$$

and $\rho_*$ is the density at $z_*$.

Light intensity as photosynthetically available radiation (PAR) at depth $z$ ($I_z$, in mol $m^{-2}$ $day^{-1}$) was calculated based on the Lambert-Beer law:

$$I_z = \alpha\beta I_0 e^{-\varepsilon z} \qquad (5.7)$$

where $\alpha$ is 0.4 which is the conversion factor from Watts into mol PAR $day^{-1}$, $\beta$ is the fraction of solar radiation penetrating the water surface, which is 0.45 as recommended in Williams (1981), $I_0$ is the solar radiation at the water surface (in W $m^{-2}$), $\varepsilon$ is the light extinction coefficient which is set as 0.55 $m^{-1}$ according to the model calibration result shown above. Then the averaged light intensity within the mixed-layer ($I_m$) was obtained by integrating the expression above over the layer:

$$I_m = \frac{\alpha\beta I_0}{\varepsilon Z_{ML}}(1 - e^{-\varepsilon Z_{ML}}) \qquad (5.8)$$

where $z_{ML}$ is the mixed-layer thickness.

In order to aggregate the daily resolved water temperature dynamics, we calculated annual averaged water temperatures at different depths, while the other stratification indices were calculated based on their mean summer values (July to September) in each year. The non-parametric Mann-Kendall test (Hipel and McLeod 1994) and Theil-Sen method (Sen 1968) were used to assess the significance and slope of the changing trends. All the post-processing and statistical tests were performed in R version 3.3.2 (R Core Team 2016b).

## 5.4. Results

### 5.4.1. Model calibration

The calibrated model, driven by the EWEMBI climate data, performed well in capturing the main characteristics of the thermal structure in Rappbode Reservoir. Simulated water temperatures were in good agreement with observations (RMSE=0.61°C, $R^2$ = 0.98; see Figure 5.3 & Figure 5.4). The annual mean water temperature over the whole water column based on the simulation results was 6.45 °C, which was very close to the calculated mean water temperature from the measurements (6.36 °C). The model accurately reproduced the general stratification patterns and all temperature dynamics in the two summers, although it slightly underestimated the surface water temperature in the 2015/2016 winter (Figure 5.3).

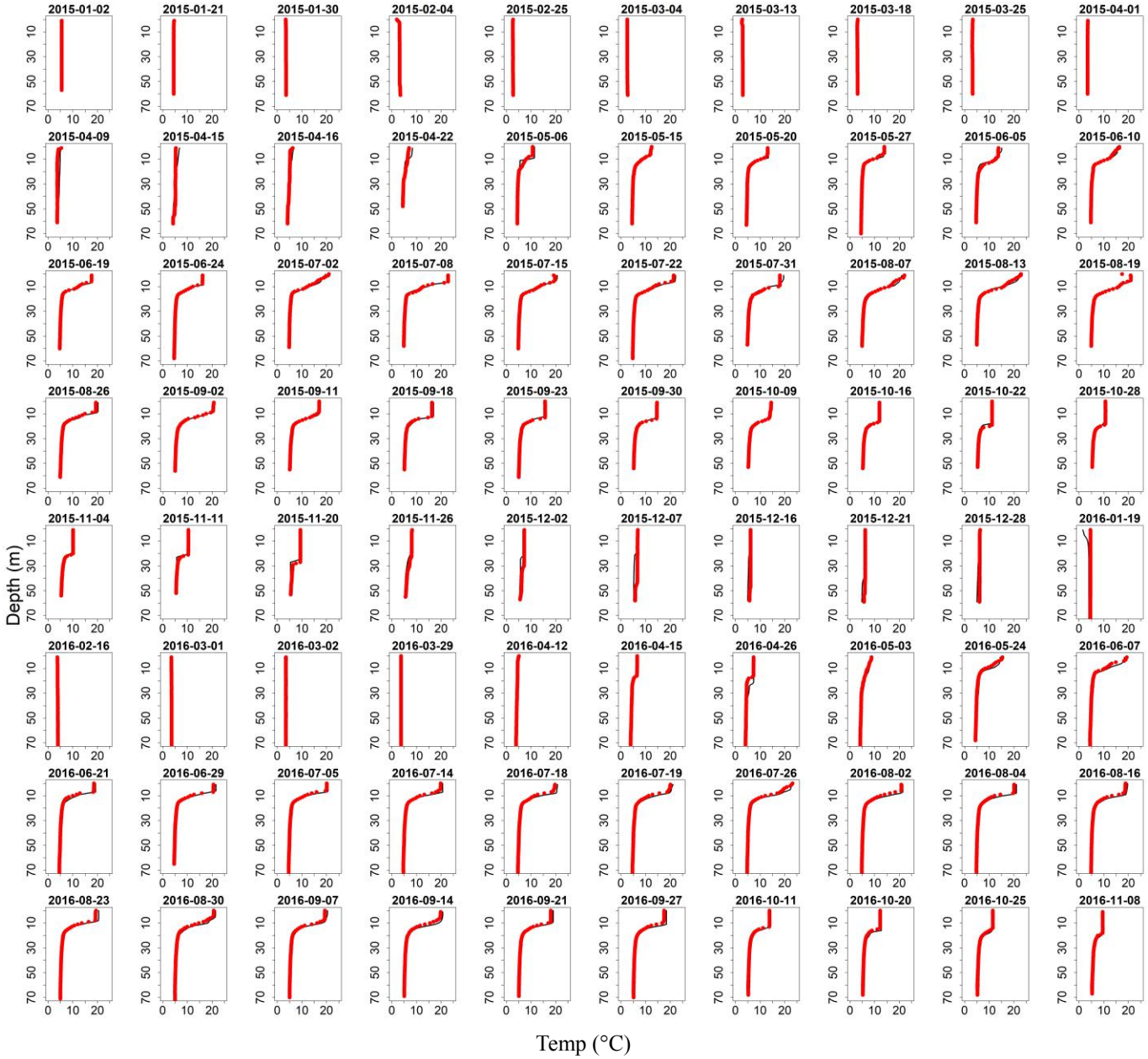


Figure 5.3. Comparison between simulated (black lines) and observed (red points) water temperature profiles in 2015 and 2016.

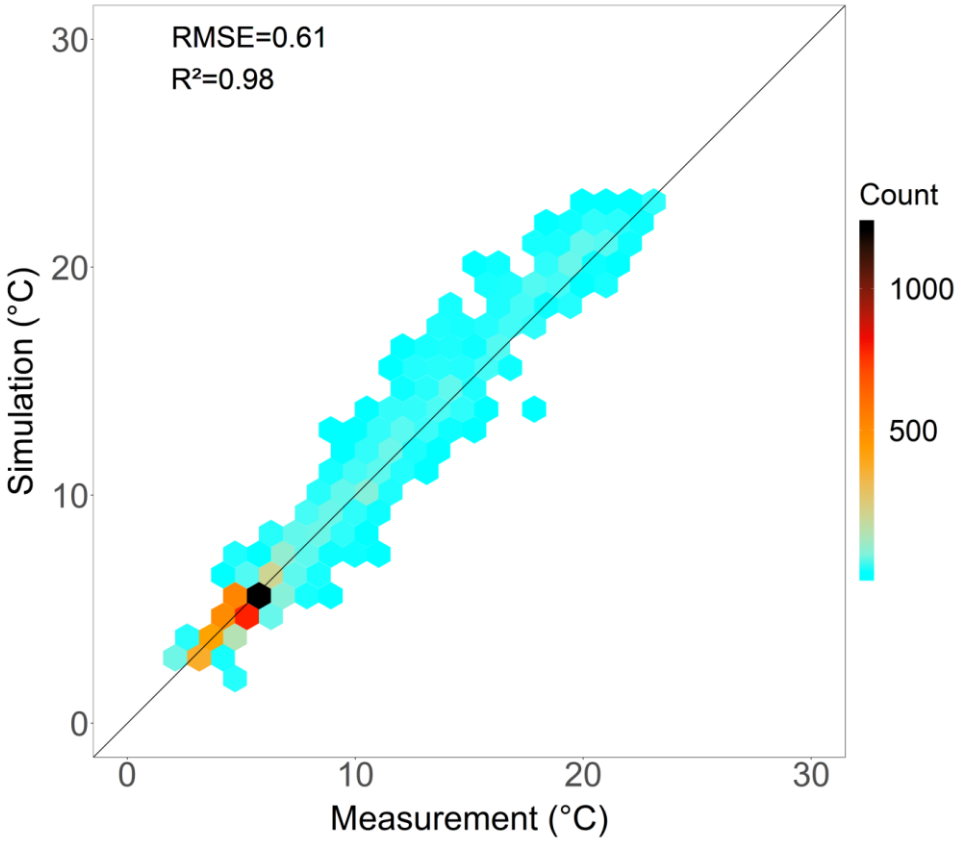


Figure 5.4. Comparison between simulated and measured water temperatures for all depths. The color bar depicts the amount of samples per hexagon. The black line has a slope of one and an intercept of zero (1:1 line).

### 5.4.2. Climate projections

The annual mean air temperature increased significantly in the future projections by 0.05, 0.3 and 0.5 °C decade$^{-1}$ under RCP 2.6, RCP 6.0 and RCP 8.5, respectively (average value over all 4 GCMs, see Table 5.1). Similar trends were evident for longwave radiation, which is directly connected to air temperatures according to the Stefan-Boltzmann law, with the strongest increases under RCP 8.5 (2.66 W m$^{-2}$ decade$^{-1}$) and weakest increases under RCP 2.6 (0.24 W m$^{-2}$ decade$^{-1}$). Shortwave radiation increased at a similar rate under RCP 6.0 (1.09 W m$^{-2}$ decade$^{-1}$) and RCP 8.5 (1.07 W m$^{-2}$ decade$^{-1}$), which was 1.6 times higher than that under RCP 2.6 (0.68 W m$^{-2}$ decade$^{-1}$). The projected wind speed did not change significantly under RCP 2.6 and RCP 6.0, but slightly decreased by 0.03 m s$^{-1}$ decade$^{-1}$ under RCP 8.5 (see Table 5.1).

Table 5.1. Projected trends (2006-2099) in climate variables, under RCP 2.6, 6.0, 8.5 climate scenarios (values represent averages over all four GCMs, ns: not significant,*: p<0.001, d: decade).

| | RCP 2.6 | RCP 6.0 | RCP 8.5 |
|---|---|---|---|
| Shortwave radiation | 0.68 W $m^{-2}$ $d^{-1}$ (*) | 1.09 W $m^{-2}$ $d^{-1}$ (*) | 1.07 W $m^{-2}$ $d^{-1}$ (*) |
| Air temp | 0.05 °C $d^{-1}$ (*) | 0.3 °C $d^{-1}$ (*) | 0.5 °C $d^{-1}$ (*) |
| Longwave radiation | 0.24 W $m^{-2}$ $d^{-1}$ (*) | 1.35 W $m^{-2}$ $d^{-1}$ (*) | 2.66 W $m^{-2}$ $d^{-1}$ (*) |
| Wind speed | ns | ns | -0.03 m $s^{-1}$ $d^{-1}$ (*) |

Although the climate trends in the projections of the four climate models were qualitatively similar, there were some quantitative differences (Figure S2 in Appendix 4). HadGEM2 predicted the highest longwave radiation and air temperature, whereas GFDL showed the lowest values for these variables. In general, the inter-model spread among the projections increases over time, especially in the more severe warming scenarios (e.g. RCP 6.0 and RCP 8.5). In RCP 8.5, for example, the longwave radiation and air temperature at the end of the century projected by these two models deviated by up to 20 W $m^{-2}$ and 4 °C, respectively (Figure S2 c&l in Appendix 4). In comparison, MIROC5 projected the highest shortwave radiation, while the values from GFDL remained much lower than those from the other three models. For the projected wind speed, results from GFDL were somewhat higher than the others under RCP 2.6 and there was no significant difference under RCP 6.0 and RCP 8.5 (Figure S2 g-h-i in Appendix 4).

### 5.4.3. Response of thermal structure to climate change

Surface water temperatures in the reservoir showed a pronounced increase under the three climate scenarios and warming rates were comparable to those of air temperature, with the fastest rate under RCP 8.5 (0.5 °C $decade^{-1}$) and lowest rate under RCP 2.6 (0.09 °C $decade^{-1}$, Figure 5.5, Table 5.2). Whereas surface temperature warmed continuously until the end of this century under RCP 8.5, it levelled off in the middle of the century or towards the end of the century under RCP 2.6 and RCP 6.0, respectively. The spread of temperatures around the median among the different ensemble members rose with increasing average temperature. Metalimnetic water (measured at 10m depth) warmed far slower than surface water, although the increasing trends were still significant in all three scenarios (Table 5.2). Bottom temperatures did not show clear future trend under RCP 2.6 and only marginally increased under RCP 6.0 (0.06 °C $decade^{-1}$, Table 5.2). Under RCP 8.5, however, bottom temperatures increased comparatively rapidly at a rate of 0.19 °C $decade^{-1}$. Moreover, the annual mean value rose to approximately 8 °C by the end of the century, which is about 3 °C higher than the 5 °C that was projected at the beginning of the century (see Figure 5.5, Table 5.2). Hypolimnetic warming under RCP 8.5 followed a discontinuous trajectory and remained relatively stable until the middle of the century but afterwards entered a phase of intense and continuous warming.

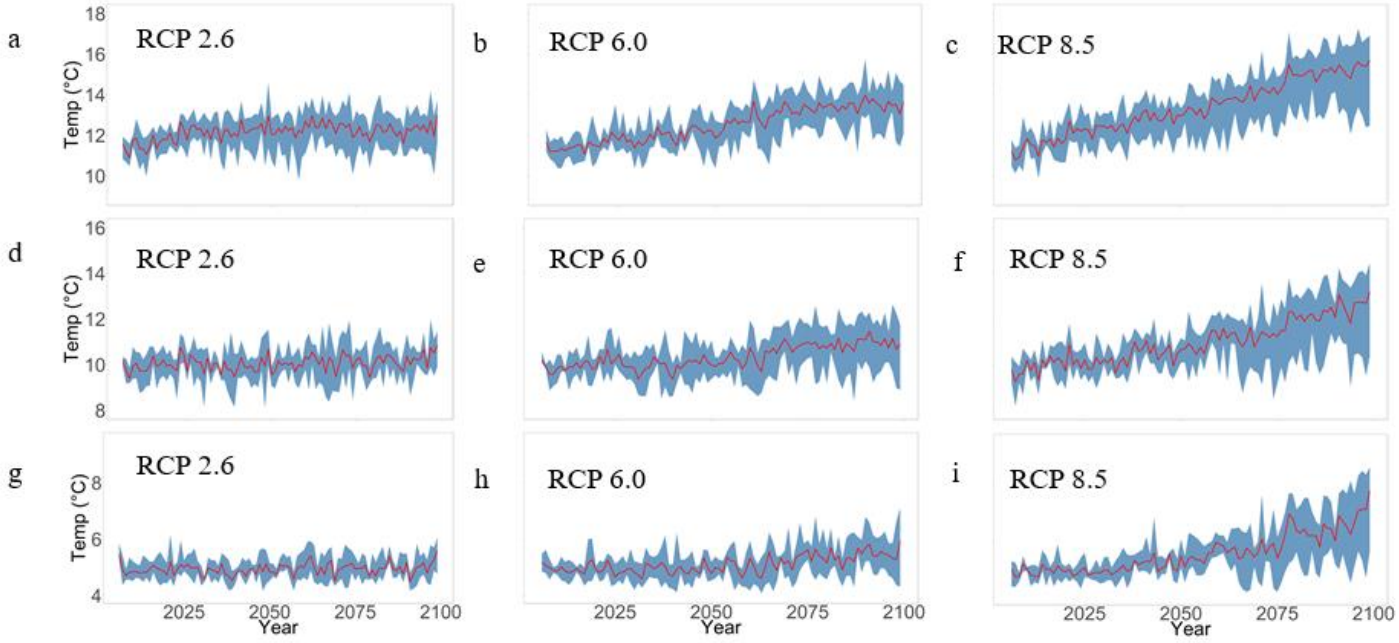


Figure 5.5. Time series of the simulated annual mean water temperature at depths of 1 m (a-b-c), 10 m (d-e-f), 50 m (g-h-i) in Rappbode Reservoir during the period 2006-2099 under RCP 2.6 (left column), RCP 6.0 (middle column) and RCP 8.5 (right column). The red lines show the annual ensemble mean values, the blue shaded areas show the annual minimum and maximum values from the ensemble.

Table 5.2. Projected trends (2006-2099) in thermal indices in Rappbode Reservoir, under RCP 2.6, 6.0, 8.5 climate scenarios (values represent averages over all four GCMs, ns: not significant,*: $p<0.001$, d: decade)

| | RCP 2.6 | RCP 6.0 | RCP 8.5 |
|---|---|---|---|
| Water temp (1m depth) | 0.09 °C $d^{-1}$ (*) | 0.32 °C $d^{-1}$ (*) | 0.50 °C $d^{-1}$ (*) |
| Water temp (10m depth) | 0.02 °C $d^{-1}$ (p=0.008) | 0.15 °C $d^{-1}$ (*) | 0.34 °C $d^{-1}$ (*) |
| Water temp (50m depth) | ns | 0.06 °C $d^{-1}$ (*) | 0.19 °C $d^{-1}$ (*) |
| Schmidt stability | ns | 53.9 J $m^{-2}$ $d^{-1}$ (*) | 88.1 J $m^{-2}$ $d^{-1}$ (*) |
| Mixed layer thickness | ns | -0.10 m $d^{-1}$ (*) | -0.13 m $d^{-1}$ (*) |
| Light intensity in mixed layer | 0.04 mol $m^{-2}$ $day^{-1}$ $d^{-1}$ (p=0.02) | 0.13 mol $m^{-2}$ $day^{-1}$ $d^{-1}$ (*) | 0.16 mol $m^{-2}$ $day^{-1}$ $d^{-1}$ (*) |

The water temperature trends driven by the different climate models in the same RCP scenario differed considerably (Table S1 in Appendix 4). Water temperatures at 1 m, 10 m, and 50 m increased much more slowly under GFDL forcing than under the other climate models. Under RCP 8.5, for example, water temperature in the surface layer (1m depth) increased at a

rate of 0.27 °C decade$^{-1}$ under GFDL, which was half of the rate under the other models. Moreover, hypolimnetic temperatures remained rather stable under GFDL, whereas they increased at rates of more than 0.2 °C decade$^{-1}$ under the other climate models. Similar patterns were also observed under RCP 2.6 and RCP 6.0. Interestingly, hypolimnetic temperatures forced by GFDL under RCP 2.6 and RCP 6.0 scenarios even showed weakly decreasing trends, which was not the case in projections of the other climate models (Table S1 in Appendix 4).

Since the surface water heats up much faster than the bottom water, more stable stratification was predicted under future climate warming. Average Schmidt stability in the period 2090-2099, for example, was projected to reach 2628 ± 87 J m$^{-2}$ and 2894 ± 115 J m$^{-2}$ under RCP 6.0 and RCP 8.5, respectively, whereas at the beginning of the century values mostly remained below 2400 J m$^{-2}$ (Figure 5.6). In contrast to this, Schmidt stability under RCP 2.6 remained rather constant during the whole simulation period (on average around 2300 J m$^{-2}$, see Figure 5.6) and showed no significant increase (Table 5.2).

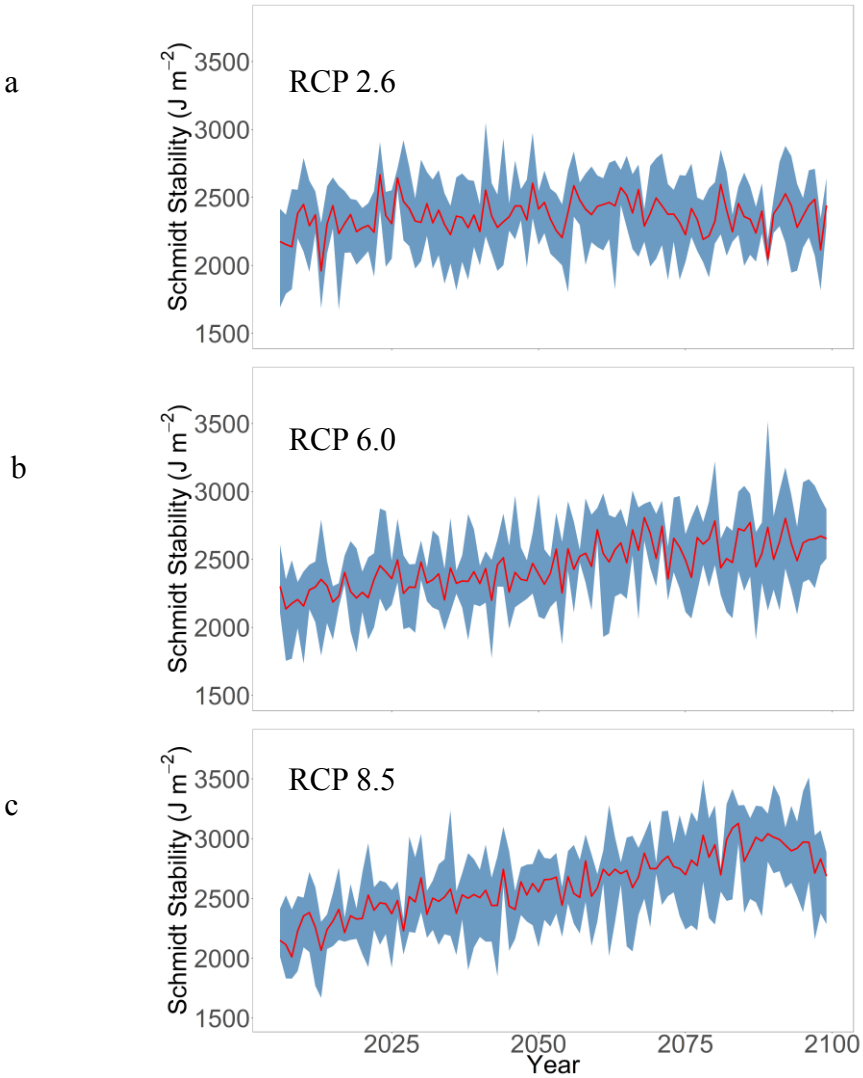


Figure 5.6. Time series of the simulated summer mean Schmidt stability in Rappbode Reservoir during the period 2006-2099 under RCP 2.6 (a), RCP 6.0 (b) and RCP 8.5 (c). The red lines show the annual ensemble mean values, the blue shaded areas show the annual minimum and maximum values in the ensemble.

Mixed layer thickness was projected to decrease at a similar rate under RCP 6.0 (-0.1 m decade$^{-1}$) and RCP 8.5 (-0.13 m decade$^{-1}$) leading to mixed layer thicknesses nearly 1m shallower by the end of the century. The mixed layer thickness did not show a significant trend under RCP 2.6 (Table 5.2, Figure 5.7). Combining the increasing shortwave radiation and decreasing mixed layer thickness, the average photosynthetically available radiation intensity within the epilimnion increased gradually under RCP 6.0 (0.13 mol m$^{-2}$ day$^{-1}$ decade$^{-1}$) and RCP 8.5 (0.16 mol m$^{-2}$ day$^{-1}$ decade$^{-1}$). Only a weak (but nevertheless significant) trend was detected under RCP 2.6 (0.04 mol m$^{-2}$ day$^{-1}$ decade$^{-1}$, Table 5.2, Figure 5.8).

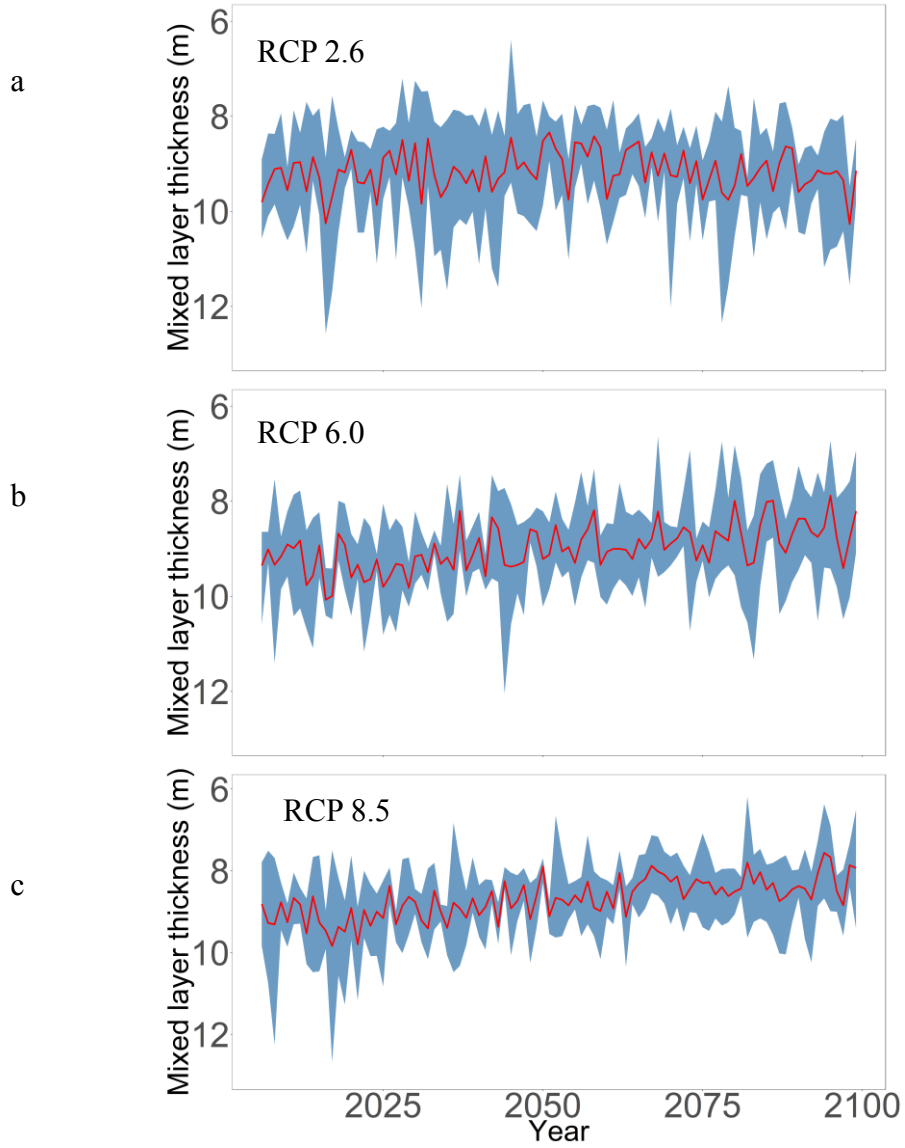


Figure 5.7. Time series of the simulated summer mixed layer thickness in Rappbode Reservoir during the period 2006-2099 under RCP 2.6 (a), RCP 6.0 (b) and RCP 8.5 (c). The red lines show the annual ensemble mean values, the blue shaded areas show the annual minimum and maximum values in the ensemble. Note the reversed y-axis.

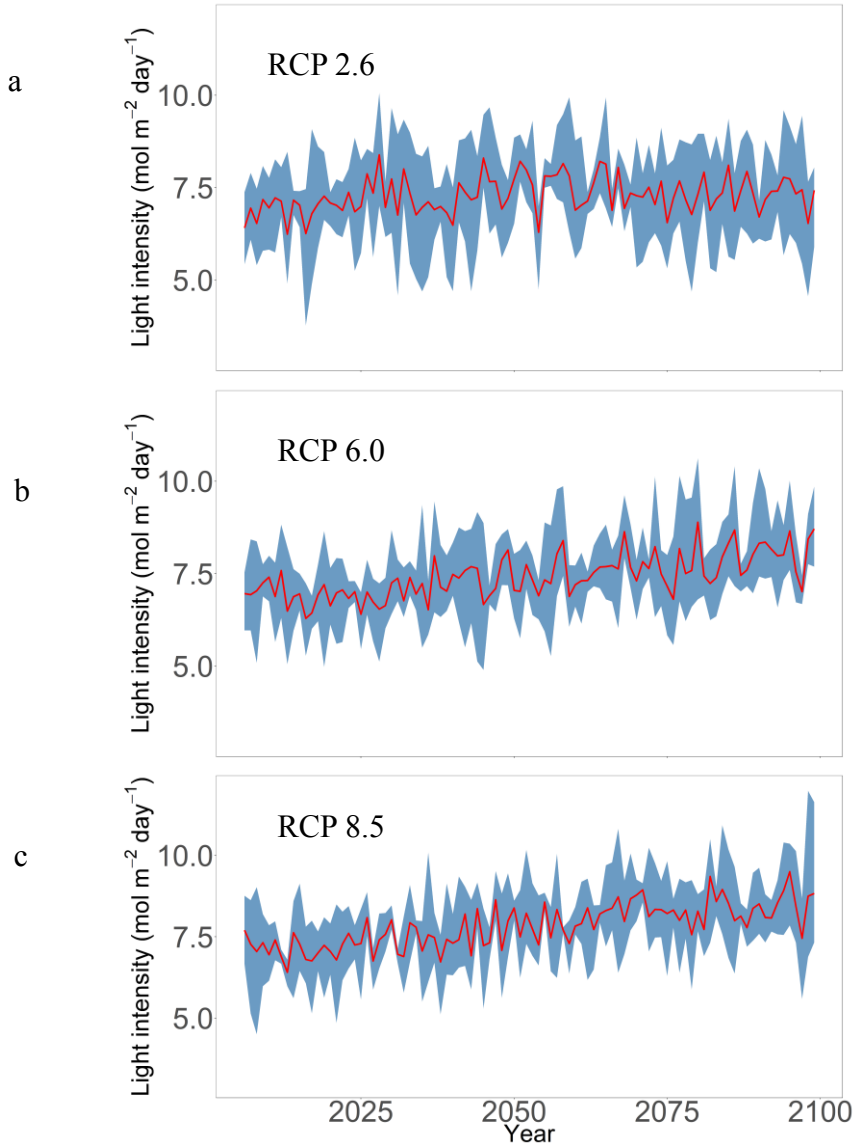


Figure 5.8. Time series of the simulated light intensity within the summer mixed layer of the Rappbode Reservoir during the period 2006-2099 under the RCP 2.6 (a), RCP 6.0 (b) and RCP 8.5 (c) climate scenarios. The red lines show the annual ensemble mean values, the blue shaded areas show the annual minimum and maximum values from the ensemble.

### 5.4.4. Interaction between climate warming and alternative withdrawal scenarios

Surface withdrawal turned out to be an effective strategy to reduce the heat content of the water body and resulted in lower water temperatures under severe climate warming (i.e. RCP 8.5 climate scenario, see Figure 5.9). This cooling effect was also evident at all depths as projected water temperatures at all three depths remained lower than those under the current withdrawal strategy and the difference between them increased over time. For example, at 10 m depth the annual mean water temperature in 2099 was 13.19 ± 1.92 °C under current withdrawal, while the temperature decreased to 12.28 ± 1.85 °C under the partial surface withdrawal scenario and

further down to 10.86 ± 1.49 °C in the complete surface withdrawal scenario. Interestingly, the cooling effect of the surface withdrawal was also effective in the deep water, where the differences in water temperatures between the withdrawal strategies were even larger than at the surface. For instance, at 1m depth the difference in the mean water temperature between the current withdrawal scenario and the complete surface withdrawal was 0.7 °C in 2099. At 50 m depth however, the difference was projected to be 2.7 °C (Figure 5.9). Most importantly, the water temperatures at 50 m depth showed no warming or only a very weak warming trend under the two surface withdrawal scenarios, regardless of the continuous surface warming under the climate conditions (Figure 5.9). In conclusion, surface withdrawal is an effective measure to suppress hypolimnetic warming in the reservoir and can strongly buffer the effects of climate warming on the thermal structure in Rappbode Reservoir.

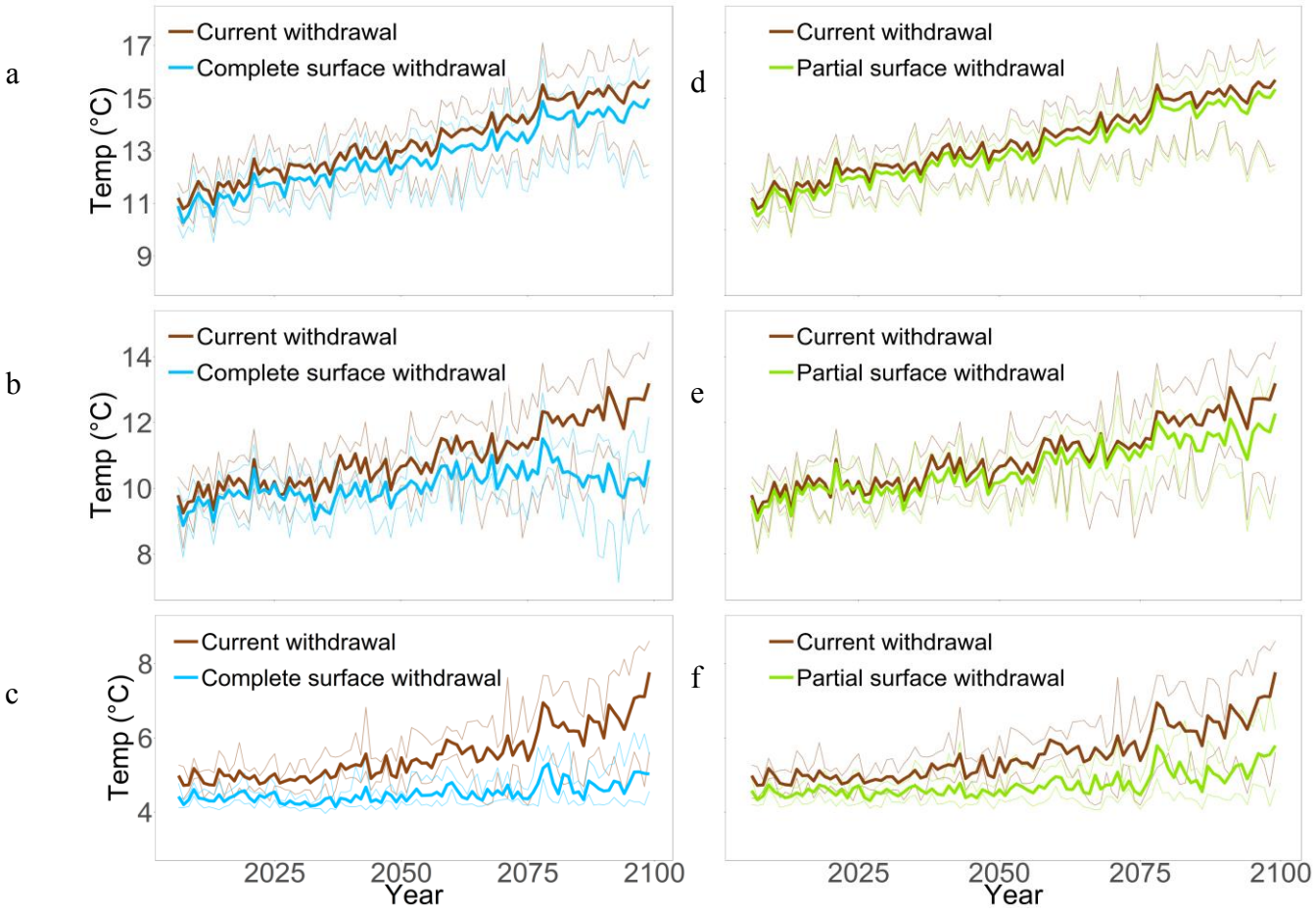


Figure 5.9. Comparison of the simulated annual mean water temperatures at 1 m (a & d), 10 m (b & e), and 50 m (c & f) depth in the Rappbode Reservoir during 2006-2099 under the RCP 8.5 climate scenario. Red lines depict the current withdrawal management. In the "complete surface withdrawal" all the water is discharged from the top outlet, while in the “partial surface withdrawal” all raw water for drinking water supply is still taken from the bottom waters and only downstream flow is withdrawn from the surface layer. The thick lines show the annual mean values, the thinner lines show the annual minimum and maximum values from the ensemble.

## 5.5. Discussion and conclusions

In this study, a well-established 2-dimensional hydrodynamic model, W2, was used to analyze the response of the thermal structure in Germany's largest drinking water reservoir to future climate conditions. Since we used projected climates from different GCMs, as provided within the ISIMIP-project, we were not only able to quantify the impact of warming on the reservoir thermal structure, but also estimate its uncertainty and expected year-to-year variations. The calibrated model was shown to perform well in capturing the observed water temperatures between January 2015 and December 2017, with the RMSE lower than that in recent studies on the same topic (Ayala et al. 2019,Chuo et al. 2019,Jin et al. 2019,Park et al. 2018a). According to a meta-analysis of the performance of aquatic ecosystem models (Arhonditsis and Brett 2004), the simulation accuracy of water temperature in our research can be regarded as the top level.

***Climate warming effects on physical structure***

The results showed that stratification intensity in the reservoir will significantly increase under severe climate warming (i.e. RCP 6.0 and RCP 8.5), but remain rather constant under low climate warming (RCP 2.6), which is in line with the study by Fenocchi et al. (2018). The most rapid increase in water temperature was projected under HadGEM2 forcing, while the least warming was projected under GFDL forcing, which is similar to the results shown in Ayala et al. (2019). We observed an increasing spread in thermal metrics towards the end of the century under RCP 8.5, which was also shown in other related studies (Huber and Zanna 2017,Tan et al. 2018) and indicates that variability in projections scales with the average change from current conditions. The water temperatures in the surface layer respond more strongly to climate change than in deeper layers – an observation that is reasonable and has been reported elsewhere (Fan and Kao 2008,Zhang et al. 2014). Whereas the surface temperature is directly controlled by the climate variables, the response of bottom temperature to climate change is highly non-linear (Winslow et al. 2017b). This differential warming over depth intensifies temperature gradients and stabilizes the stratification.

An important outcome of our analysis is that under intense climate warming (i.e. RCP 8.5) the water temperature at 50 m depth was projected to react discontinuously, with almost no warming in the first half of the century but strong warming (0.35 °C decade$^{-1}$) in the second half, albeit at a lower rate than in the surface layer. This increase in hypolimnetic water temperature decreased the temperature gradient in the water column, which accounted for the decrease of Schmidt stability at the end of the century (see Figure 5.6). This discontinuous change in deep temperature could be attributed to the transformation of mixing type. Our simulations suggest that ice will nearly disappear in the reservoir in the second half of the century (Figure S3 in Appendix 4), shifting the mixing regime from dimictic to warm monomictic. This transition will allow heat to accumulate in the bottom layers when the resetting effect of the winter inverse stratification on deep water temperature disappears (Kirillin 2010). In this case, the annual mean bottom water temperature at the end of the 21$^{st}$ century would reach nearly 8 °C. This means that by the end of this century Rappbode Reservoir will have its winter overturn at a water

temperature of 7-8°C and minimum temperatures will no longer drop to 4°C as is the current case. Such conditions could induce oligomixis in deep water bodies as observed and described, for example, in Lake Constance (Straile et al. 2003,Straile et al. 2010). In Lake Constance, inter mixing does not occur when a rather warm winter follows a very cold winter because vertical temperature gradients persist throughout the warm winter. Such findings will be valid for many other lakes and reservoirs in the temperate zone. Lakes in a far colder climate, however, will not show deep water warming or tendencies to oligomixis as long as their winter conditions allow the water to cool down to the temperature of maximum water density at 4°C. A study by Tan et al. (2018), for example, predicted that the bottom temperature in Harp Lake (Ontario, Canada) would remain between 4 °C and 5 °C for the whole century under RCP 8.5 climate scenario.

***Reservoir management can mitigate climate warming effects***

The deep water warming in Rappbode Reservoir is also partly supported by the current management practice in Rappbode Reservoir of withdrawing water from the bottom. This deep water withdrawal enables a deeper advective intrusion of heat and a loss of the coldest water layers (Lewis Jr et al. 2019). As shown in our alternative management scenario, the hypolimnetic warming can be completely avoided in Rappbode Reservoir if all water is withdrawn from the surface layer. In this scenario, the response of bottom temperature to climate warming in the reservoir is comparable to that in natural lakes where outflows are also withdrawn from the surface layer. Furthermore, the surface withdrawal strategy would not only avoid hypolimnetic warming, but also considerably decrease water temperature in the epilimnion and metalimnion (Figure 5.9).

Even under the partial surface withdrawal scenario, i.e. when drinking water withdrawal is still taken from the hypolimnion and downstream withdrawal is shifted to the epilimnion, deep water warming was not as pronounced as in the scenario of withdrawing all water from the hypolimnion (Figure 5.9). The results from both scenarios illustrate that the surface withdrawal strategy can be used as an effective way to alleviate the climate warming effects on the physical structure. We expect that this strategy is also applicable to many other deep reservoirs located in the temperate zone. An adapted withdrawal management can therefore be used as an effective climate adaptation strategy.

It has to be noted, however, that potential side effects on water quality variables (e.g. oxygen, see Weber et al. (2017)), have to be taken into account. Surface withdrawal reduces the water exchange in the deep hypolimnion and therefore intensifies oxygen depletion. We believe that such problems could be completely circumvented if withdrawal is switched back to bottom withdrawal in the second half of the cooling phase. For Rappbode Reservoir, a corresponding time would be around mid-October. Such a switch-back to bottom withdrawal at that time would still avoid hypolimnetic warming but would also improve oxygen conditions at the lake bottom and reduce the risk of oligomixis.

***Light conditions and phytoplankton composition***

Besides the commonly used thermal indices (e.g. water temperatures at different depths, Schmidt stability), we also analyzed how the mixed layer thickness and the mean light intensity

in the mixed layer will change under climate warming. The results show that the mixed layer tends to shoal and light intensity becomes higher with warming, which is consistent with the conclusion in Saros et al. (2016). Such changes, combined with intensified stratification as shown above, are presumed to encourage the growth of phytoplankton in surface layers if nutrients are available (Tan et al. 2017). The stronger stratification will particularly favor motile (e.g. cryptophytes or dinoflagellates) and buoyant (e.g. cyanobacteria) over fast sinking diatoms and a shift in phytoplankton communities can be expected (Wentzky et al. 2018b). Interestingly, Horn et al. (2015) found such a shift from diatoms towards cyanobacteria over the last decades within another German drinking water reservoir. These authors also considered climate warming and the associated changes in thermal structure as the main drivers of this change. Furthermore, they emphasize that nutrients could not have been the driver here because these changes in phytoplankton community structure were not paralleled by increasing nutrient loadings. All this points to the necessity that we urgently need to link the (existing) sophisticated hydrophysical models with (still non-existing) sophisticated models of lake biogeochemistry and plankton dynamics.

Notably, in our scenarios we only elucidated the effects of climate change on the mixed layer indices and kept the light attenuation coefficient (i.e. transparency) of the water at a constant level. Previous studies illustrated that the effects of climate change on the mixed layer thickness can be modified when the transparency changes at the same time (Rose et al. 2016,Shatwell et al. 2019). Therefore, it is valuable for the further modelling scenarios to check the response of the mixed layer indices to different transparency conditions, under future climate warming.

In this study, a well-established hydrodynamic model was employed to derive local thermal impacts from global climate projections and demonstrate how reservoir management can be adapted to minimize these impacts. Our results also illustrate that the adaptation requirements differ strongly depending on the projected warming rates: the most intense warming scenario, i.e. RCP 8.5, requires comprehensive climate adaptation while the mitigation scenario (RCP 2.6) requires little or no adaptation in reservoir management during this century. A valuable next step would be to extend the current model applications to analyze the influence of climate changes and management strategies on the aquatic ecosystem and water quality variables (e.g. nutrients, phytoplankton, zooplankton, oxygen). Of particular interest for water managers will be the expected changes in oxygen dynamics, nutrient cycling, and algal community dynamics. For that purpose, the existing model needs to be extended to include ecological routines that account for the biogeochemical dynamics in the open water and the sediments. This is a big step for aquatic ecosystem modelling because it is questionable whether our current models are still valid under climate conditions that can be as much as 5 °C warmer than now (England et al. 2015). A way out of this problem could be to confront existing models for temperate lakes or reservoirs with new applications in warmer regions, e.g. in Mediterranean reservoirs. A major benefit of a sound water quality modelling will be the ability to identify new reservoir management strategies that may help to dampen potential negative effects of climate warming on water quality or to identify new restoration targets that maintain water quality.

# 6. General discussion

## 6.1. Evaluating performance of the applied models

In the thesis, three hydrodynamic models were used to simulate water temperatures in Lake Arendsee and Rappbode Reservoir: (i) the one-dimensional (1D) model GLM, (ii) the two-dimensional (2D) model W2 and (iii) the three-dimensional (3D) model EFDC. The simulation results from all models were in good agreement with measurements (research question A1) and the overall RMSE from the four studies ranged between 0.61 °C and 0.89 °C. These model errors were lower than those presented in recent studies in which the three models were applied before (Bai et al. 2018,Bueche et al. 2017,Lee et al. 2018,Park et al. 2018b,Weber et al. 2017,Zheng et al. 2018). Based on a meta-analysis of the performance of different water quality models (Arhonditsis and Brett 2004), the simulation accuracy of water temperature in the thesis can be regarded as top level. In contrast to Stepanenko et al. (2010) in which the authors concluded that temperature dynamics below the thermocline cannot be properly mimicked by 1D models, the calibrated GLM in this study was shown to satisfactorily capture the water temperature from the top to the bottom (see Chapter 3 & 4). It is also interesting to see that W2 model can always accurately reproduce the thermal structure of Rappbode Reservoir, no matter whether it is driven by the measured climate data (Chapter 4) or the bias-corrected reanalysis data from EWEMBI dataset (Chapter 5), demonstrating that the model performance is robust under small changes in the boundary conditions.

Unlike other studies using hydrodynamic models, this study not only used the dynamics of water temperature for model assessment but also explicitly check its suitability to reproduce vertical diffusivity quantitatively. Evaluating the model performance in reproducing vertical diffusivity is a powerful approach since it allows us to link emerging deviations between modelled and observed state variables to the underlying processes. The study followed the research by Wahl and Peeters (2014), who used a 3D model for comparing observed and simulated vertical diffusivity in deep Lake Constance and it is extended by including a detailed analysis of vertical diffusivity within the metalimnion. The results calculated from observed temperatures showed that in Lake Arendsee the metalimnetic diffusivity was much lower than that in other layers with the lowest value occurring in mid-July. Such features were well reproduced by the 3D model EFDC (research question A2), regardless of different approaches (i.e. from water temperature as well as tracer concentration) used for the calculation of diffusivity. Additionally, by comparing the simulated results under different horizontal and vertical grid resolution, we further clarified that the model performance for capturing the vertical diffusivity is grid independent (research question A2).

## 6.2. The response of thermal dynamics and vertical diffusion to climate change

In this thesis, firstly the influence of two important climate factors (i.e. air temperature and wind speed) on the thermal structure and vertical diffusion was studied. Then the hydrodynamic model was driven by the results from ensemble climate models, to draw a more comprehensive picture of climate change impacts on lakes and reservoirs. The utilization of model outputs from climate simulations provides not only a more coherent meteorological data basis because all meteorological variables were propagated through the model but it also includes estimates of uncertainties.

### 6.2.1. The response of thermal structure and vertical exchange to variations in wind speed

The response of stratification and vertical exchange to variations in wind speed was studied in chapters 2 and 3. The results showed that wind intensification can move the 10 °C isotherm depth downwards and decrease the stratification duration and intensity, addressing research question B1. The finding is in line with the research by Desai et al. (2009) who illustrated that elevated wind speed is increasing the vertical mixing strength and the surface layer thickness in Lake Superior. A similar conclusion can be drawn from our results in Chapter 2, in which it suggested that elevated wind speed can markedly decrease the duration of periods with very low vertical diffusion in the metalimnion of Lake Arendsee. In Chapter 2, we further demonstrated that compared to air temperature, wind speed is a more influential factor for the vertical exchange within the metalimnion (research question A3).

To our best knowledge, this is the first modelling research on the response of thermal structure to episodic strong wind events. The findings identified the end of April to the start of July as the sensitive time window and the strong wind events outside the period do not have a big influence on the stratification of Rappbode Reservoir (research question B2). It also demonstrated that although the wind strength and duration can quantitatively affect the wind-induced perturbation on the stratification phenology, the sensitive time window shown above is not changed which further strengthens the related conclusion, confirming research question B3. Our finding about this time window can be explained from several perspectives. In Chapter 3 it was explained by the development of Schmidt stability in different periods. From another perspective, the results for Lake Arendsee (see Chapter 2) can also be used to account for this sensitive time window. Although research was done for different water bodies in Chapter 2 and 3, both of them belong to dimictic types and locate in the same climate zone, so their patterns of vertical diffusivity should be similar to each other. It showed that during this sensitive time period, the minimum diffusivity in the metalimnion of Lake Arendsee was kept at a high level (i.e. higher than $2\times10^{-6}$ $m^2$ $s^{-1}$, see Figure 2.7), which facilitated the strong wind to mix the whole water column. By contrast, after this period (i.e. in the midsummer) the minimum diffusivity

dropped below $1\times10^{-6}$ $m^2$ $s^{-1}$ so that metalimnion played as an efficient barrier which strongly suppressed influence of episodic strong wind events on the thermal structure. Additionally, the recent study by Andersen et al. (2020) used thermocline depth before the episodic wind events to explain this sensitive time window. When the thermocline was located shallow in the reservoir at the beginning of a wind event (i.e. from late spring to early summer), the small volume of the surface mixed layer facilitated the impact of events; and vice versa, when the thermocline became deeper at the start of a wind event (i.e. in the midsummer), a relatively large volume of water was affected so the effect was strongly dampened.

A higher frequency of episodic strong wind events are expected in the future (Aumann et al. 2018,Hawcroft et al. 2018), and results in this thesis confirmed the influence from these events on stratification structure. Comparing such results with the findings from Poschke et al. (2015), it is interesting to see that the spring upwelling events in temperature lakes also appear within this sensitive time period, of which the intensity is positively related to the magnitude of episodic wind events. Both the break of stratification and upwelling due to catastrophic strong wind events can significantly influence the biogeochemical cycling in aquatic ecosystems, since they facilitate mixing of nutrients from the hypolimnion into the epilimnion, oxygenation of the deep water column and release of the sediment-produced methane into the atmosphere (Klug et al. 2012). To extend the current research, therefore, a valuable next step would be to establish an integrated physical-biological model to further analyze the response of water quality variables (e.g. nutrients, oxygen, algae groups) to the episodic strong wind events.

Besides the conclusions shown above, this research also can be seen as a good start to systemically check the response of aquatic systems to climate extremes. Previous studies have confirmed that more and more climate extremes will appear (e.g. extreme precipitation, tropical storms, and severe droughts) due to global warming trend (King et al. 2017,Sillmann et al. 2017), which may strongly affect aquatic ecosystems in inland waters (Bergkemper and Weisse 2017). Our research provides a template for the subsequent modelling studies to check the influence from such extreme weather conditions, which can help opening the sensitive time window for other episodic events.

### 6.2.2. The response of winter stratification to increase in air temperature

Winter stratification, occurring when water temperature in the surface is lower than that in the bottom, is an important indicator in differentiating between dimictic and monomictic waters, and this kind of stratification is not well studied in the previous research. In the current study, to fill in the gap, two well-established hydrodynamic models (i.e. GLM and W2) were used to systemically check the development of winter stratification in Rappbode Reservoir and analyze its response to two important influencing factors (i.e. air temperature and withdrawal elevations). In Chapter 4, it was shown that the duration of winter stratification will decrease under climate warming. Moreover, the winter stratification can totally disappear if air temperature is increased high enough, which means that under intense climate warming Rappbode Reservoir may transform into a monomictic mixing type (hypothesis C1). This conclusion corresponds well with that shown in Chapter 5 suggesting that the reservoir will become warm monomictic at the

second half of 21st century under RCP 8.5 climate projection. Similar results were reported in previous studies (Ficker et al. 2017,Kirillin 2010,Peeters et al. 2002). This change in mixing patterns have been shown to increase hypolimnetic water temperature, extend the time window for the formation of hypoxia and anoxia, and potentially increases the release of the phosphorus from the sediment so as to pose a significant threat to water quality (Foley et al. 2012,North et al. 2014). Therefore, it is valuable to see whether management strategies (selective water withdrawal in the thesis) can be used as an effective way to mitigate climate warming effects on the winter stratification, which is discussed in detail in section 6.3.

The method adopted in Chapter 4 followed that in most of the traditional simulation studies, which gradually increased air temperature in the referenced scenario and checked its influence on lakes and reservoirs (see Fink et al. 2014b,Trolle et al. 2011). It is admitted that this is a direct and effective way to analyze the influence of air temperature, but it strongly simplifies climate change dynamics, especially neglects the effect caused by heat waves. Actually, meteorologists have clarified that in this century heat waves will become the new normal at a global scale, due to increased emission of greenhouse gas (Herring et al. 2020,Stillman 2019). Recent examples are Australia heatwave in December 2019 and exceptionally hot weather in Europe in July 2018. It has been shown that such events can suddenly increase the water temperature difference between epilimnion and hypolimnion, reduce the vertical exchange in water column and lead to severe oxygen depletion in the lake bottom (Jeppesen et al. 2009,Jeppesen et al. 2014). High frequency of heat waves and their threats to aquatic ecosystems pose a new challenge to modelers, which is whether we can use the coupled hydrodynamic-ecological models to accurately predict the influence of expected heat waves on inland waters. If the answer is yes, then it will be definitely helpful to improve our management strategies to mitigate the negative effects caused by such climate events. From the literature review, it is found that there are already some aquatic modelers focusing on this topic (for example Chen et al. 2020,Trolle et al. 2011). However, most of such research just duplicated the historical heat waves into the future to project the effects of such events on lake ecosystems, and cannot accurately evaluate the influence due to the future development of heat waves. To fix the problem, it is suggested in the next step to take out the heat wave events from high-resolution regional climate projections (e.g. ISIMIP, CORDEX) and use them as the climate boundary conditions to drive the aquatic models, which can also be seen as a good extension of the thesis.

Additionally, when combining the conclusion from Chapter 3 and Chapter 4, another interesting topic to extend the current research is to check whether projected episodic strong wind events can effectively offset influence of climate warming on aquatic ecosystems. Considering strong impact of wind on stratification dynamics shown in Chapter 3, it is possible that changes within stratified lakes and reservoirs, due to increase in air temperature for the whole year, can be partly or even totally offset by a single strong wind event during the sensitive time period. To my best knowledge, there is no previous research which illustrated the combined effect, attributed to the two kinds of expected climate changes (i.e. episodic strong wind and increase in air temperature), on lentic waters and this topic should attract attention in future studies. It is believed that analyzing this combined effect will be helpful for limnologists to better understand the response of freshwater systems to future climate change.

### 6.2.3. The response of thermal dynamics to different future climate projections

Based on the data repository of the ISIMIP2b project, the response of thermal structure in Rappbode Reservoir to future climate projections have been analyzed in detail. Here the climate projections were drawn from three RCP scenarios and each scenario was driven by four GCMs. From the perspective of climatologists, large uncertainties exist in the long-term climate projections from different GCMs due to their inconsistencies in the calculation of radiative forcing by $CO_2$ (Soden et al. 2018), which will lead to different physical processes in lentic waters (Ayala et al. 2019). Results in Chapter 5 further confirmed this point. In Rappbode Reservoir, difference of climate projections from four GCMs become larger over time, especially for RCP 6.0 and RCP 8.5 (see Figure S2 in Appendix 4) and similar patterns were shown in the corresponding projections of water temperature (hypothesis D2). It was supposed that using several GCMs (i.e. climate ensembles) to mimic climate change and take out their mean results as the representation of future can effectively reduce uncertainties from climate projections (Kundzewicz et al. 2018). The same method was adopted in this thesis to project future stratification structure in Rappbode Reservoir, and the results suggested that stratification intensity in the reservoir will significantly increase under severe climate warming (RCP 8.5), but keep rather constant under low climate warming (RCP 2.6), supporting hypothesis D1. Our results are comparable to those from Sahoo et al. (2015) who illustrated that during 2014-2098, stratification duration in Lake Tahoe will increase more than one month under IPCC A2 scenario in which greenhouse-gas emissions will increase rapidly in the 21$^{st}$ century, while keep unchanged under IPCC B1 scenario representing low-level emissions of greenhouse-gas in the century.

An interesting finding in Chapter 5 is that under RCP 8.5, not only the surface water temperature but also the hypolimnetic water temperature was predicted to strongly warm up (0.35 °C decade$^{-1}$) in the second half of 21$^{st}$ century (hypothesis D3). This result goes against to that from Richardson et al. (2017) in which it showed that deep-water temperature in several dimictic lakes across Northeastern North America did not significantly change under climate warming. This difference can be attributed to two reasons: firstly due to climate warming, ice cover in Rappbode Reservoir is supposed to gradually disappear from 2050 onwards (Figure S3 in Appendix 4), which leads to the change of mixing regime from dimictic to warm monomictic. Waters with warm monomictic type, compared to dimictic type, tends to preserve more heat in deep layers during stratified period so as to facilitate warming in hypolimnion (Kirillin 2010). Moreover, according to current management strategy, water in the reservoir is always taken out from hypolimnion which helps in replacing hypolimnetic cold water with warm water in upper layers. Similar results about hypolimnetic warming were also shown in the 35-year temperature record for Lake Dillion (Lewis Jr et al. 2019) and the authors even assumed that under future climate warming, increase in bottom water temperatures due to hypolimnetic withdrawal will be expected for reservoirs in general.

Also in the study, a shoaling of the mixed layer in Rappbode Reservoir was projected under

future climate warming, which is consistent with the research from Jang et al. (2011) and Capotondi et al. (2012). From the view of physical limnology, the thinning of mixed layer in response to climate warming is caused by strengthening of density gradient at the lower boundary of this layer (Hondzo and Stefan 1993,Lewis Jr et al. 2019). However, the opposite conclusion was drawn from other previous studies. Fee et al. (1996) reported that 2 x $CO_2$ climate change would strongly decrease concentration of DOC and increase transparency in Canadian Shield lakes, which leads to increase in the mixed layer depth by 2 m. Additionally, Flaim et al. (2016) suggested that due to increase in transparency of Lake Caldonazzo through removal of point source sewage inputs, mixed layer depth in the lake increased 3.9 m from 1973 to 2014, although air temperature during that time also markedly elevated. Such results indicated that not only climate conditions but also transparency has a big influence on mixed layer depth. In Chapter 5, the dynamics of transparency in Rappbode Reservoir was ignored in the scenario, which can reduce projection accuracy for the mixed layer. Therefore, it is suggested in the future research to embed an ecological part into the current hydrodynamic model, in order to take into account the effects of transparency and to obtain more promising projections for mixed layer depth under future climate change.

Another important point is that this study is involved in the lake sector of ISIMIP, which collects historical observations and future climate data for 66 water bodies around the world. Therefore, it provides modelers a great platform to predict the response of waters, in the global scale, to future climate conditions and our research can be seen as a protocol for these projections. The hydrodynamic model and R scripts used in this research are easily transferred to other case studies, indicating that the importance of our work is beyond the case of Rappbode Reservoir and conclusion from the research should be useful for other aquatic modelers involved in the ISIMIP project. Additionally based on the long-term observations, influence of climate change on different freshwater systems is strongly controlled by their basin morphometry and latitudes (i.e. geographic properties, see Kraemer et al. 2015). Therefore, it is a valuable next step to extend the current study into the whole lake sector of ISIMIP, to evaluate how the geographic properties of different waters affect their response to future climate warming. Clearly this extension will improve our understanding about the effects of climate change on the global population of lakes, and help in optimizing management strategies to mitigate negative effects by climate warming.

## 6.3. The effect of selective withdrawal strategy on modifying the thermal structure in Rappbode Reservoir under climate change

Two well-estabilished hydrodynamics models, GLM and CE-QUAL-W2,were applied in Chapter 4 to illustrate how selective withdrawal strategy can be used to adapt climate warming effects on winter inversed stratifation in Rappbode Reserovir. Compared to most of traditional studies, which analyzed hydrodynamic processes by one model, the conclusion from different models is more robust and the results will provide valuable information for further developments of such modelling tools (Perroud et al. 2009). Actually there is already a scientific project,

among aquatic modelers, specifically focusing on comparing simulation results from different hydrodynamic models (i.e. Lake MIP, see Stepanenko et al. 2010). However, studies in the project mainly tested performance of different models in reproducing summer stratification (Stepanenko et al. 2014,Thiery et al. 2014), while neglected physical processes in winter. Our research filled in this gap and to make the results more promising, it is suggested in future studies to apply other models in LakeMIP, e.g. SIMSTRAT, Flake, Minlake, on this topic. The current study clearly indicated that although simulation results, from two models, showed some quantitative differences, their qualitative outcomes about the response of winter stratification to different withdrawal elevations are the same. Our study confirmed that the surface water withdrawals can help extend duration of winter stratification under climate warming, so as to stabilize the dimictic mixing type of the reservoir (supporting hypothesis C2 & C3).

Similar conclusion about the effect of selective withdrawal strategy was obtained from Chapter 5, which illustrated that under severe climate warming (i.e. RCP 8.5), bottom withdrawal will transform the reservoir from dimictic to warm monomictic type and significantly increase the annual averaged bottom temperature from current 4 °C to 8 °C at the end of 21$^{st}$ century. By contrast under the same climate projection, surface withdrawal will help cooling down the water body, while keeping the bottom temperature unchanged over the whole century (hypothesis D4). Different response of bottom temperature to these two withdrawal strategies, under future climate warming, may change the known relationship between hypolimnetic oxygen condition and water withdrawal elevations. A bunch of previous studies have clarified that compared to surface withdrawal, bottom water withdrawal fuels the exchange between epilimnion and hypolimnion, increases vertical diffusivity in water column and reduces hypolimnetic oxygen depletion (Aghasian et al. 2019,Çalışkan and Elçi 2009,Carr et al. 2019). Considering the results in our research, it is suggested that this conclusion about hypolimnetic oxygen may be only valid under current climate condition, and may change under severe climate warming. Based on our latest paper disentangling the contributions of different processes to oxygen depletion in Rappbode Reservoir (Mi et al. 2020), sediment oxygen demand (SOD) in the hypolimnion reached up to 0.72 $gO_2$ $m^{-2}$ $day^{-1}$ at the water temperature of 8 °C, which is more than twice compared with the value at 4 °C (0.3 $gO_2$ $m^{-2}$ $day^{-1}$). These results showed that under future climate warming, hypolimnetic oxygen concentration may be lower under bottom water withdrawal than that under surface withdrawal, due to the increased oxygen consumption by sediment. Clearly this is just a hypothesis inferred from our current findings. How the oxygen dynamics will be changed under combined effects from climate warming and withdrawal strategies is still unknown and should attract more attention in future studies.

The recent paper by Feldbauer et al. (2020), of which the topic was similar to our study, not only checked the influence of different withdrawal elevations but also the period to conduct selective withdrawal strategies on the thermal dynamics in deep researvoirs. Here comes another interesting topic when combining their research with ours: when to apply surface withdrawal can most effectively reduce water temperatures under severe climate warming? In other words, is there a sensitive time window of selective withdrawal strategy in cooling down the water column? This is supposed to be a key point for the future research, since opening this time window can help reservoir operators better control water quality conditions in the face of climate

warming, by encouraging vertical mixing to transport more oxygen into the hypolimnion, and meanwhile reducing water temperatures to decrease oxygen consumption rate by sediment. Due to the thermal characteristics in dicmic waters (i.e. fully mixed in spring and autumn while weakly stratified in winter), changing withdrawal elevations in such three seasons should not strongly affect their physical processes. To achieve the goal shown above, therefore, it is planned in future modelling studies to apply the surface withdrawal, under RCP 8.5, at three periods of every year, which is the beginning of summer stratification (May 1$^{st}$ to June 20$^{th}$), middle of summer stratification (June 21$^{st}$ to August 10$^{th}$) and end of summer stratifcation (August 11$^{st}$ to September 30$^{th}$), while keep the bottom withdrawal at other time, and then compare simulated water temperatures with those under bottom withdrawal over the whole year, to illustrate the best time to take out water from surface.

## 6.4. Additional perspectives

Several suggestions for future research, following the specific research point, have been put forward in sector 6.2 and 6.3. From a general view in this section, extension of the current study is illustrated based on three perspectives which are shown as below.

### 6.4.1. Modelling in connective systems

In this thesis, the influence of climate change and management strategies on stratification structure in two dimictic waters (i.e. Lake Arendsee and Rappbode Reservoir) was illustrated in detail. As shown from Chapter 2 to 5, however, all the research was done in the local scale while neglected the influence across the nearby catchment. This is a critical point since the functioning of aquatic systems can only be understood if we take their connectedness with the surrounding watershed into account (Teurlincx et al. 2019). On the one hand inflow discharge and temperatures, which are highly sensitive to climate conditions, control the energy transporting into the water body and thus significantly affect its thermal structure (Read et al. 2014). On the other hand withdrawal elevations of a reservoir determine temperatures of its outflow into downstream rivers, which may have far-reaching ecological effects on the downstream ecosystems due to the disruption of natural stratification (Aghasian et al. 2019). To extend the current research, therefore, future studies should think about using simulation tools to connect upstream-lakes/reservoirs-downstream together, so as to better understand the influence of climate change and human activities on aquatic systems in a catchment scale.

### 6.4.2. Future changes of vertical diffusion

In Chapter 2, response of vertical turbulent diffusivity to general changes of air temperature and wind speed was illustrated by the hydrodynamic model. Considering importance of the diffusivity in freshwater ecosystems, more attention should be paid to this topic and my thesis can be seen as a first attempt for future related studies. Influenced by global warming, not only the two climate variables above but also the other variables (e.g. cloud cover, shortwave

radiation, precipitation) will be changed (Donat et al. 2016,Pryor et al. 2009), and all such changes can affect vertical diffusion in water column (Joehnk et al. 2008,Richardson et al. 2017). Therefore, it is suggested in future research to check the response of turbulent diffusivity to real climate projections, and thus draw a more promising conclusion in this topic.

Elucidating the development of vertical diffusivity and its influencing factors will improve our understanding about transportation processes of oxygen in lentic waters. An interesting phenomenon about vertical distribution of dissolved oxygen, in both Rappbode Reservoir and Lake Arendsee, is that its minimum concentration in summer does not appear in the hypolimnion but instead in the metalimnion, which is supposed to be closely related to the minimum of vertical diffusivity in this layer (Kreling et al. 2017,Mi et al. 2020). Actually this metalimnetic oxygen minimum (i.e. MOM) is a well-known phenomenon (McClure et al. 2018,Wentzky et al. 2019), but did not get enough attention in the previous studies. It has been shown that MOM can cause fish kills (Rice et al. 2013), change greenhouse gas dynamics (McClure et al. 2018) and help release of manganese or other unwanted substances in deep reservoirs (Carraro et al. 2012). Consequently, identifying drivers for MOM and finding out management strategies to control the phenomenon should be important topics for the future research. Results in this thesis give reservoir authorities a hint to deal with MOM that it may be an effective way to solve the problem by withdrawing water from the metalimnion, since this strategy can increase vertical diffusivity in this layer and thus facilitate more oxygen penetrating into it.

### 6.4.3. Near-term forecast

The research in this thesis mainly focused on the response of thermal dynamics in lentic waters to long-term climate projections (i.e. multidecadal time scales) or general changes of specific climate variables (e.g. wind speed, air temperature). It is suggested in the next step to pay more attention to near-term (daily to monthly) physical or ecological forecasts. On the one hand, traditional calibration-validation process for coupled hydrodynamic-water quality models cannot guarantee that they always perform well under changing external drivers, actually they always fail to do so (Cole and Wells 2006). This near-term forecast allows modelers to get feedback from new observations more quickly, effectively optimize the parameterization during the continuous predictions and iteratively test models. In other words, near-term forecasts help models to be continually updated with new data and make their future predictions more precise (Dietze et al. 2018). Furthermore, from the pragmatic view, environmental decision-making is based on near-term, rather than long-term, predictions. This is clear to us all since the stakeholders cannot change their current management strategies due to the projections after one hundred years. Based on this near-term forecast, stakeholders can have a couple of days' notice so as to have enough time to react for the potential water quality problems. After optimizing their management strategies, based on the simulation results, modelers will get back new data for the next forecast. It means that this kind of forecast can support human-in-the-loop decisions and increase the adaptive capacity of the water utility. To the best of our knowledge, there are already some modelers focusing on this near-term forecast for aquatic ecosystems (see Li et al. 2014,Vinçon-Leite et al. 2017,Zhang et al. 2013). However, most of the related research made

the near-term forecast for shallow lakes, while very few of them did the forecast for vertical structure of stratified waters. Also, the forecasts in the current research were always based on the fixed parameterization and the modelling tools were not advanced enough to do the self-optimization, which limits their prediction accuracy. All in all, this near-term forecast for lentic waters is still in its infancy and has much space for development. Just as shown in Berdalet et al. (2018), the societal demand for this forecast, which was already high, is growing considerably, so now is the best time to further develop the near-term aquatic forecast and it should be an important extension of this thesis. Maybe it is still a long way to go since the current modelling skills are not "good enough" to make the perfect near-term forecast, but we should keep in mind that learning by doing is the fastest route to drive the science forward.

# 7. References


Adrian, R., C. M. O'Reilly, H. Zagarese, S. B. Baines, D. O. Hessen, W. Keller, D. M. Livingstone, R. Sommaruga, D. Straile, E. Van Donk, G. A. Weyhenmeyer, M. Winder, 2009. Lakes as sentinels of climate change. Limnology and Oceanography 54(6):2283-2297.

Aghasian, K., A. Moridi, A. Mirbagheri, M. Abbaspour, 2019. Selective withdrawal optimization in a multipurpose water use reservoir. Int J Environ Sci Technol (Tehran) 16(10):5559-5568.

Ajami, N. K., Q. Duan, S. Sorooshian, 2007. An integrated hydrologic Bayesian multimodel combination framework: Confronting input, parameter, and model structural uncertainty in hydrologic prediction. Water Resources Research 43(1).

Andersen, M. R., E. de Eyto, M. Dillane, R. Poole, E. Jennings, 2020. 13 Years of Storms: An Analysis of the Effects of Storms on Lake Physics on the Atlantic Fringe of Europe. Water 12(2):318.

Appt, J., J. Imberger, H. Kobus, 2004. Basin‐scale motion in stratified Upper Lake Constance. Limnology and Oceanography 49(4):919-933.

Arhonditsis, G. B., M. T. Brett, 2004. Evaluation of the current state of mechanistic aquatic biogeochemical modeling. Mar Ecol Prog Ser 271:13-26.

Aumann, H. H., A. Behrangi, Y. Wang, 2018. Increased frequency of extreme tropical deep convection: AIRS observations and climate model predictions. Geophysical Research Letters 45(24):13,530-13,537.

Austin, J. A., J. Allen, 2011. Sensitivity of summer Lake Superior thermal structure to meteorological forcing. Limnology and Oceanography 56(3):1141-1154.

Ayala, A. I., S. Moras, D. C. Pierson, 2019. Simulations of future changes in thermal structure of Lake Erken: Proof of concept for ISIMIP2b lake sector local simulation strategy. Hydrol Earth Syst Sci Discuss 2019:1-25.

Bai, H., Y. Chen, D. Wang, R. Zou, H. Zhang, R. Ye, W. Ma, Y. Sun, 2018. Developing an EFDC and Numerical Source-Apportionment Model for Nitrogen and Phosphorus Contribution Analysis in a Lake Basin. Water 10(10):1315.

Bastviken, D., L. J. Tranvik, J. A. Downing, P. M. Crill, A. Enrich-Prast, 2011. Freshwater methane emissions offset the continental carbon sink. Science 331(6013):50-50.

Berdalet, E., R. M. Kudela, N. S. Banas, E. Bresnan, M. A. Burford, K. Davidson, C. J. Gobler, B. Karlson, P. T. Lim, L. Mackenzie, 2018. GlobalHAB: fostering international coordination on harmful algal bloom research in aquatic systems Global Ecology and Oceanography of Harmful Algal Blooms. Springer, 425-447.

Bergkemper, V., T. Weisse, 2017. Phytoplankton response to the summer 2015 heat wave–a case study from prealpine Lake Mondsee, Austria. Inland Waters 7(1):88-99.

Bernhardt, J., G. Kirillin, 2013. Seasonal pattern of rotation‐affected internal seiches in a small temperate lake. Limnology and Oceanography 58(4):1344-1360.

Bocaniov, S. A., C. Ullmann, K. Rinke, K. G. Lamb, B. Boehrer, 2014. Internal waves and mixing in a stratified reservoir: insights from three-dimensional modeling. Limnologica 49:52-67.
Boehrer, B., 2000. Modal response of a deep stratified lake: western Lake Constance. Journal of Geophysical Research: Oceans 105(C12):28837-28845.
Boehrer, B., J. Ilmberger, K. O. Münnich, 2000. Vertical structure of currents in western Lake Constance. Journal of Geophysical Research: Oceans 105(C12):28823-28835.
Boehrer, B., U. Kiwel, K. Rahn, M. Schultze, 2014. Chemocline erosion and its conservation by freshwater introduction to meromictic salt lakes. Limnologica 44:81-89.
Boehrer, B., M. Schultze, 2008. Stratification of lakes. Rev Geophy 46:RG 2005.
Boehrer, B., M. Schultze, 2009a. Density Stratification and Stability.
Boehrer, B., M. Schultze, 2009b. Density Stratification and Stability. Encyclopedia of Inland Waters 1:583-593.
Bolton, D., 1980. The computation of equivalent potential temperature. Mon Weather Rev 108(7):1046-1053.
Bonnet, M. P., M. Poulin, J. Devaux, 2000. Numerical modeling of thermal stratification in a lake reservoir. Methodology and case study. Aquatic Sciences 62(2):105-124.
Brito, D., T. B. Ramos, M. C. Gonçalves, M. Morais, R. Neves, 2018. Integrated modelling for water quality management in a eutrophic reservoir in south-eastern Portugal. Environmental Earth Sciences 77(2):40.
Bromirski, P. D., R. E. Flick, D. R. Cayan, 2003. Storminess variability along the California coast: 1858-2000. Journal of Climate 16(6):982-993.
Bruce, L. C., M. A. Frassl, G. B. Arhonditsis, G. Gal, D. P. Hamilton, P. C. Hanson, A. L. Hetherington, J. M. Melack, J. S. Read, K. Rinke, A. Rigosi, D. Trolle, L. Winslow, R. Adrian, A. I. Ayala, S. A. Bocaniov, B. Boehrer, C. Boon, J. D. Brookes, T. Bueche, B. D. Busch, D. Copetti, A. Cortes, E. de Eyto, J. A. Elliott, N. Gallina, Y. Gilboa, N. Guyennon, L. Huang, O. Kerimoglu, J. D. Lenters, S. MacIntyre, V. Makler-Pick, C. G. McBride, S. Moreira, D. Ozkundakci, M. Pilotti, F. J. Rueda, J. A. Rusak, N. R. Samal, M. Schmid, T. Shatwell, C. Snorthheim, F. Soulignac, G. Valerio, L. van der Linden, M. Vetter, B. Vincon-Leite, J. B. Wang, M. Weber, C. Wickramaratne, R. I. Woolway, H. X. Yao, M. R. Hipsey, 2018. A multi-lake comparative analysis of the General Lake Model (GLM): Stress-testing across a global observatory network. Environmental Modelling & Software 102:274-291.
Bryant, L. D., H. Hsu-Kim, P. A. Gantzer, J. C. Little, 2011. Solving the problem at the source: controlling Mn release at the sediment-water interface via hypolimnetic oxygenation. Water research 45(19):6381-6392.
Bueche, T., D. P. Hamilton, M. Vetter, 2017. Using the General Lake Model (GLM) to simulate water temperatures and ice cover of a medium-sized lake: a case study of Lake Ammersee, Germany. Environmental Earth Sciences 76:461.
Bueche, T., M. Vetter, 2015. Future alterations of thermal characteristics in a medium-sized lake simulated by coupling a regional climate model with a lake model. Clim Dynam 44(1-2):371-384.
Burger, D. F., D. P. Hamilton, C. A. Pilditch, 2008. Modelling the relative importance of internal and external nutrient loads on water column nutrient concentrations and phytoplankton biomass in a shallow polymictic lake. Ecological Modelling 211(3-4):411-423.
Butcher, J. B., D. Nover, T. E. Johnson, C. M. Clark, 2015. Sensitivity of lake thermal and mixing dynamics to climate change. Climatic Change 129:295-305.
Çalışkan, A., Ş. Elçi, 2009. Effects of selective withdrawal on hydrodynamics of a stratified reservoir. Water Resour Manag 23(7):1257-1273.
Cao, J., Z. Chu, Y. Du, Z. Hou, S. Wang, 2016. Phytoplankton dynamics and their relationship with environmental variables of Lake Poyang. Hydrology Research 47(S1):249-260.
Capotondi, A., M. A. Alexander, N. A. Bond, E. N. Curchitser, J. D. Scott, 2012. Enhanced upper ocean stratification with climate change in the CMIP3 models. Journal of Geophysical Research: Oceans 117(C4).
Carr, M. K., A. Sadeghian, K.-E. Lindenschmidt, K. Rinke, L. Morales-Marin, 2019. Impacts of Varying Dam Outflow Elevations on Water Temperature, Dissolved Oxygen, and Nutrient Distributions in a Large Prairie Reservoir. Environ Eng Sci.

Carraro, E., N. Guyennon, D. Hamilton, L. Valsecchi, E. C. Manfredi, G. Viviano, F. Salerno, G. Tartari, D. Copetti, 2012. Coupling high-resolution measurements to a three-dimensional lake model to assess the spatial and temporal dynamics of the cyanobacterium Planktothrix rubescens in a medium-sized lake Hydrobiologia. Springer, 77-95.

Casamitjana, X., T. Serra, J. Colomer, C. Baserba, J. Pérez-Losada, 2003. Effects of the water withdrawal in the stratification patterns of a reservoir. Hydrobiologia 504(1):21-28.

Chai, T., R. R. Draxler, 2014. Root mean square error (RMSE) or mean absolute error (MAE)?–Arguments against avoiding RMSE in the literature. Geoscientific Model Development 7(3):1247-1250.

Chang, C. H., L. Y. Cai, T. F. Lin, C. L. Chung, L. van der Linden, M. Burch, 2015. Assessment of the Impacts of Climate Change on the Water Quality of a Small Deep Reservoir in a Humid-Subtropical Climatic Region. Water 7(4):1687-1711.

Chen, C. T. A., F. J. Millero, 1986. Thermodynamic properties for natural waters covering only the limnological range 1. Limnology and Oceanography 31(3):657-662.

Chen, W., A. Nielsen, T. K. Andersen, F. Hu, Q. Chou, M. Søndergaard, E. Jeppesen, D. Trolle, 2020. Modeling the Ecological Response of a Temporarily Summer-Stratified Lake to Extreme Heatwaves. Water 12(1):94.

Chuo, M., J. Ma, D. Liu, Z. Yang, 2019. Effects of the impounding process during the flood season on algal blooms in Xiangxi Bay in the Three Gorges Reservoir, China. Ecological Modelling 392:236-249.

Churchill, J. H., W. C. Kerfoot, 2007. The impact of surface heat flux and wind on thermal stratification in Portage Lake, Michigan. Journal of Great Lakes Research 33(1):143-155.

Cole, T. M., S. A. Wells, 2006. CE-QUAL-W2: A two-dimensional, laterally averaged, hydrodynamic and water quality model, version 3.5.

Coloso, J. J., J. J. Cole, M. L. Pace, 2011. Short-term variation in thermal stratification complicates estimation of lake metabolism. Aquatic Sciences 73(2):305-315.

Cowx, I., M. Portocarrero Aya, 2011. Paradigm shifts in fish conservation: moving to the ecosystem services concept. J Fish Biol 79(6):1663-1680.

Craig, P., D. Chung, N. Lam, P. Son, N. Tinh, 2014. Sigma-Zed: A Computationally Efficient Approach To Reduce The Horizontal Gradient Error In The EFDC's Vertical Sigma Grid. ICHD.

Desai, A. R., J. A. Austin, V. Bennington, G. A. McKinley, 2009. Stronger winds over a large lake in response to weakening air-to-lake temperature gradient. Nature Geoscience 2(12):855-858.

Dietz, S., D. Lessmann, B. Boehrer, 2012. Contribution of solutes to density stratification in a meromictic lake (Waldsee/Germany). Mine Water Environ 31(2):129-137.

Dietze, M. C., A. Fox, L. M. Beck-Johnson, J. L. Betancourt, M. B. Hooten, C. S. Jarnevich, T. H. Keitt, M. A. Kenney, C. M. Laney, L. G. Larsen, H. W. Loescher, C. K. Lunch, B. C. Pijanowski, J. T. Randerson, E. K. Read, A. T. Tredennick, R. Vargas, K. C. Weathers, E. P. White, 2018. Iterative near-term ecological forecasting: Needs, opportunities, and challenges. Proceedings of the National Academy of Sciences 115(7):1424-1432.

Donat, M. G., A. L. Lowry, L. V. Alexander, P. A. O'Gorman, N. Maher, 2016. More extreme precipitation in the world's dry and wet regions. Nature Climate Change 6(5):508-513.

Easterling, D. R., G. A. Meehl, C. Parmesan, S. A. Changnon, T. R. Karl, L. O. Mearns, 2000. Climate extremes: Observations, modeling, and impacts. Science 289(5487):2068-2074.

Edlund, M. B., J. E. Almendinger, X. Fang, J. M. R. Hobbs, D. D. VanderMeulen, R. L. Key, D. R. Engstrom, 2017. Effects of Climate Change on Lake Thermal Structure and Biotic Response in Northern Wilderness Lakes. Water 9(9):678.

Engelhardt, C., G. Kirillin, 2014. Criteria for the onset and breakup of summer lake stratification based on routine temperature measurements. Fundamental and Applied Limnology/Archiv für Hydrobiologie 184(3):183-194.

England, M. H., J. B. Kajtar, N. Maher, 2015. Robust warming projections despite the recent hiatus. Nature Climate Change 5(5):394-396.

Fan, C.-W., S.-J. Kao, 2008. Effects of climate events driven hydrodynamics on dissolved oxygen in a subtropical deep reservoir in Taiwan. Science of the total environment 393(2):326-332.

Fang, X., H. G. Stefan, 1999. Projections of climate change effects on water temperature characteristics of

small lakes in the contiguous US. Climatic Change 42(2):377-412.
Fang, X., H. G. Stefan, 2009. Simulations of climate effects on water temperature, dissolved oxygen, and ice and snow covers in lakes of the contiguous United States under past and future climate scenarios. Limnology and Oceanography 54:2359-2370.
Fee, E., R. Hecky, S. Kasian, D. Cruikshank, 1996. Effects of lake size, water clarity, and climatic variability on mixing depths in Canadian Shield lakes. Limnology and Oceanography 41(5):912-920.
Feldbauer, J., D. Kneis, T. Hegewald, T. U. Berendonk, T. Petzoldt, 2020. Managing climate change in drinking water reservoirs: potentials and limitations of dynamic withdrawal strategies. Environmental Sciences Europe 32(1):48.
Fenocchi, A., M. Rogora, G. Morabito, A. Marchetto, S. Sibilla, C. Dresti, 2019. Applicability of a one-dimensional coupled ecological-hydrodynamic numerical model to future projections in a very deep large lake (Lake Maggiore, Northern Italy/Southern Switzerland). Ecological Modelling 392:38-51.
Fenocchi, A., M. Rogora, S. Sibilla, M. Ciampittiello, C. Dresti, 2018. Forecasting the evolution in the mixing regime of a deep subalpine lake under climate change scenarios through numerical modelling (Lake Maggiore, Northern Italy/Southern Switzerland). Clim Dynam:1-16.
Fenocchi, A., M. Rogora, S. Sibilla, C. Dresti, 2017. Relevance of inflows on the thermodynamic structure and on the modeling of a deep subalpine lake (Lake Maggiore, Northern Italy/Southern Switzerland). Limnologica 63:42-56.
Fenocchi, A., S. Sibilla, 2016. Hydrodynamic modelling and characterisation of a shallow fluvial lake: a study on the Superior Lake of Mantua. J Limnol 75(3).
Ficker, H., M. Luger, H. Gassner, 2017. From dimictic to monomictic: Empirical evidence of thermal regime transitions in three deep alpine lakes in Austria induced by climate change. Freshwater Biology 62(8):1335-1345.
Findlay, D., H. Kling, H. Rönicke, W. Findlay, 1998. A paleolimnological study of eutrophied Lake Arendsee (Germany). J Paleolimnol 19(1):41-54.
Fink, G., M. Schmid, B. Wahl, T. Wolf, A. Wuest, 2014a. Heat flux modifications related to climate-induced warming of large European lakes. Water Resources Research 50(3):2072-2085.
Fink, G., M. Schmid, A. Wüest, 2014b. Large lakes as sources and sinks of anthropogenic heat: Capacities and limits. Water Resources Research 50(9):7285-7301.
Flaim, G., E. Eccel, A. Zeileis, G. Toller, L. Cerasino, U. Obertegger, 2016. Effects of re‐oligotrophication and climate change on lake thermal structure. Freshwater Biology 61(10):1802-1814.
Foley, B., I. D. Jones, S. C. Maberly, B. Rippey, 2012. Long‐term changes in oxygen depletion in a small temperate lake: effects of climate change and eutrophication. Freshwater Biology 57(2):278-289.
Frassl, M. A., B. Boehrer, P. L. Holtermann, W. Hu, K. Klingbeil, Z. Peng, J. Zhu, K. Rinke, 2018. Opportunities and Limits of Using Meteorological Reanalysis Data for Simulating Seasonal to Sub-Daily Water Temperature Dynamics in a Large Shallow Lake. Water 10(5):594.
Frassl, M. A., K.-O. Rothhaupt, K. Rinke, 2014. Algal internal nutrient stores feedback on vertical phosphorus distribution in large lakes. Journal of Great Lakes Research 40:162-172.
Frieler, K., S. Lange, F. Piontek, C. P. Reyer, J. Schewe, L. Warszawski, F. Zhao, L. Chini, S. Denvil, K. Emanuel, 2017. Assessing the impacts of 1.5 C global warming–simulation protocol of the Inter-Sectoral Impact Model Intercomparison Project (ISIMIP2b). Geoscientific Model Development.
Friese, K., M. Schultze, B. Boehrer, O. Büttner, P. Herzsprung, M. Koschorreck, B. Kuehn, H. Rönicke, K. Wendt‐Potthoff, U. Wollschläger, 2014. Ecological response of two hydro‐morphological similar pre‐dams to contrasting land‐use in the Rappbode reservoir system (Germany). International Review of Hydrobiology 99(5):335-349.
Gantzer, P. A., L. D. Bryant, J. C. Little, 2009. Effect of hypolimnetic oxygenation on oxygen depletion rates in two water-supply reservoirs. Water research 43(6):1700-1710.
Gaudard, A., R. Schwefel, L. R. Vinnå, M. Schmid, A. Wüest, D. Bouffard, 2017. Optimizing the parameterization of deep mixing and internal seiches in one-dimensional hydrodynamic models: a case study with Simstrat v1. 3. Geoscientific Model Development 10(9):3411-3423.

Giling, D. P., J. C. Nejstgaard, S. A. Berger, H. P. Grossart, G. Kirillin, A. Penske, M. Lentz, P. Casper, J. Sareyka, M. O. Gessner, 2017a. Thermocline deepening boosts ecosystem metabolism: evidence from a large-scale lake enclosure experiment simulating a summer storm. Global Change Biology 23(4):1448-1462.

Giling, D. P., P. A. Staehr, H. P. Grossart, M. R. Andersen, B. Boehrer, C. Escot, F. Evrendilek, L. Gómez‐Gener, M. Honti, I. D. Jones, 2017b. Delving deeper: Metabolic processes in the metalimnion of stratified lakes. Limnology and Oceanography 62(3):1288-1306.

Goudsmit, G. H., F. Peeters, M. Gloor, A. Wüest, 1997. Boundary versus internal diapycnal mixing in stratified natural waters. Journal of Geophysical Research: Oceans 102(C13):27903-27914.

Hamrick, J. M., 1992. A three-dimensional environmental fluid dynamics computer code: Theoretical and computational aspects.

Hamrick, J. M., 1996. User's manual for the environmental fluid dynamics computer code.

Hawcroft, M., E. Walsh, K. Hodges, G. Zappa, 2018. Significantly increased extreme precipitation expected in Europe and North America from extratropical cyclones. Environmental research letters 13(12):124006.

Heinz, G., J. Ilmberger, M. Schimmele, 1990. Vertical mixing in Überlinger See, western part of Lake Constance. Aquatic Sciences 52(3):256-268.

Henderson-Sellers, B., 1986. Calculating the surface energy balance for lake and reservoir modeling: A review. Rev Geophy 24(3):625-649.

Herring, S. C., N. Christidis, A. Hoell, M. P. Hoerling, P. A. Stott, 2020. Explaining Extreme Events of 2018 from a Climate Perspective. B Am Meteorol Soc 101(1):S1-S128.

Hillmer, I., P. van Reenen, J. Imberger, T. Zohary, 2008. Phytoplankton patchiness and their role in the modelled productivity of a large, seasonally stratified lake. Ecological Modelling 218(1-2):49-59.

Hipel, K. W., A. I. McLeod, 1994. Time series modelling of water resources and environmental systems, vol 45. Elsevier.

Hipsey, M. R., L. C. Bruce, C. Boon, B. Busch, C. C. Carey, D. P. Hamilton, P. C. Hanson, J. S. Read, E. de Sousa, M. Weber, L. A. Winslow, 2017. A General Lake Model (GLM 2.4) for linking with high‐frequency sensor data from the Global Lake Ecological Observatory Network (GLEON). Geoscientific Model Development.

Hipsey, M. R., L. C. Bruce, D. P. Hamilton, 2014. GLM - General Lake Model: Model overview and user information. The

University of Western Australia, Perth, Australia. AED Report #26.

Hodges, B., J. Imberger, B. Laval, J. Appt, Modeling the hydrodynamics of stratified lakes. In: Hydroinformatics 2000 Conference, 2000a. vol 4. p 23-27.

Hodges, B. R., J. Imberger, A. Saggio, K. B. Winters, 2000b. Modeling basin‐scale internal waves in a stratified lake. Limnology and oceanography 45(7):1603-1620.

Hondzo, M., H. G. Stefan, 1993. Regional water temperature characteristics of lakes subjected to climate change. Climatic change 24(3):187-211.

Horn, H., L. Paul, W. Horn, D. Uhlmann, I. Röske, 2015. Climate change impeded the re‐oligotrophication of the Saidenbach Reservoir. International Review of Hydrobiology 100(2):43-60.

Hu, F., K. Bolding, J. Bruggeman, E. Jeppesen, M. R. Flindt, L. Van Gerven, J. H. Janse, A. B. Janssen, J. J. Kuiper, W. M. Mooij, 2016. FABM-PCLake–linking aquatic ecology with hydrodynamics. Geoscientific Model Development 9(6):2271-2278.

Huber, M. B., L. Zanna, 2017. Drivers of uncertainty in simulated ocean circulation and heat uptake. Geophysical Research Letters 44(3):1402-1413.

Hupfer, M., K. Reitzel, A. Kleeberg, J. Lewandowski, 2016. Long-term efficiency of lake restoration by chemical phosphorus precipitation: Scenario analysis with a phosphorus balance model. Water research 97:153-161.

Hutchinson, G. E., H. Loffler, 1956. THE THERMAL CLASSIFICATION OF LAKES. Proc Natl Acad Sci U S A 42(2):84-86.

Idso, 1973. On the concept of lake stability. Limnology and Oceanography 18:681-683.

Imberger, J., 1981. A dynamic reservoir simulation model-DYRESM. Transport models for inland and coastal waters:310-361.

Imboden, D. M., U. Lemmin, T. Joller, M. Schurter, 1983. MIXING PROCESSES IN LAKES - MECHANISMS AND ECOLOGICAL RELEVANCE. Schweizerische Zeitschrift Fur Hydrologie-Swiss Journal of Hydrology 45(1):11-44.

IPCC, 2014. Climate change 2014: synthesis report. Contribution of Working Groups I,II and III to the Fifth Assessment Report of the intergovernmental panel on Climate Change. e [Core Writing Team, R.K. Pachauri and L.A. Meyer (eds.)].IPCC, Geneva, Switzerland. 151.

Ishikawa, T., M. Tanaka, 2010. Diurnal stratification and its effects on wind-induced currents and water qualities in Lake Kasumigaura, Japan. Journal of Hydraulic Research 31(3):307-322.

Jang, C. J., J. Park, T. Park, S. Yoo, 2011. Response of the ocean mixed layer depth to global warming and its impact on primary production: a case for the North Pacific Ocean. Ices J Mar Sci 68(6):996-1007.

Jansen, M. F., 2017. Glacial ocean circulation and stratification explained by reduced atmospheric temperature. Proceedings of the National Academy of Sciences 114(1):45-50.

Janssen, A. B. G., G. B. Arhonditsis, A. Beusen, K. Bolding, L. Bruce, J. Bruggeman, R. M. Couture, A. S. Downing, J. A. Elliott, M. A. Frassl, G. Gal, D. J. Gerla, M. R. Hipsey, F. J. Hu, S. C. Ives, J. H. Janse, E. Jeppesen, K. D. Johnk, D. Kneis, X. Z. Kong, J. J. Kuiper, M. K. Lehmann, C. Lemmen, D. Ozkundakci, T. Petzoldt, K. Rinke, B. J. Robson, R. Sachse, S. A. Schep, M. Schmid, H. Scholten, S. Teurlincx, D. Trolle, T. A. Troost, A. A. Van Dam, L. P. A. Van Gerven, M. Weijerman, S. A. Wells, W. M. Mooij, 2015. Exploring, exploiting and evolving diversity of aquatic ecosystem models: a community perspective. Aquat Ecol 49(4):513-548.

Jennings, E., S. Jones, L. Arvola, P. A. Staehr, E. Gaiser, I. D. Jones, K. C. Weathers, G. A. Weyhenmeyer, C. Y. CHIU, E. De Eyto, 2012. Effects of weather‐related episodic events in lakes: an analysis based on high‐frequency data. Freshwater Biology 57(3):589-601.

Jeppesen, E., B. Kronvang, M. Meerhoff, M. Sondergaard, K. M. Hansen, H. E. Andersen, T. L. Lauridsen, L. Liboriussen, M. Beklioglu, A. Ozen, J. E. Olesen, 2009. Climate Change Effects on Runoff, Catchment Phosphorus Loading and Lake Ecological State, and Potential Adaptations. J Environ Qual 38(5):1930-1941.

Jeppesen, E., M. Meerhoff, T. A. Davidson, D. Trolle, M. SondergaarD, T. L. Lauridsen, M. Beklioglu, S. Brucet Balmaña, P. Volta, I. González-Bergonzoni, 2014. Climate change impacts on lakes: an integrated ecological perspective based on a multi-faceted approach, with special focus on shallow lakes.

Jin, J., S. A. Wells, D. Liu, G. Yang, S. Zhu, J. Ma, Z. Yang, 2019. Effects of water level fluctuation on thermal stratification in a typical tributary bay of Three Gorges Reservoir, China. PeerJ 7:e6925.

Joehnk, K. D., J. Huisman, J. Sharples, B. Sommeijer, P. M. Visser, J. M. Stroom, 2008. Summer heatwaves promote blooms of harmful cyanobacteria. Global change biology 14(3):495-512.

Józsa, J., 2014. On the internal boundary layer related wind stress curl and its role in generating shallow lake circulations. Journal of Hydrology and Hydromechanics 62(1):16-23.

Karpowicz, M., J. Ejsmont-Karabin, 2017. Effect of metalimnetic gradient on phytoplankton and zooplankton (Rotifera, Crustacea) communities in different trophic conditions. Environ Monit Assess 189(8):367.

Kerimoglu, O., K. Rinke, 2013. Stratification dynamics in a shallow reservoir under different hydro‐meteorological scenarios and operational strategies. Water Resources Research 49(11):7518-7527.

King, A. D., D. J. Karoly, B. J. Henley, 2017. Australian climate extremes at 1.5 °C and 2 °C of global warming. Nature Climate Change 7(6):412-416.

Kirillin, G., 2010. Modeling the impact of global warming on water temperature and seasonal mixing regimes in small temperate lakes. Boreal Environ Res 15:279-293.

Kirillin, G., T. Shatwell, 2016. Generalized scaling of seasonal thermal stratification in lakes. Earth-sci Rev 161:179-190.

Kirillin, G., T. Shatwell, P. Kasprzak, 2013. Consequences of thermal pollution from a nuclear plant on lake temperature and mixing regime. Journal of Hydrology 496:47-56.

Klug, J. L., D. C. Richardson, H. A. Ewing, B. R. Hargreaves, N. R. Samal, D. Vachon, D. C. Pierson, A. M. Lindsey, D. M. O'Donnell, S. W. Effler, 2012. Ecosystem effects of a tropical cyclone on a network of lakes in northeastern North America. Environmental science & technology 46(21):11693-11701.

Kobler, U. G., A. Wüest, M. Schmid, 2018. Effects of Lake–Reservoir Pumped-Storage Operations on Temperature and Water Quality. Sustainability 10(ARTICLE):1968.
Koue, J., H. Shimadera, T. Matsuo, A. Kondo, 2018. Numerical assessment of the impact of strong wind on thermal stratification in Lake Biwa, Japan. International Journal 14(45):35-40.
Kraemer, B. M., O. Anneville, S. Chandra, 2015. Morphometry and average temperature affect lake stratification responses to climate change. Geophysical Research Letters 42:4981-4988.
Kreling, J., J. Bravidor, C. Engelhardt, M. Hupfer, M. Koschorreck, A. Lorke, 2017. The importance of physical transport and oxygen consumption for the development of a metalimnetic oxygen minimum in a lake. Limnology and Oceanography 62(1):348-363.
Kundzewicz, Z., V. Krysanova, R. Benestad, Ø. Hov, M. Piniewski, I. Otto, 2018. Uncertainty in climate change impacts on water resources. Environ Sci Policy 79:1-8.
Ladwig, R., E. Furusato, G. Kirillin, R. Hinkelmann, M. Hupfer, 2018. Climate Change Demands Adaptive Management of Urban Lakes: Model-Based Assessment of Management Scenarios for Lake Tegel (Berlin, Germany). Water 10(2).
Laval, B., B. R. Hodges, J. Imberger, 2003. Reducing numerical diffusion effects with pycnocline filter. Journal of Hydraulic Engineering 129(3):215-224.
Lawrence, M. G., 2005. The relationship between relative humidity and the dewpoint temperature in moist air: A simple conversion and applications. B Am Meteorol Soc 86(2):225-234.
Laybourn-Parry, J., J. L. Wadham, 2014. Antarctic Lakes.
Leach, T. H., B. E. Beisner, C. C. Carey, P. Pernica, K. C. Rose, Y. Huot, J. A. Brentrup, I. Domaizon, H. P. Grossart, B. W. Ibelings, 2018. Patterns and drivers of deep chlorophyll maxima structure in 100 lakes: The relative importance of light and thermal stratification. Limnology and Oceanography 63(2):628-646.
Lee, R., T. Biggs, X. Fang, 2018. Thermal and Hydrodynamic Changes under a Warmer Climate in a Variably Stratified Hypereutrophic Reservoir. Water 10(9):1284.
Lehner, B., P. Döll, 2004. Development and validation of a global database of lakes, reservoirs and wetlands. Journal of Hydrology 296(1-4):1-22.
Lewis Jr, W. M., J. H. McCutchan Jr, J. Roberson, 2019. Effects of Climatic Change on Temperature and Thermal Structure of a Mountain Reservoir. Water Resources Research 55(3):1988-1999.
Lewis, W. M., 1983. A REVISED CLASSIFICATION OF LAKES BASED ON MIXING. Canadian Journal of Fisheries and Aquatic Sciences 40(10):1779-1787.
Li, W., B. Qin, G. Zhu, 2014. Forecasting short‐term cyanobacterial blooms in Lake Taihu, China, using a coupled hydrodynamic–algal biomass model. Ecohydrology 7(2):794-802.
Lopez, A., E. B. Suckling, F. Otto, A. Lorenz, D. Rowlands, M. Allen, 2015. Towards a typology for constrained climate model forecasts. Climatic Change 132(1):15-29.
Luo, Y., Y. Zhao, K. Yang, K. Chen, M. Pan, X. Zhou, 2018. Dianchi Lake watershed impervious surface area dynamics and their impact on lake water quality from 1988 to 2017. Environ Sci Pollut R 25(29):29643-29653.
Ma, S., S. C. Kassinos, D. Fatta Kassinos, E. Akylas, 2008. Effects of selective water withdrawal schemes on thermal stratification in Kouris Dam in Cyprus. Lakes & Reservoirs: Research & Management 13(1):51-61.
Magee, M. R., C. H. Wu, 2016. Response of water temperatures and stratification to changing climate in three lakes with different morphometry. Hydrology and Earth System Sciences, in review.
Magee, M. R., C. H. Wu, 2017. Response of water temperatures and stratification to changing climate in three lakes with different morphometry. Hydrology and Earth System Sciences 21(12):6253-6274.
Malmqvist, B., S. Rundle, 2002. Threats to the running water ecosystems of the world. Environ Conserv 29(2):134-153.
Mao, M., A. J. Van Der Westhuysen, M. Xia, D. J. Schwab, A. Chawla, 2016. Modeling wind waves from deep to shallow waters in Lake Michigan using unstructured SWAN. Journal of Geophysical Research: Oceans 121(6):3836-3865.
Marmorino, G., 1978. Warm bottom water in lake Michigan. Limnology and Oceanography 23(5):1017-1020.
McClure, R. P., K. D. Hamre, B. Niederlehner, Z. W. Munger, S. Chen, M. E. Lofton, M. E. Schreiber, C. C. Carey, 2018. Metalimnetic oxygen minima alter the vertical profiles of carbon dioxide and

methane in a managed freshwater reservoir. Science of The Total Environment 636:610-620.
McVicar, T. R., M. L. Roderick, 2010. Atmospheric science: winds of change. Nature Geoscience 3(11):747.
Meinikmann, K., M. Hupfer, J. Lewandowski, 2015. Phosphorus in groundwater discharge–A potential source for lake eutrophication. Journal of Hydrology 524:214-226.
Meinshausen, M., S. J. Smith, K. Calvin, J. S. Daniel, M. Kainuma, J.-F. Lamarque, K. Matsumoto, S. Montzka, S. Raper, K. Riahi, 2011. The RCP greenhouse gas concentrations and their extensions from 1765 to 2300. Climatic change 109(1-2):213.
Mellor, G. L., T. Yamada, 1982. Development of a turbulence closure model for geophysical fluid problems. Rev Geophy 20(4):851-875.
Mi, C., M. A. Frassl, B. Boehrer, K. Rinke, 2018. Episodic wind events induce persistent shifts in the thermal stratification of a reservoir (Rappbode Reservoir, Germany). International Review of Hydrobiology 103:71-82.
Mi, C., A. Sadeghian, K.-E. Lindenschmidt, K. Rinke, 2019. Variable withdrawal elevations as a management tool to counter the effects of climate warming in Germany's largest drinking water reservoir. Environmental Sciences Europe 31(1):19.
Mi, C., T. Shatwell, J. Ma, V. C. Wentzky, B. Boehrer, Y. Xu, K. Rinke, 2020. The formation of a metalimnetic oxygen minimum exemplifies how ecosystem dynamics shape biogeochemical processes: A modelling study. Water Research.
Moshfeghi, H., A. Etemad-Shahidi, J. Imberger, 2005. Modelling of bubble plume destratification using DYRESM. Journal of Water Supply: Research and Technology-Aqua 54(1):37-46.
Moss, R., W. Babiker, S. Brinkman, E. Calvo, T. Carter, J. Edmonds, I. Elgizouli, S. Emori, L. Erda, K. Hibbard, 2008. Towards new scenarios for the analysis of emissions: Climate change, impacts and response strategies. Intergovernmental Panel on Climate Change Secretariat (IPCC).
Müller, B., L. D. Bryant, A. Matzinger, A. Wüest, 2012. Hypolimnetic oxygen depletion in eutrophic lakes. Environmental Science & Technology 46(18):9964-9971.
North, R. P., R. L. North, D. M. Livingstone, O. Köster, R. Kipfer, 2014. Long‐term changes in hypoxia and soluble reactive phosphorus in the hypolimnion of a large temperate lake: consequences of a climate regime shift. Global change biology 20(3):811-823.
O'Reilly, C. M., S. Sharma, D. K. Gray, S. E. Hampton, J. S. Read, R. J. Rowley, P. Schneider, J. D. Lenters, P. B. McIntyre, B. M. Kraemer, 2015. Rapid and highly variable warming of lake surface waters around the globe. Geophysical Research Letters 42(24):10,773-10,781.
O'Reilly, C. M., S. Sharma, 2015a. Rapid and highly variable warming of lake surface waters around the globe. Geophysical Research Letters 42:10773-10781.
O'Reilly, C. M., S. Sharma, 2015b. Rapid and highly variable warming of lake surface
waters around the globe. Geophysical Research Letters 42:10773-10781.
Paerl, H. W., J. Huisman, 2009. Climate change: a catalyst for global expansion of harmful cyanobacterial blooms. Environ Microbiol Rep 1(1):27-37.
Park, H., S. Chung, E. Cho, K. Lim, 2018a. Impact of climate change on the persistent turbidity issue of a large dam reservoir in the temperate monsoon region. Climatic Change 151(3-4):365-378.
Park, H., S. Chung, E. Cho, K. Lim, 2018b. Impact of climate change on the persistent turbidity issue of a large dam reservoir in the temperate monsoon region. Climatic Change:1-14.
Peeters, F., D. M. Livingstone, G. H. Goudsmit, R. Kipfer, R. Forster, 2002. Modeling 50 years of historical temperature profiles in a large central European lake. Limnology and Oceanography 47(1):186-197.
Peeters, F., D. Straile, A. Lorke, D. Ollinger, 2007. Turbulent mixing and phytoplankton spring bloom development in a deep lake. Limnology and oceanography 52(1):286-298.
Pekel, J.-F., A. Cottam, N. Gorelick, A. S. Belward, 2016. High-resolution mapping of global surface water and its long-term changes. Nature 540(7633):418.
Perroud, M., S. Goyette, A. Martynov, M. Beniston, O. Anneville, 2009. Simulation of multiannual thermal profiles in deep Lake Geneva: A comparison of one-dimensional lake models. Limnology and Oceanography 54(5):1574-1594.
Persson, I., I. D. Jones, 2008. The effect of water colour on lake hydrodynamics: A modelling study. Freshwater Biology 53(12):2345-2355.

Piccolroaz, S., N. C. Healey, J. D. Lenters, S. G. Schladow, S. J. Hook, G. B. Sahoo, M. Toffolon, 2018. On the predictability of lake surface temperature using air temperature in a changing climate: A case study for Lake Tahoe (USA). Limnology and Oceanography 63(1):243-261.
Piccolroaz, S., M. Toffolon, B. Majone, 2015. The role of stratification on lakes' thermal response: The case of Lake Superior. Water Resources Research 51(10):7878-7894.
Posch, T., O. Koster, M. M. Salcher, J. Pernthaler, 2012. Harmful filamentous cyanobacteria favoured by reduced water turnover with lake warming. Nature Climate Change 2(11):809-813.
Pöschke, F., J. Lewandowski, C. Engelhardt, K. Preuß, M. Oczipka, T. Ruhtz, G. Kirillin, 2015. Upwelling of deep water during thermal stratification onset—A major mechanism of vertical transport in small temperate lakes in spring? Water Resources Research 51(12):9612-9627.
Poschke, F., o. Lewandowski, C. Engelhardt, K. Preuß, M. Oczipka, T. Ruhtz, G. Kirillin1, 2015. Upwelling of deep water during thermal stratification onset - A major mechanism of vertical transport in small temperate lakes in spring. Water Resources Research.
Pryor, S. C., R. J. Barthelmie, D. T. Young, E. S. Takle, R. W. Arritt, D. Flory, W. J. Gutowski Jr., A. Nunes, J. Roads, 2009. Wind speed trends over the contiguous United States. Journal of Geophysical Research: Atmospheres 114(D14).
Read, J. S., D. P. Hamilton, I. D. Jones, K. Muraoka, L. A. Winslow, R. Kroiss, C. H. Wu, E. Gaiser, 2011. Derivation of lake mixing and stratification indices from high-resolution lake buoy data. Environmental Modelling and Software 26:1325-1336.
Read, J. S., L. A. Winslow, G. J. A. Hansen, J. Van den Hoek, P. C. Hanson, L. C. Bruce, C. D. Markfort, 2014. Simulating 2368 temperate lakes reveals weak coherence in stratification phenology. Ecological Modelling 291:142-150.
Rice, J. A., J. S. Thompson, J. A. Sykes, C. T. Waters, The role of metalimnetic hypoxia in striped bass summer kills: consequences and management implications. In: Am Fish Soc Symp, 2013. vol 80. p 000-000.
Richardson, D. C., S. J. Melles, R. M. Pilla, A. L. Hetherington, L. B. Knoll, C. E. Williamson, B. M. Kraemer, J. R. Jackson, E. C. Long, K. Moore, 2017. Transparency, geomorphology and mixing regime explain variability in trends in lake temperature and stratification across Northeastern North America (1975–2014). Water 9(6):442.
Riley, M. J., H. G. Stefan, 1988. MINLAKE: A dynamic lake water quality simulation model. Ecological Modelling 43(3-4):155-182.
Rinke, K., A. M. R. Huber, S. Kempke, M. Eder, T. Wolf, W. N. Probst, K. O. Rothhaupt, 2009. Lake-wide distributions of temperature, phytoplankton, zooplankton, and fish in the pelagic zone of a large lake. Limnology and Oceanography 54(4):1306-1322.
Rinke, K., P. S. Keller, X. Kong, D. Borchardt, M. Weitere, 2019. Ecosystem services from inland waters and their aquatic ecosystems Atlas of Ecosystem Services. Springer, 191-195.
Rinke, K., B. Kuehn, S. Bocaniov, K. Wendt-Potthoff, O. Büttner, J. Tittel, M. Schultze, P. Herzsprung, H. Rönicke, K. Rink, 2013a. Reservoirs as sentinels of catchments: the Rappbode Reservoir Observatory (Harz Mountains, Germany). Environmental Earth Sciences 69(2):523-536.
Rinke, K., B. Kuehn, S. Bocaniov, K. Wendt-Potthoff, O. Buttner, J. Tittel, M. Schultze, P. Herzsprung, H. Ronicke, K. Rink, K. Rinke, M. Dietze, M. Matthes, L. Paul, K. Friese, 2013b. Reservoirs as sentinels of catchments: the Rappbode Reservoir Observatory (Harz Mountains, Germany). Environmental Earth Sciences 69(2):523-536.
Roderick, M. L., L. D. Rotstayn, G. D. Farquhar, M. T. Hobbins, 2007. On the attribution of changing pan evaporation. Geophysical research letters 34(17):L17403.
Rose, K. C., L. A. Winslow, J. S. Read, G. J. Hansen, 2016. Climate‐induced warming of lakes can be either amplified or suppressed by trends in water clarity. Limnology and Oceanography Letters 1(1):44-53.
Rosner, R., D. C. Muller-Navarra, E. Zorita, 2012. Trend analysis of weekly temperatures and oxygen concentrations during summer stratification in Lake Plusssee: A long-term study. Limnology and Oceanography 57(5):1479-1491.
Saber, A., D. E. James, D. F. Hayes, 2018. Effects of seasonal fluctuations of surface heat flux and wind stress on mixing and vertical diffusivity of water column in deep lakes. Adv Water Resour 119:150-163.

Sadeghian, A., S. C. Chapra, J. Hudson, H. Wheater, K.-E. Lindenschmidt, 2018. Improving in-lake water quality modeling using variable chlorophyll a/algal biomass ratios. Environmental Modelling & Software 101:73-85.
Sahoo, G., A. Forrest, S. Schladow, J. Reuter, R. Coats, M. Dettinger, 2015. Climate change impacts on lake thermal dynamics and ecosystem vulnerabilities. Limnology and Oceanography 61:496-507.
Sahoo, G., S. Schladow, J. Reuter, R. Coats, M. Dettinger, J. Riverson, B. Wolfe, M. Costa-Cabral, 2013. The response of Lake Tahoe to climate change. Climatic Change 116(1):71-95.
Saros, J. E., R. M. Northington, C. L. Osburn, B. T. Burpee, N. John Anderson, 2016. Thermal stratification in small arctic lakes of southwest Greenland affected by water transparency and epilimnetic temperatures. Limnology and Oceanography 61(4):1530-1542.
Schlabing, D., M. A. Frassl, M. M. Eder, K. Rinke, A. Bárdossy, 2014. Use of a weather generator for simulating climate change effects on ecosystems: A case study on Lake Constance. Environmental modelling & software 61:326-338.
Schmidt, W., 1928. Über die Temperatur-und Stabilitätsverhältnisse von Seen. Geografiska Annaler 10:145-177.
Schwefel, R., A. Gaudard, A. Wüest, D. Bouffard, 2016. Effects of climate change on deep‐water oxygen and winter mixing in a deep lake (Lake Geneva)–Comparing observational findings and modeling. Water Resources Research 52:8811-8826.
Sen, P. K., 1968. Estimates of the regression coefficient based on Kendall's tau. J Am Stat Assoc 63(324):1379-1389.
Shatwell, T., W. Thiery, G. Kirillin, 2019. Future projections of temperature and mixing regime of European temperate lakes. Hydrology and Earth System Sciences 23(3):1533-1551.
Shimoda, Y., M. E. Azim, G. Perhar, M. Ramin, M. A. Kenney, S. Sadraddini, A. Gudimov, G. B. Arhonditsis, 2011. Our current understanding of lake ecosystem response to climate change: What have we really learned from the north temperate deep lakes? Journal of Great Lakes Research 37(1):173-193.
Sillmann, J., T. Thorarinsdottir, N. Keenlyside, N. Schaller, L. V. Alexander, G. Hegerl, S. I. Seneviratne, R. Vautard, X. Zhang, F. W. Zwiers, 2017. Understanding, modeling and predicting weather and climate extremes: Challenges and opportunities. Weather and climate extremes 18:65-74.
Smith, L. A., 2002. What might we learn from climate forecasts? Proc Natl Acad Sci U S A 99:2487-2492.
Snortheim, C. A., P. C. Hanson, K. D. McMahon, J. S. Read, C. C. Carey, H. A. Dugan, 2017. Meteorological drivers of hypolimnetic anoxia in a eutrophic, north temperate lake. Ecological Modelling 343:39-53.
Soden, B. J., W. D. Collins, D. R. Feldman, 2018. Reducing uncertainties in climate models. Science 361(6400):326-327.
Sommer, U., Z. M. Gliwicz, W. Lampert, A. Duncan, 1986. The PEG-model of seasonal succession of planktonic events in fresh waters. Arch Hydrobiol 106(4):433-471.
Stepanenko, V., K. D. Jöhnk, E. Machulskaya, M. Perroud, Z. Subin, A. Nordbo, I. Mammarella, D. Mironov, 2014. Simulation of surface energy fluxes and stratification of a small boreal lake by a set of one-dimensional models. Tellus A: Dynamic Meteorology and Oceanography 66(1):21389.
Stepanenko, V. M., S. Goyette, A. Martynov, M. Perroud, X. Fang, D. Mironov, 2010. First steps of a Lake Model Intercomparison Project: LakeMIP. Boreal Environ Res 15(2):191-202.
Stillman, J. H., 2019. Heat waves, the new normal: summertime temperature extremes will impact animals, ecosystems, and human communities. Physiology 34(2):86-100.
Straile, D., K. Jöhnk, R. Henno, 2003. Complex effects of winter warming on the physicochemical characteristics of a deep lake. Limnology and oceanography 48(4):1432-1438.
Straile, D., O. Kerimoglu, F. Peeters, M. C. Jochimsen, R. Kümmerlin, K. Rinke, K. O. ROTHHAUPT, 2010. Effects of a half a millennium winter on a deep lake–a shape of things to come? Global Change Biology 16(10):2844-2856.
Swinbank, W. C., 1963. Long‐wave radiation from clear skies. Quarterly Journal of the Royal Meteorological Society 89(381):339-348.
Tan, Z., H. Yao, Q. Zhuang, 2018. A small temperate lake in the 21st century: Dynamics of water temperature, ice phenology, dissolved oxygen and chlorophyll a. Water Resources Research.
Tan, Z., Q. Zhuang, N. J. Shurpali, M. E. Marushchak, C. Biasi, W. Eugster, K. Walter Anthony, 2017.

Modeling CO 2 emissions from A rctic lakes: Model development and site‐level study. Journal of Advances in Modeling Earth Systems 9(5):2190-2213.
Team, R. C., 2016a. R: A language and environment for statistical computing. R Foundation for Statistical Computing, Vienna, Austria.
Team, R. C., 2016b. R: A language and environment for statistical computing. R Foundation for Statistical Computing, Vienna, Austria.
Tebaldi, C., R. Knutti, 2007. The use of the multi-model ensemble in probabilistic climate projections. Philosophical transactions of the royal society A: mathematical, physical and engineering sciences 365(1857):2053-2075.
Terry, J. A., A. Sadeghian, K.-E. Lindenschmidt, 2017. Modelling dissolved oxygen/sediment oxygen demand under ice in a shallow eutrophic prairie reservoir. Water 9(2):131.
Tetra , T., 2007. The Environmental Fluid Dynamics Code Theory and Computation Volume 3: Water Quality Module. Fairfax, VA.
Teurlincx, S., D. van Wijk, W. M. Mooij, J. J. Kuiper, I. Huttunen, R. J. Brederveld, M. Chang, J. H. Janse, B. Woodward, F. Hu, 2019. A perspective on water quality in connected systems: modelling feedback between upstream and downstream transport and local ecological processes. Current Opinion in Environmental Sustainability 40:21-29.
Thiery, W., V. M. Stepanenko, X. Fang, K. D. Johnk, Z. S. Li, A. Martynov, M. Perroud, Z. M. Subin, F. Darchambeau, D. Mironov, N. P. M. Van Lipzig, 2014. LakeMIP Kivu: evaluating the representation of a large, deep tropical lake by a set of one-dimensional lake models. Tellus A 66.
Tian, X., H. Pan, P. Köngäs, J. Horppila, 2017. 3D-modelling of the thermal circumstances of a lake under artificial aeration. Applied Water Science:1-8.
Trolle, D., J. A. Elliott, W. M. Mooij, J. H. Janse, K. Bolding, D. P. Hamilton, E. Jeppesen, 2014. Advancing projections of phytoplankton responses to climate change through ensemble modelling. Environmental modelling & software 61:371-379.
Trolle, D., D. P. Hamilton, M. R. Hipsey, K. Bolding, J. Bruggeman, W. M. Mooij, J. H. Janse, A. Nielsen, E. Jeppesen, J. A. Elliott, 2012. A community-based framework for aquatic ecosystem models. Hydrobiologia 683(1):25-34.
Trolle, D., D. P. Hamilton, C. A. Pilditch, I. C. Duggan, E. Jeppesen, 2011. Predicting the effects of climate change on trophic status of three morphologically varying lakes: Implications for lake restoration and management. Environmental Modelling & Software 26(4):354-370.
Trolle, D., A. Nielsen, H. E. Andersen, H. Thodsen, J. E. Olesen, C. D. Børgesen, J. C. Refsgaard, T. O. Sonnenborg, I. B. Karlsson, J. P. Christensen, 2019. Effects of changes in land use and climate on aquatic ecosystems: Coupling of models and decomposition of uncertainties. Science of the Total Environment 657:627-633.
Uhlmann, W., 2017. A model-based study on the discharge of iron-rich groundwater into the Lusatian post-mining lake Lohsa, Germany. Mine Water and Circular Economy
Valerio, G., M. Pilotti, S. Barontini, B. Leoni, 2015. Sensitivity of the multiannual thermal dynamics of a deep pre-alpine lake to climatic change. Hydrological Processes 29:767-779.
Valerio, G., M. Pilotti, C. L. Marti, J. r. Imberger, 2012. The structure of basin‐scale internal waves in a stratified lake in response to lake bathymetry and wind spatial and temporal distribution: Lake Iseo, Italy. Limnology and Oceanography 57(3):772-786.
Vautard, R., J. Cattiaux, P. Yiou, J.-N. Thépaut, P. Ciais, 2010. Northern Hemisphere atmospheric stilling partly attributed to an increase in surface roughness. Nature geoscience 3(11):756.
Vilhena, L. C., I. Hillmer, J. rg Imberger, 2010. The role of climate change in the occurrence of algal blooms: Lake Burragorang, Australia. Limnology and Oceanography 55(3):1188-1200.
Vinçon-Leite, B., A. Fadel, B. J. Lemaire, C. Bonhomme, Y. Li, G. Le Divechen, J. Zhang, Y. Luo, 2017. Short-term forecasting of cyanobacteria blooms in Yuqiao reservoir, China. LHBl(2):35-44.
Wahl, B., F. Peeters, 2014. Effect of climatic changes on stratification and deep‐water renewal in Lake Constance assessed by sensitivity studies with a 3D hydrodynamic model. Limnology and Oceanography 59(3):1035-1052.
Wang, Q., S. Li, P. Jia, C. Qi, F. Ding, 2013. A review of surface water quality models. The Scientific World Journal 2013.
Warszawski, L., K. Frieler, V. Huber, F. Piontek, O. Serdeczny, J. Schewe, 2014. The inter-sectoral impact

model intercomparison project (ISI–MIP): project framework. Proceedings of the National Academy of Sciences 111(9):3228-3232.
Weber, M., K. Rinke, M. Hipsey, B. Boehrer, 2017. Optimizing withdrawal from drinking water reservoirs to reduce downstream temperature pollution and reservoir hypoxia. Journal of Environmental Management 197:96-105.
Wentzky, V., J. Tittel, C. Jäger, K. Rinke, 2018a. Mechanisms preventing a decrease in phytoplankton biomass after phosphorus reductions in a German drinking
water reservoir—results from more than 50 years of
observation. Freshwater Biology 00:1-14.
Wentzky, V. C., M. A. Frassl, K. Rinke, B. Boehrer, 2019. Metalimnetic oxygen minimum and the presence of Planktothrix rubescens in a low-nutrient drinking water reservoir. Water Research(148):208-218.
Wentzky, V. C., J. Tittel, C. G. Jäger, K. Rinke, 2018b. Mechanisms preventing a decrease in phytoplankton biomass after phosphorus reductions in a German drinking water reservoir—results from more than 50 years of observation. Freshwater biology 63(9):1063-1076.
Wiens, J. A., D. Stralberg, D. Jongsomjit, C. A. Howell, M. A. Snyder, 2009. Niches, models, and climate change: assessing the assumptions and uncertainties. Proceedings of the National Academy of Sciences 106(Supplement 2):19729-19736.
Wilhelm, S., R. Adrian, 2008. Impact of summer warming on the thermal characteristics of a polymictic lake and consequences for oxygen, nutrients and phytoplankton. Freshwater Biology 53(2):226-237.
Wilkinson, G. M., J. J. Cole, M. L. Pace, R. A. Johnson, M. J. Kleinhans, 2015. Physical and biological contributions to metalimnetic oxygen maxima in lakes. Limnology and Oceanography 60(1):242-251.
Williams, D. T., Determination of light extinction coefficients in lakes and reservoirs. In: Proceeding of the Symposium on Surface Water Impoundments, American Society of Civil Engineers, 1981. vol 2. p 1329-1335.
Winslow, L. A., G. J. A. Hansen, J. S. Read, M. Notaro, 2017a. Large-scale modeled contemporary and future water temperature estimates for 10774 Midwestern US Lakes. Scientific Data 4.
Winslow, L. A., J. S. Read, G. J. Hansen, K. C. Rose, D. M. Robertson, 2017b. Seasonality of change: Summer warming rates do not fully represent effects of climate change on lake temperatures. Limnology and Oceanography 62(5):2168-2178.
Winton, R. S., E. Calamita, B. Wehrli, 2019. Reviews and syntheses: Dams, water quality and tropical reservoir stratification. BGeo 16(8):1657-1671.
Wood, T. M., S. A. Wherry, S. Piccolroaz, S. F. Girdner, 2016. Simulation of deep ventilation in Crater Lake, Oregon, 1951–2099: U.S. Geological Survey Scientific Investigations Report 2016–5046, 43 p., http://dx.doi.org/10.3133/sir20165046.
Woolway, R. I., S. C. Maberly, I. D. Jones, H. Feuchtmayr, 2014. A novel method for estimating the onset of thermal stratification in lakes from surface water measurements. Water Resources Research 50(6):5131-5140.
Woolway, R. I., C. J. Merchant, 2017. Amplified surface temperature response of cold, deep lakes to inter-annual air temperature variability. Sci Rep 7(1):4130.
Woolway, R. I., C. J. Merchant, 2019. Worldwide alteration of lake mixing regimes in response to climate change. Nature Geoscience 12(4):271.
Woolway, R. I., C. J. Merchant, J. Van Den Hoek, C. Azorin-Molina, P. Nõges, A. Laas, E. B. Mackay, I. D. Jones, 2019. Northern Hemisphere Atmospheric Stilling Accelerates Lake Thermal Responses to a Warming World. Geophysical Research Letters 46(21):11983-11992.
Wu, G., Z. Xu, 2011. Prediction of algal blooming using EFDC model: Case study in the Daoxiang Lake. Ecological Modelling 222(6):1245-1252.
Wüest, A., A. Lorke, 2003. Small-scale hydrodynamics in lakes. Annu Rev Fluid Mech 35(1):373-412.
Yang, K., Z. Yu, Y. Luo, Y. Yang, L. Zhao, X. Zhou, 2018. Spatial and temporal variations in the relationship between lake water surface temperatures and water quality-A case study of Dianchi Lake. Science of the Total Environment 624:859-871.
Yang, K., Z. Yu, Y. Luo, X. Zhou, C. Shang, 2019. Spatial‐Temporal Variation of Lake Surface Water

Temperature and its Driving Factors in Yunnan‐Guizhou Plateau. Water Resources Research.
Yang, P., Z. Xing, D. A. Fong, S. G. Monismith, K. M. Tan, E. Y. Lo, 2015. Observations of vertical eddy diffusivities in a shallow tropical reservoir. Journal of Hydro-environment Research 9(3):441-451.
Yao, H., N. Samal, K. Joehnk, X. Fang, L. Bruce, D. Pierson, J. Rusak, A. James, 2014. Comparing ice and temperature simulations by four dynamic lake models in Harp Lake: past performance and future predictions. Hydrological Processes 28(16):4587-4601.
Yeates, P., J. Imberger, 2003. Pseudo two‐dimensional simulations of internal and boundary fluxes in stratified lakes and reservoirs. International Journal of River Basin Management 1(4):297-319.
You, Q., S. Kang, W.-A. Flügel, N. Pepin, Y. Yan, J. Huang, 2010. Decreasing wind speed and weakening latitudinal surface pressure gradients in the Tibetan Plateau. Climate Research 42(1):57-64.
Zhang, H., W. Hu, K. Gu, Q. Li, D. Zheng, S. Zhai, 2013. An improved ecological model and software for short-term algal bloom forecasting. Environmental Modelling & Software 48:152-162.
Zhang, Y., Z. Wu, M. Liu, J. He, K. Shi, M. Wang, Z. Yu, 2014. Thermal structure and response to long-term climatic changes in Lake Qiandaohu, a deep subtropical reservoir in China. Limnology and Oceanography 59(4):1193-1202.
Zhang, Y., Z. Wu, M. Liu, J. He, K. Shi, Y. Zhou, M. Wang, X. Liu, 2015. Dissolved oxygen stratification and response to thermal structure and long-term climate change in a large and deep subtropical reservoir (Lake Qiandaohu, China). Water Research 75:249-258.
Zheng, H., X. Lei, Y. Shang, Y. Duan, L. Kong, Y. Jiang, H. Wang, 2018. Sudden water pollution accidents and reservoir emergency operations: impact analysis at Danjiangkou Reservoir. Environ Technol 39(6):787-803.

# References to own articles used in this thesis

**Chapter 2** has been already published under the title:
Dong, F., **Mi, C.,** Hupfer, M., Lindenschmidt, K. E., Peng, W., Liu, X., and Rinke, K.: Assessing vertical diffusion in a stratified lake using a 3D hydrodynamic model, Hydrological Processes, 2019. **(co-first and corresponding author)**.

**Chapter 3** has been already published under the title:
**Mi, C.,** Frassl, M. A., Boehrer, B., and Rinke, K.: Episodic wind events induce persistent shifts in the thermal stratification of a reservoir (Rappbode Reservoir, Germany), International Review of Hydrobiology, 103, 71-82, 2018.

**Chapter 4** has been already published under the title:
**Mi, C.,** Sadeghian, A., Lindenschmidt, K.-E., and Rinke, K.: Variable withdrawal elevations as a management tool to counter the effects of climate warming in Germany's largest drinking water reservoir, Environmental Sciences Europe, 31, 19, 2019.

**Chapter 5** has been resubmitted to Science of the Total Environment after revision, under the title:
**Mi, C.**, Shatwell, T., Ma, J., Xu, Y., Su, F., and Rinke, K: Ensemble warming projections in Germany's largest drinking water reservoir and potential adaptation strategies.

# Other papers accepted or under review during the PhD study

**Mi, C.**, Shatwell, T., Ma, J., Wentzky, V. C., Boehrer, B., Xu, Y., and Rinke, K.: The formation of a metalimnetic oxygen minimum exemplifies how ecosystem dynamics shape biogeochemical processes: A modelling study, Water Research, 115701, 2020.

Dai, L., Dai, H., Liu, H., Wang, Y., Guo, J., Cai, Z., and **Mi, C**.: Development of an Optimal Model for the Xiluodu-Xiangjiaba Cascade Reservoir System Considering the Downstream Environmental Flow, Sustainability, 12, 966, 2020.

**Mi, C.,** Wang, L., Lin, H., and Mi, Y.: Analysis of water quality tendency of Shenwo Reservoir with seasonal kendall method, Science Technology and Engineering, 2017.

Song, F., Su, F., **Mi, C**., and Sun, D: Analysis of Driving Forces on Wetland Ecosystem Services Value Change: A Case in Northeast China, resubmitted to Science of the Total Environment after revision.

# Appendix 2

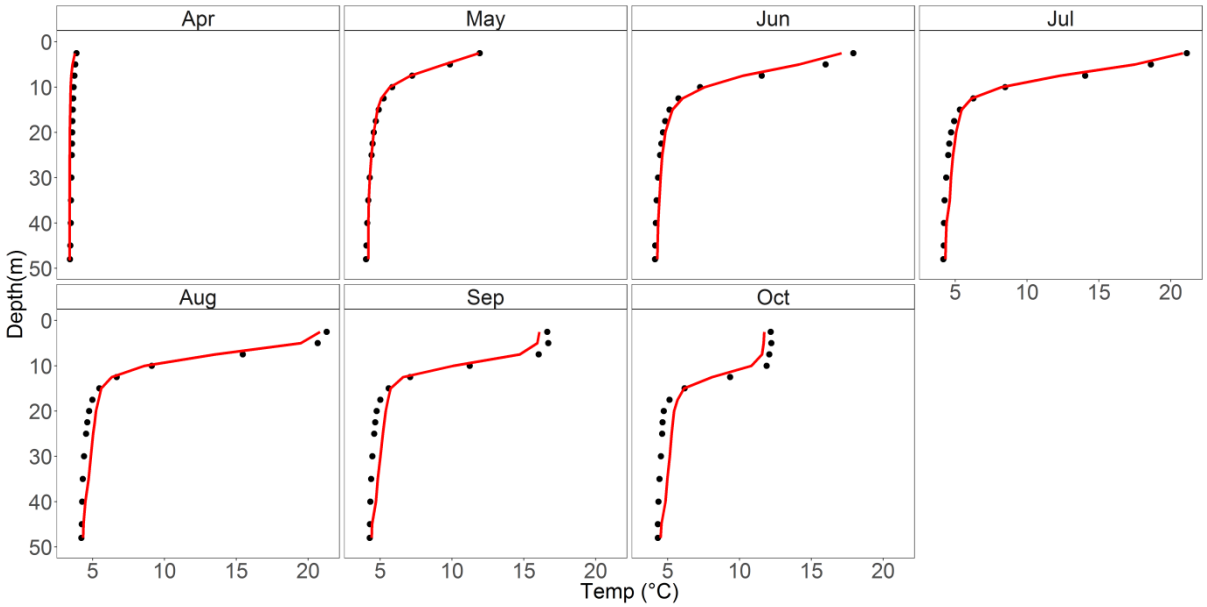


Figure S1. Simulated (lines) versus observed (points) water temperatures in Lake Arendsee, based on monthly averaged results.

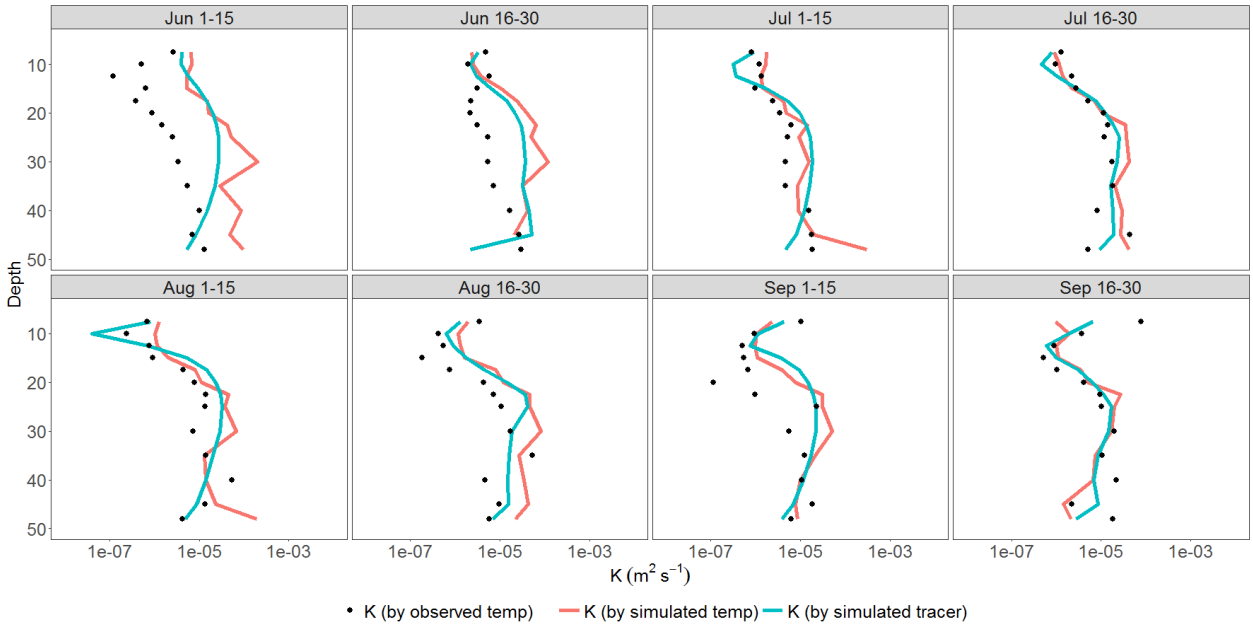


Figure S2. Comparison of simulated vertical diffusion coefficient $K_z$ (derived from water temperature and tracer concentration results from the model with gird size of 100*100m) with observed $K_z$ (calculated from observed water temperature dynamics) over biweekly intervals in Lake Arendsee.

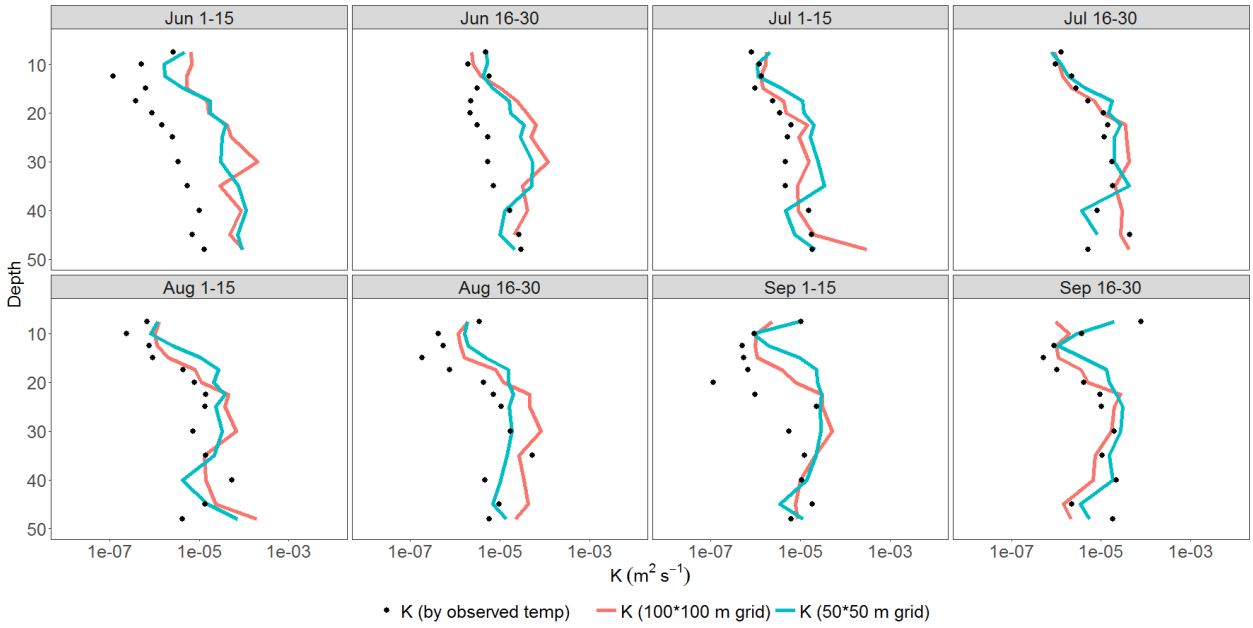


Figure S3. Comparison of simulated vertical diffusion coefficient $K_z$ at different horizontal grid resolution (derived from water temperature in the models) with observed $K_z$ (calculated from observed water temperature dynamics) over biweekly intervals in Lake Arendsee.

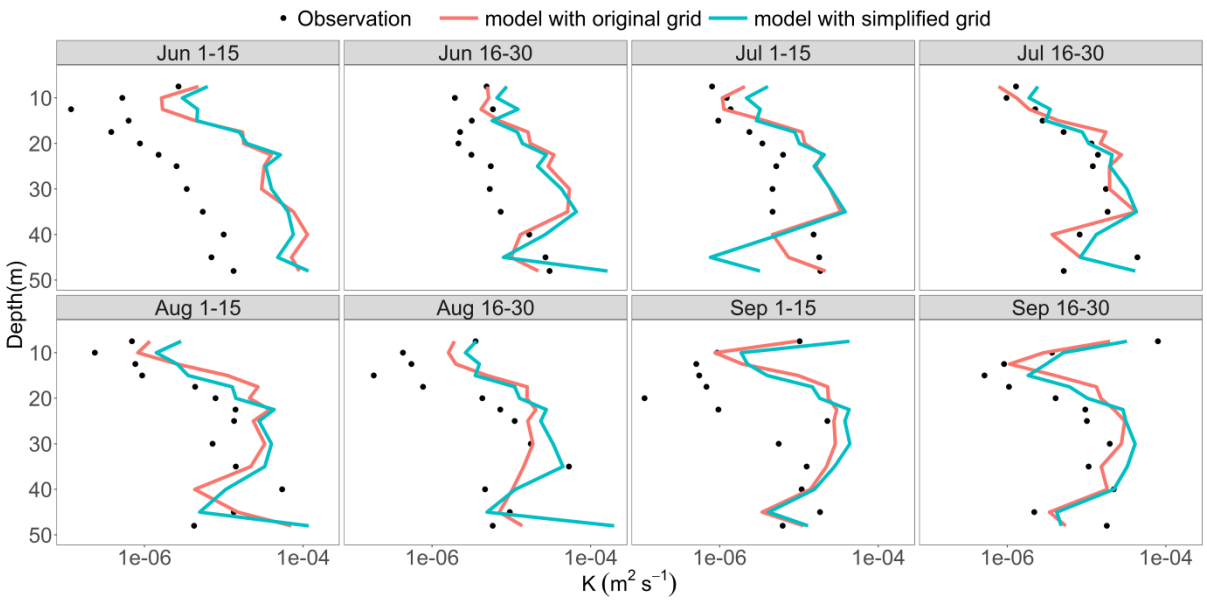


Figure S4. Comparison of vertical diffusion coefficient $K_z$ calculated from the original calibrated model with refined vertical resolution in the metalimnion (red line) and simulation using a model with a homogeneous layer thickness (blue line) in the metalimnion. Observed $K_z$, calculated from observed water temperature over biweekly intervals in Lake Arendsee, are shown as points.

# Appendix 3

a

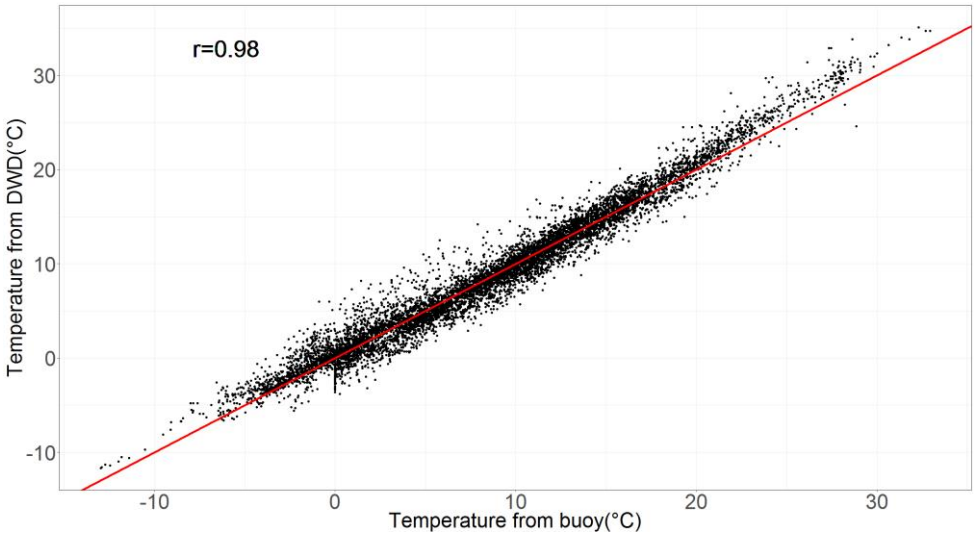


b

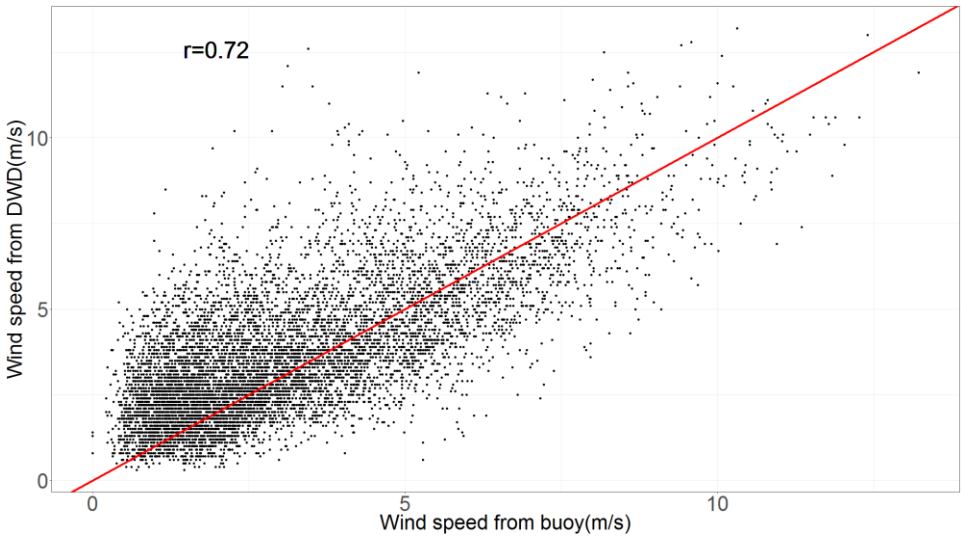


c

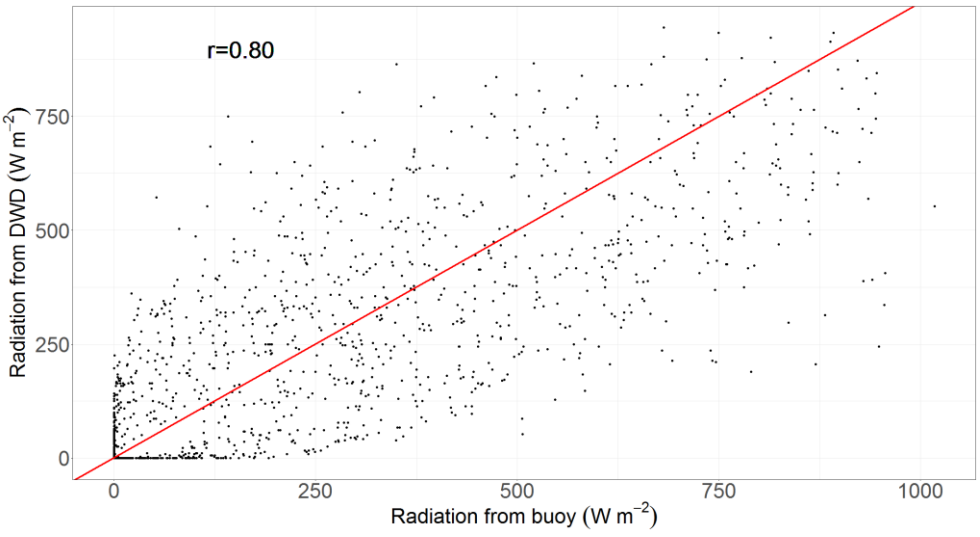

d

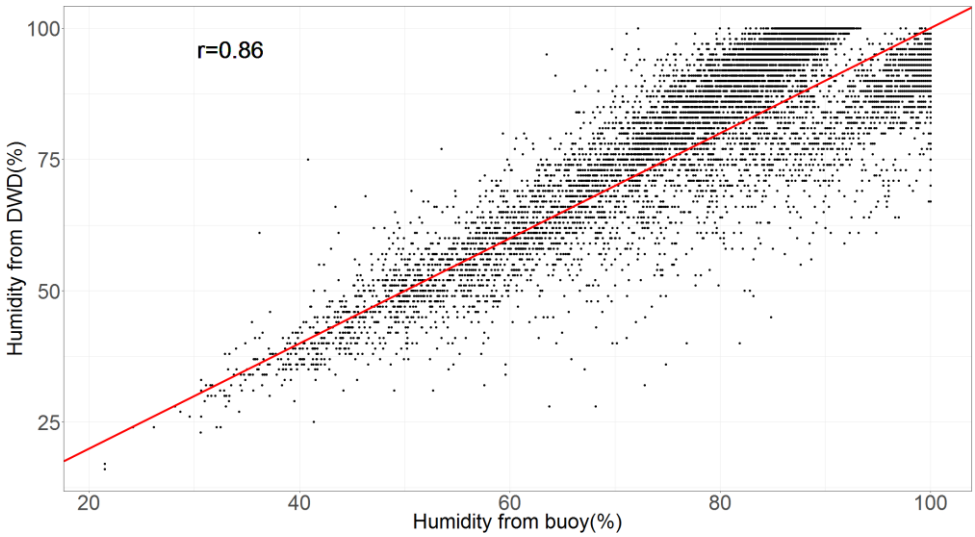


Figure S1. Comparison between the measured meteorological data in 2015 from weather station Harzgerode (German weather service, DWD) and from our buoy at the Rappbode Reservoir: (a) air temperature, (b) wind speed, (c) shortwave radiation, (d) relative humidity. The red line is the 1:1 line.


Figure S2. The comparison between median meteorological conditions at Rappbode Reservoir (Table 3.2) and the respective time series of 2015. The number in each plots shows the mean±sd of median conditions for the variables.

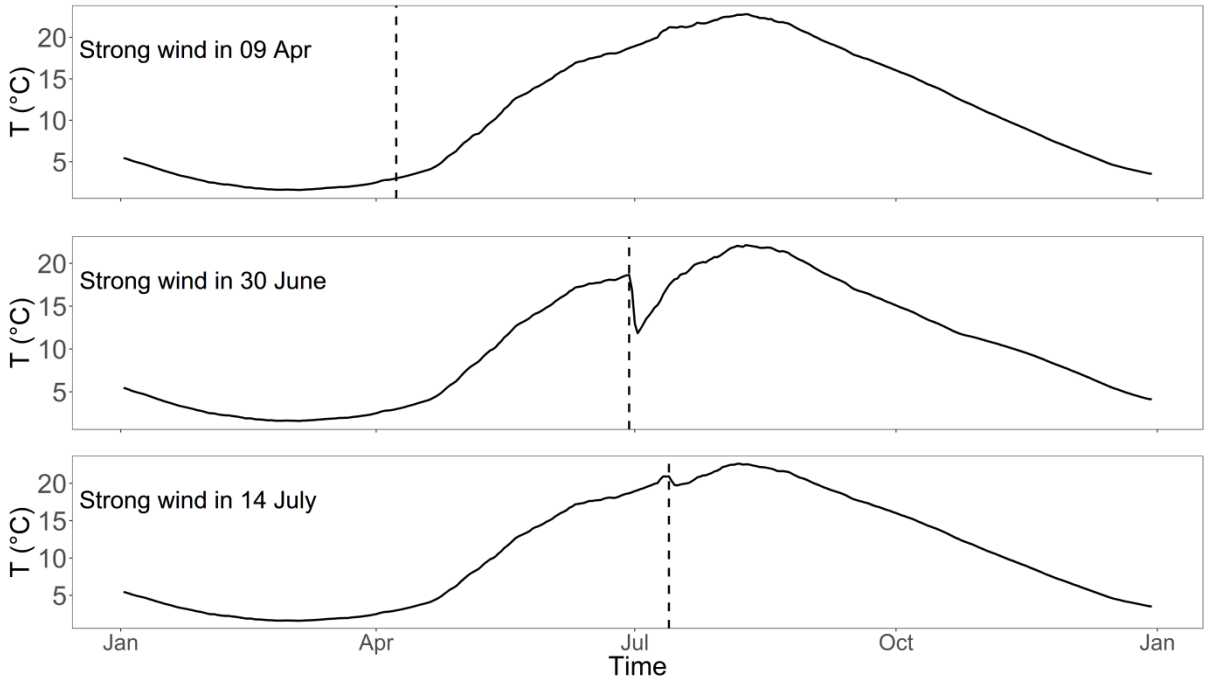


Figure S3. The surface water temperature dynamics under different strong wind events (Scenario S3) taking place at the date indicated by the vertical dashed line (April 09$^{th}$, June 30$^{th}$ and July 14$^{th}$, respectively).

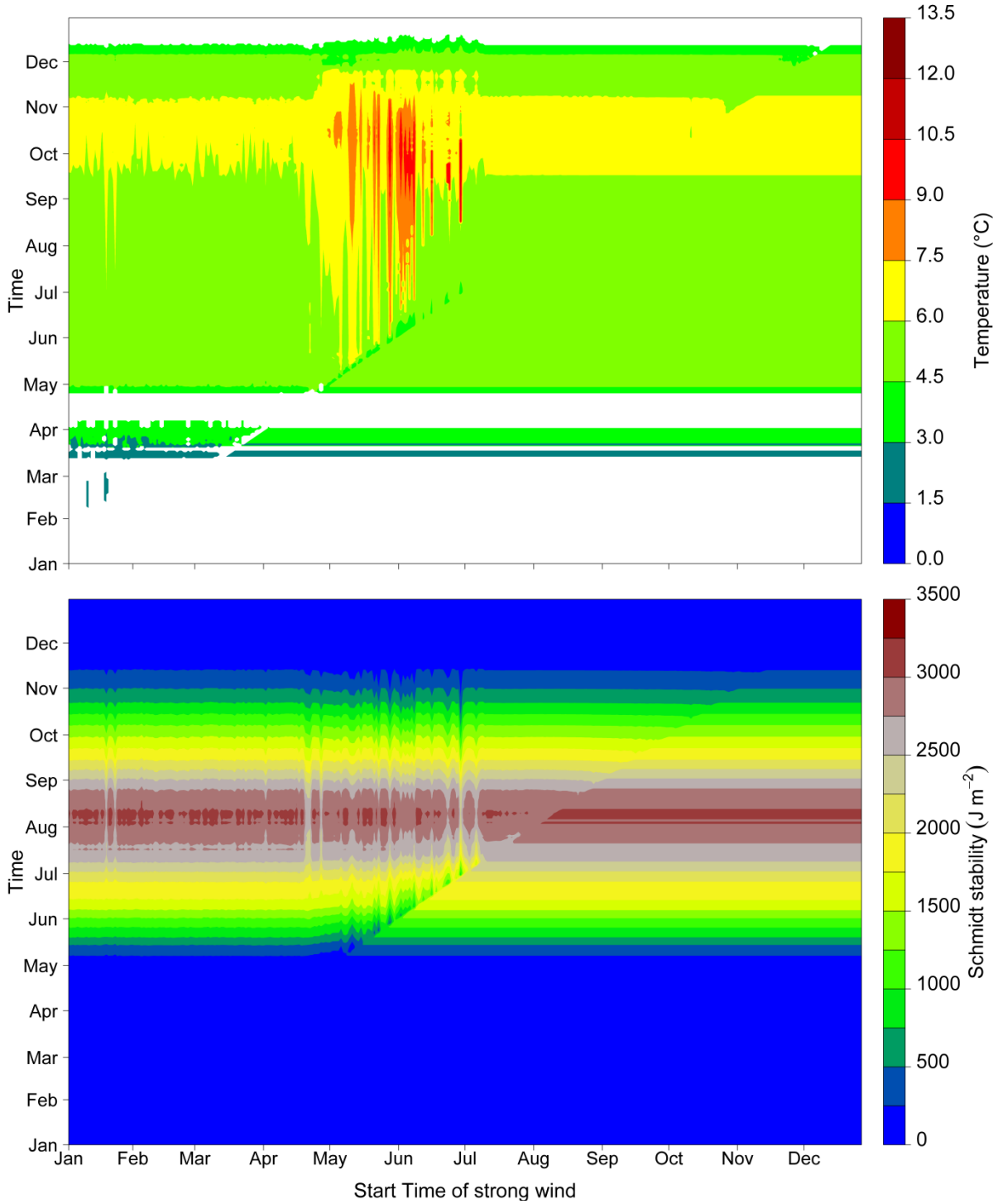


Figure S4. Hypolimnetic temperature (top) and Schmidt stability (bottom) in the scenario S4 for a strong wind event lasting over one day modeled over the entire year (vertical axis) for different timing of the strong wind event (horizontal axis).

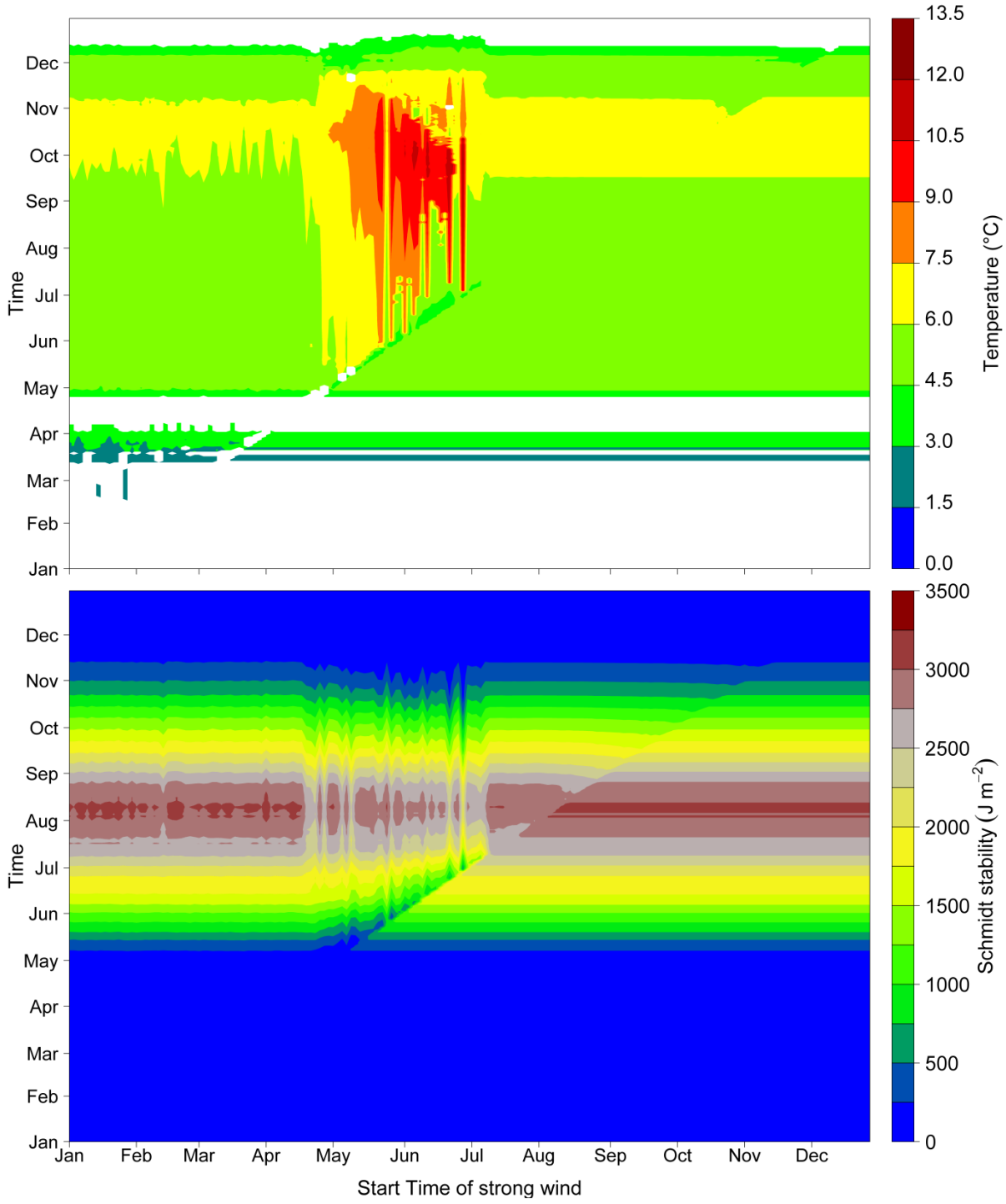


Figure S5. Hypolimnetic temperature (top) and Schmidt stability (bottom) in the scenario S4 for a strong wind event lasting over two days modeled over the entire year (vertical axis) for different timing of the strong wind event (horizontal axis).

# Appendix 4

Table S1. Projected water temperature trends (2006-2099), under RCP 2.6, 6.0, 8.5 forced by different climate models (ns: not significant, *: p<0.001, d: decade)

| | Model | Water temp (1m depth) | Water temp (10m depth) | Water temp (50m depth) |
|---|---|---|---|---|
| RCP 2.6 | GFDL | ns | ns | -0.04 °C $d^{-1}$ (p=0.002) |
| | HadGEM2 | 0.12 °C $d^{-1}$ (*) | 0.11 °C $d^{-1}$ (p=0.0018) | 0.07 °C $d^{-1}$ (p=0.0013) |
| | IPSL | 0.10 °C $d^{-1}$ (*) | ns | ns |
| | MIROC5 | 0.07 °C $d^{-1}$ (*) | 0.07 °C $d^{-1}$ (*) | 0.05 °C $d^{-1}$ (*) |
| RCP 6.0 | GFDL | 0.15 °C $d^{-1}$ (*) | ns | -0.04 °C $d^{-1}$ (p=0.03) |
| | HadGEM2 | 0.39 °C $d^{-1}$ (*) | 0.29 °C $d^{-1}$ (*) | 0.12 °C $d^{-1}$ (*) |
| | IPSL | 0.29 °C $d^{-1}$ (*) | 0.07 °C $d^{-1}$ (*) | 0.05 °C $d^{-1}$ (p=0.002) |
| | MIROC5 | 0.37 °C $d^{-1}$ (*) | 0.29 °C $d^{-1}$ (*) | 0.13 °C $d^{-1}$ (*) |
| RCP 8.5 | GFDL | 0.27 °C $d^{-1}$ (*) | 0.07 °C $d^{-1}$ (*) | ns |
| | HadGEM2 | 0.57 °C $d^{-1}$ (*) | 0.43 °C $d^{-1}$ (*) | 0.29 °C $d^{-1}$ (*) |
| | IPSL | 0.55 °C $d^{-1}$ (*) | 0.40 °C $d^{-1}$ (*) | 0.28 °C $d^{-1}$ (*) |
| | MIROC5 | 0.52 °C $d^{-1}$ (*) | 0.37 °C $d^{-1}$ (*) | 0.22 °C $d^{-1}$ (*) |

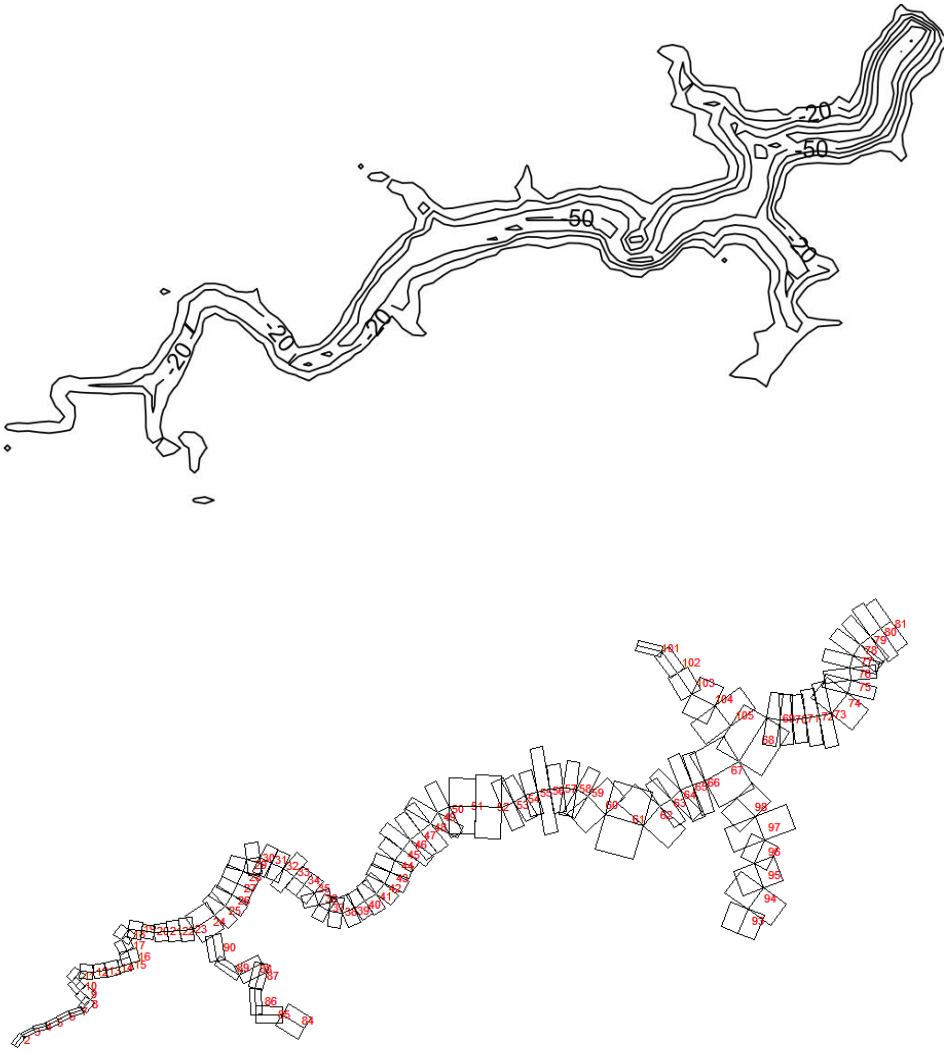


Figure S1. Comparison between observed bathymetry (top) and that established in CE-QUAL-W2 (bottom)

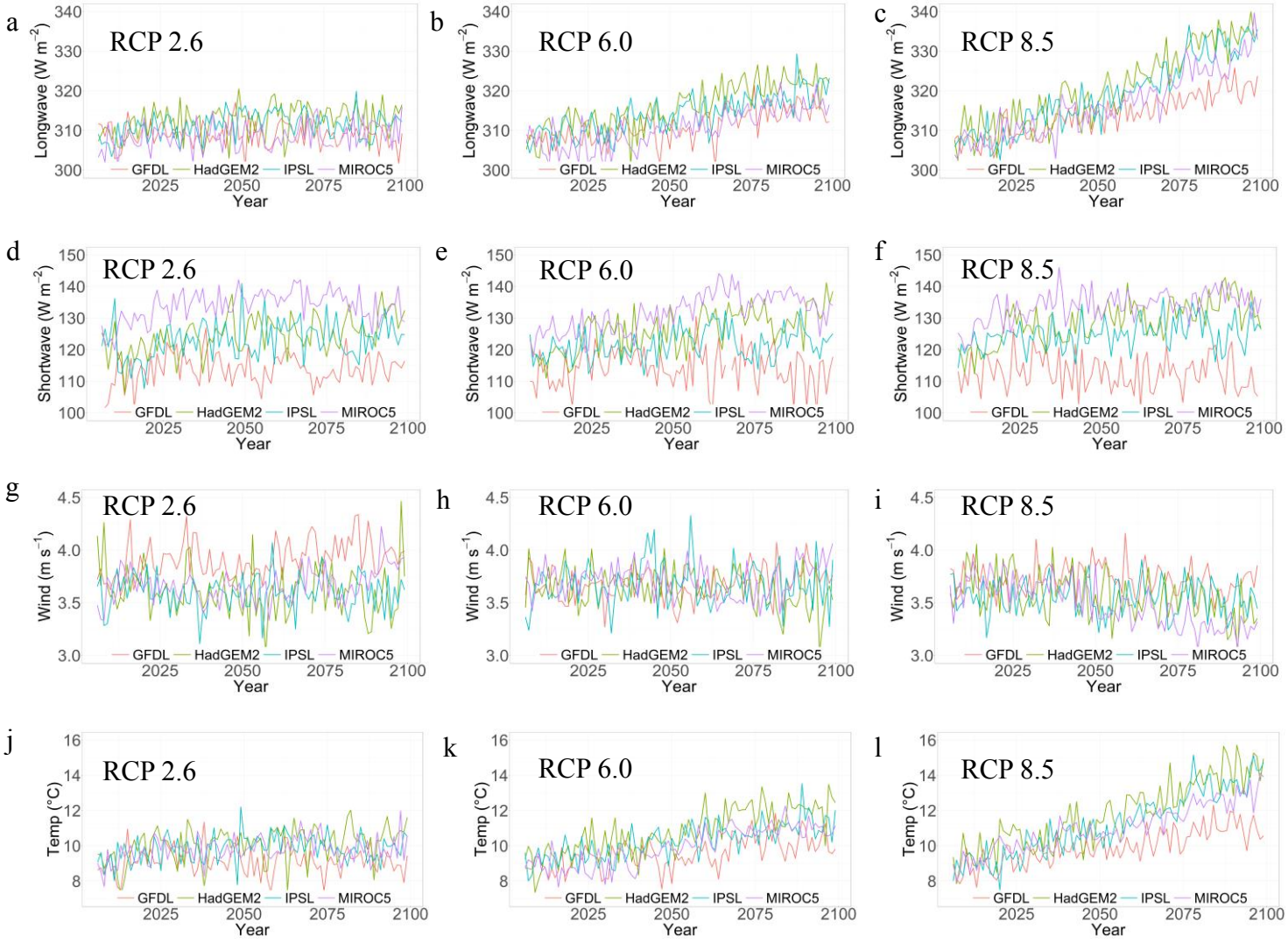


Figure S2. Time series of projected longwave radiation (a-b-c), shortwave radiation (d-e-f), wind speed (g-h-i) and air temperature (j-k-l) during 2006-2099 under RCP 2.6 (left column), RCP 6.0 (middle column) and RCP 8.5 (right column).

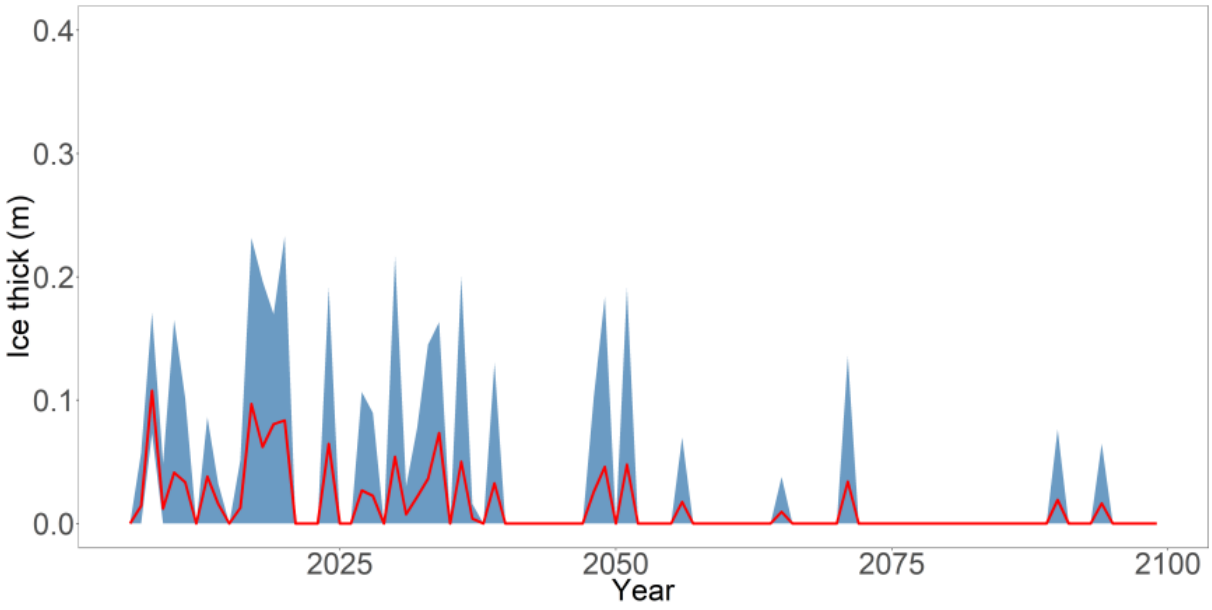


Figure S3. Annual mean ice thickness in Rappbode Reservoir during the period 2006-2099 under RCP 8.5 .The red lines show the annual mean values, the blue shaded areas show the annual minimum and maximum values from the ensemble.